NAVAL POSTGRADUATE SCHOOL

MONTEREY, CALIFORNIA

THESIS

CONVECTIVE INDICES FOR THE CENTRAL AND WESTERN TROPICAL PACIFIC

by

Matthew B. Stratton

March 2006

Thesis Advisor:	Patrick A. Harr
Second Reader:	Russell L. Elsberry

THIS PAGE INTENTIONALLY LEFT BLANK

REPORT DOCUMENTATION PAGE			Form Approved OMB No. 0704-0188
Public reporting burden for this collection of information is estimated to average 1 hour per response, including the time for reviewing instruction, searching existing data sources, gathering and maintaining the data needed, and completing and reviewing the collection of information. Send comments regarding this burden estimate or any other aspect of this collection of information, including suggestions for reducing this burden, to Washington headquarters Services, Directorate for Information Operations and Reports, 1215 Jefferson Davis Highway, Suite 1204, Arlington, VA 22202-4302, and to the Office of Management and Budget, Paperwork Reduction Project (0704-0188) Washington DC 20503.			
1. AGENCY USE ONLY *(Leave blank)*	**2. REPORT DATE** March 2006	**3. REPORT TYPE AND DATES COVERED** Master's Thesis	
4. TITLE AND SUBTITLE: Convective Indices for the Central and Western Tropical Pacific			**5. FUNDING NUMBERS**
6. AUTHOR(S) Matthew B. Stratton			
7. PERFORMING ORGANIZATION NAME(S) AND ADDRESS(ES) Naval Postgraduate School Monterey, CA 93943-5000			**8. PERFORMING ORGANIZATION REPORT NUMBER**
9. SPONSORING /MONITORING AGENCY NAME(S) AND ADDRESS(ES) N/A			**10. SPONSORING/MONITORING AGENCY REPORT NUMBER**
11. SUPPLEMENTARY NOTES The views expressed in this thesis are those of the author and do not reflect the official policy or position of the Department of Defense or the U.S. Government.			
12a. DISTRIBUTION / AVAILABILITY STATEMENT Approved for public release; distribution is unlimited.			**12b. DISTRIBUTION CODE**

13. ABSTRACT (maximum 200 words)

Within the Pacific Air Forces (PACAF) area of responsibility, tropical deep convection that is not associated with tropical cyclones can cause significant impacts to operations. In this study, convective indices calculated from five sites in the central and western tropical North Pacific are examined with respect to their ability to predict the onset and intensity of deep convection. Two predictands are utilized: measures of convection derived from surface weather observations and the Naval Research Laboratory (NRL) Blended Rainrate estimates, which are derived from infrared and microwave satellite observations and interpolated to the five sites. Eighteen indices derived from rawinsondes are ranked by predictive skill for specific locations and seasons. Indices that exhibit significant skill are used in a discriminant analysis to define a multivariate experimental tropical convective index, which is then evaluated for each region and season. The multivariate index was not able to discriminate between convective and non-convective environments over the central North Pacific. Although the multivariate index exhibited skill for sites in the tropical western North Pacific during summer, it did not perform better than the highest-ranked single indices. For many of the locations and seasons evaluated, the Severe Weather Threat (SWEAT) Index exhibited the most skill.

14. SUBJECT TERMS Convective Indices, Mesoscale Convection, Tropical Convection, Convective Initiation, Forecasting Convection, Operational Weather Squadron Forecasts, Point Forecasts, Area Forecasts, Naval Research Laboratory Blended Rainrate	**15. NUMBER OF PAGES** 119
	16. PRICE CODE

17. SECURITY CLASSIFICATION OF REPORT	**18. SECURITY CLASSIFICATION OF THIS PAGE**	**19. SECURITY CLASSIFICATION OF ABSTRACT**	**20. LIMITATION OF ABSTRACT**
Unclassified	Unclassified	Unclassified	UL

NSN 7540-01-280-5500 Standard Form 298 (Rev. 2-89)
Prescribed by ANSI Std. 239-18

THIS PAGE INTENTIONALLY LEFT BLANK

Approved for public release; distribution is unlimited

CONVECTIVE INDICES FOR
THE CENTRAL AND WESTERN TROPICAL PACIFIC

Matthew B. Stratton
Captain, United States Air Force
B.S., North Carolina State University, 1997

Submitted in partial fulfillment of the
requirements for the degree of

MASTER OF SCIENCE IN METEOROLOGY

from the

NAVAL POSTGRADUATE SCHOOL
March 2006

Author: Matthew B. Stratton

Approved by: Patrick A. Harr
Thesis Advisor

Russell L. Elsberry
Second Reader

Philip A. Durkee
Chairman, Department of Meteorology

THIS PAGE INTENTIONALLY LEFT BLANK

ABSTRACT

Within the Pacific Air Forces (PACAF) area of responsibility, tropical deep convection that is not associated with tropical cyclones can cause significant impacts to operations. In this study, convective indices calculated from five sites in the central and western tropical North Pacific are examined with respect to their ability to predict the onset and intensity of deep convection. Two predictands are utilized: measures of convection derived from surface weather observations and the Naval Research Laboratory (NRL) Blended Rainrate estimates, which are derived from infrared and microwave satellite observations and interpolated to the five sites. Eighteen indices derived from rawinsondes are ranked by predictive skill for specific locations and seasons. Indices that exhibit significant skill are used in a discriminant analysis to define a multivariate experimental tropical convective index, which is then evaluated for each region and season. The multivariate index was not able to discriminate between convective and non-convective environments over the central North Pacific. Although the multivariate index exhibited skill for sites in the tropical western North Pacific during summer, it did not perform better than the highest-ranked single indices. For many of the locations and seasons evaluated, the Severe Weather Threat (SWEAT) Index exhibited the most skill.

THIS PAGE INTENTIONALLY LEFT BLANK

TABLE OF CONTENTS

THIS PAGE INTENTIONALLY LEFT BLANK

LIST OF FIGURES

LIST OF TABLES

THIS PAGE INTENTIONALLY LEFT BLANK

ACKNOWLEDGMENTS

First, I would like to thank God for providing everything I need, including challenging opportunities to grow. Second, I would like to thank my wife and son for their love, understanding and patience throughout my work at Naval Postgraduate School. Third, I would like to thank Dr. Pat Harr and Dr. Russell Elsberry for their immeasurable assistance in all aspect of this thesis. Finally, I would like to thank my fellow classmates at NPS for sharing their operational experiences and their opinions related to this thesis.

THIS PAGE INTENTIONALLY LEFT BLANK

I. INTRODUCTION

A. CHALLENGE OF MESOSCALE TROPICAL CONVECTION

One of the most significant obstacles to military operations in the tropics is convective weather. For that reason, military weather agencies expend considerable resources observing and forecasting tropical convective weather. Most of their attention is focused on organized convective weather systems, such as tropical cyclones and convection associated with other synoptic-scale systems. Somewhat less attention is paid to mesoscale convective weather in the tropics. Yet it is the "garden variety" convective weather, not the once-in-a-while tropical cyclones, that most frequently impacts routine U.S. Air Force operations and flight safety in tropical regions (C. Finta 2005, personal communication).

B. EFFECTS ON U.S. AIR FORCE SYSTEMS

Strong convection (including thunderstorms and heavy rain showers) can significantly affect US. military systems during training and operations. In particular, U.S. Air Force weapons, communications, and support systems are at risk. Lightning can damage sensitive electronics or composite structures of aircraft and ground systems. Additionally, lightning can injure or kill military personnel. The turbulence, icing, and low-level wind shear associated with thunderstorms can all disrupt aircraft handling and possibly cause a crash. Hail aloft can damage aircraft engines, windscreens, and leading edges. Flooding from heavy convective precipitation can slow ground transport and damage equipment. Even if areas of unanticipated convection are successfully avoided when they are encountered, extra resources are consumed as aircraft divert around convective areas and time is lost to delays.

Compounding the risk from tropical convective weather is the U.S. military's increasing exposure to it. Because of national security interests, humanitarian needs, and forward operating base locations, the U.S. military is increasingly operating in the tropics where convective weather abounds (see Figure 1). Consequently, more frequent encounters with convective weather will increase the risk of negative mission impacts.

Figure 1. Locations of US military operations, 1990-2003 (from "The Pentagon's New Map: War and Peace in the Twenty-First Century" © 2003 William McNulty).

C. RISK MANAGEMENT

To mitigate the effects of adverse weather on operations, the U.S. Air Force utilizes several risk management practices. Prior to operations, weather forecasts are incorporated into mission planning and then in preparations immediately before take-off. During operations, weather observations are continuously monitored for conditions that could negatively affect systems or personnel. After operations, weather debriefings are conducted to determine both the accuracy of the forecast and the mission impacts due to the weather conditions.

Those adverse weather conditions, often referred to as "no-go criteria," are officially documented in several publications. No-go criteria are listed in three main types of publications: Flying, Safety, and Local publications. Flying publications, such as the 11-series regulations and aircraft technical orders, document no-go criteria for aircraft operations. Safety publications, such as the 91-series regulations, document no-go criteria for ground operations and mission support. Local Publications, such as base-specific or equipment-specific operating instructions, document no-go criteria for unique locations and equipment. Each publication (Flying, Safety, and Local) also lists operating restrictions or protective actions that should be taken when no-go criteria are encountered. Before restrictions or protective actions can be implemented, accurate

weather information must be provided to operational decision-makers. Therefore, the operational risk management decisions are often only as good as the weather forecast.

D. AIR FORCE WEATHER RESPONSIBILITIES

Weather Publications, which comprise the 15-series regulations, document various responsibilities for providing weather information. At the tactical unit level, weather personnel at Combat Weather Teams (CWTs) are responsible for providing weather information to operations personnel. However, much of the information CWTs provide originates at regional Operational Weather Squadrons (OWSs). The OWSs are responsible for providing CWTs various types of weather information, including forecasts for planning purposes and resource protection. The OWSs also create forecast products for other users, which occasionally includes aircrews, commanders, and other operations personnel.

E. OWS FORECASTS

Forecasts from OWSs fall into two main categories: point forecasts and area forecasts. Point forecasts predict weather conditions within a few miles of a specific point, such as the center of an airfield. Examples of point forecasts are Terminal Aerodrome Forecasts (TAFs) and Weather Watches. By contrast, area forecasts are predictions of the weather conditions across a large geographic area. Examples of area forecasts are Forecaster-In-The-Loop (FITL) Hazard Charts and Aerial Refueling (AR) Track Forecasts. Regardless of the spatial scale, both point and area forecasts are focused, among other things, on predicting convection.

For OWSs whose regions include the tropics, opportunities to forecast tropical convection occur frequently. The OWS forecasts of tropical convection are most often found in TAFs and FITL Thunderstorm Charts. An OWS creates at least three TAFs per day for each location for which they are responsible (typically 5-10 per OWS). Each TAF then describes conditions over a 24-hour period. As for FITL Thunderstorm charts, a minimum of six charts are created per day, with each chart identifying forecast conditions across the OWS area of responsibility (often spanning continents or oceans; see Figure 2) at a specific moment in time. The six charts span a 48-hour period. The numerous locations and extended time spans make it highly likely that the forecast will include convective weather conditions.

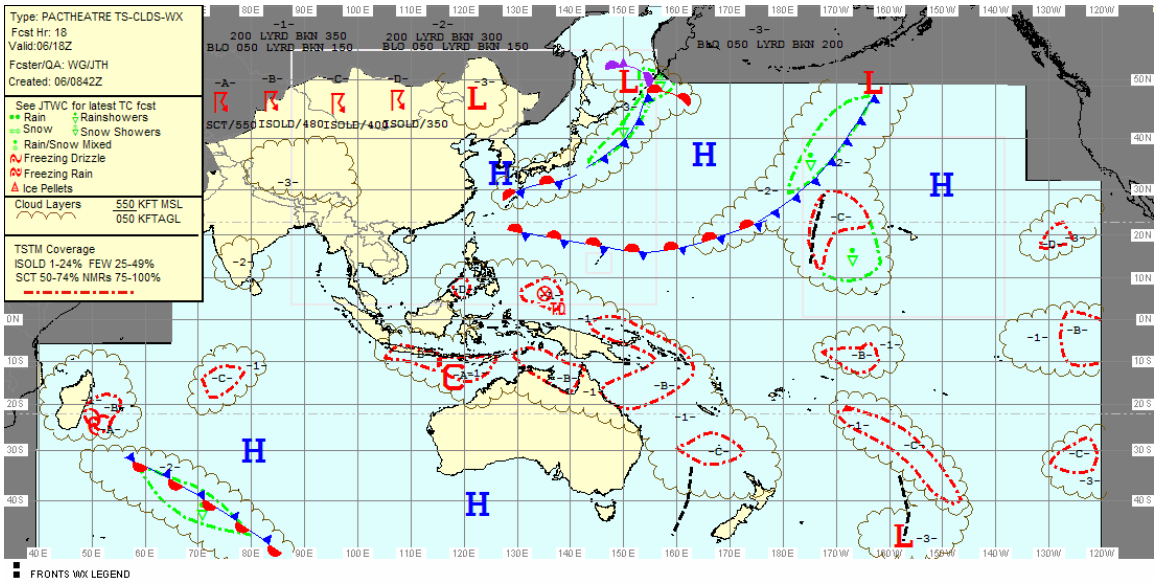

Figure 2. Sample FITL Thunderstorm Chart (from 17 OWS).

F. FORECAST METHODS

Despite these many opportunities to forecast tropical convection, the OWSs in the central and western tropical Pacific do not have a standard tool or technique to use in forecasting convection. Among the several choices left to individual forecaster discretion, Pacific Air Forces (PACAF) weather units currently use convective indices originally developed for mid-latitude locations. These indices often correlate poorly with thunderstorm and convective rain shower development in a tropical environment (Ramage 1995). Few U.S. Air Force studies have documented the effectiveness of different tools or techniques in forecasting tropical convection. Similarly, only one recent study (Sherwood 1999) has investigated predictability of tropical convection using upper-air data.

G. TECHNIQUE ANALYSIS

To address the lack of validations of any one tropical convection forecasting technique over another, a research topic titled "Tropical Convective Indices" was proposed by the 17 OWS through Air Force Weather (AFW) and Air Force Institute of Technology (AFIT) channels. This proposal identified a need for systematic evaluation of the suitability of the many indices derived from atmospheric soundings and then used to forecast convective weather in the near term (0-3 hours).

In this study, the period from August 2004 to July 2005 was chosen to investigate the utility of various sounding indices to predict convective environments at Okinawa, Guam, Kwajalein, Lihue, and Hilo. A comprehensive evaluation was undertaken in which observations were used to systematically define the pre- and post-sounding environment. Finally, satellite-derived precipitation rates are compared with observations and sounding indices to provide a comprehensive validation of the indices' performance. This final step is crucial for eventual expansion of convective forecast techniques to data-void areas that are often traversed during flight operations.

In this thesis, background material related to mesoscale tropical convection is provided in Chapter II. The methodology used during the study is described in Chapter III. The results of the study are presented in Chapter IV, and the conclusions and future recommendations are given in Chapter V.

THIS PAGE INTENTIONALLY LEFT BLANK

II. BACKGROUND

A. CONVECTION IN THE TROPICS

1. Terminology

Throughout this paper, the term "convection" is used to describe moist atmospheric convection with accompanying condensation, latent heat release, and precipitation. Dry convection is excluded because it does not create rain showers, thunderstorms, or their associated hazards to military operations. The term "initiation" refers to the onset of convection. Convective "intensity" is defined as the strength of the convective updrafts.

The term "tropics" refers to the region between the subtropical ridges of high pressure. As a rough approximation, this area lies in a latitudinal belt between 30° N and 30° S.

The term "mesoscale" refers to weather phenomena with lengths between 4 km and 400 km (Fujita 1986).

2. Physical Processes

Tropical convection is caused by the release of atmospheric instability, which may be defined by potential temperature (Θ) decreasing with height (z),

$$\frac{d\Theta}{dz} < 0 . \tag{1}$$

Several physical processes contribute to the creation of instability, which is a step sometimes referred to as "preconditioning" (Johnson and Mapes 2001). Preconditioning often occurs by synoptic-scale processes such as quasi-geostrophic forced ascent. The instability created by preconditioning is then released by mesoscale processes that initiate the convection. The release is sometimes referred to as "triggering" or "lifting." Once released, the instability causes upward vertical motion (w), which can be expressed by the vertical momentum equation

$$\rho \frac{dw}{dt} = -\frac{\partial p}{\partial z} - \rho g - \rho g (q_l + q_i) + 2\rho\Omega u \cos\phi = \rho F_z , \tag{2}$$

where ρ is density, p is pressure, g is the gravitational acceleration, q_l is the mixing ratio of liquid condensate, q_i is the mixing ratio of ice condensate, Ω is the angular rate of the earth's rotation, u is the zonal component of motion, ϕ is the latitude, and F_z is the vertical component of any external forces (viscosity). From an alternate, ingredients-based perspective, Doswell (1996) has summarized the necessary ingredients of deep moist convection as: i) instability, ii) moisture, and iii) lift.

An important characteristic of convection is its depth, which is measured from the base to the top. Often, the depth of the convection will determine what type of sensible weather will develop. Shallow convection is unlikely to have the updraft speeds necessary to generate convective hazards, such as hail or lightning (Short et al. 2004). At the other end of the spectrum is deep convection, which extends vertically from the atmospheric boundary layer (BL) to the top of the troposphere. It is primarily deep convection that provides the conditions necessary for convective hazards to form.

Field studies (Johnson et al. 1999) have shown that tropical convection tends to occur as one of three depths: i) shallow cumulus, ii) cumulus congestus, and iii) cumulonimbus. Shallow cumulus clouds tend to have tops near 2 km above ground level (AGL). In the tropics, shallow convection is often restricted by either an inversion or overlying dry air. Slightly deeper, cumulus congestus tend to have tops near 5 km AGL (near 0°C in the tropics). Cumulonimbus clouds tend to have tops near 15 km, which is approximately the height of the tropical tropopause.

3. Deep Moist Convection and its Hazards

Because cumulonimbus clouds associated with deep moist convection (DMC) are able to generate the hazards discussed in the Introduction, the focus in this thesis is on DMC in the tropics. It is the hazards (lightning, icing, turbulence, hail, heavy precipitation, and low-level wind shear) rather than the convection that threatens military operations.

Deep moist convection is caused by the same factor that causes any type of convection: release of instability. The main distinction of DMC is that strong updrafts are able to overcome any low-level inversions (such as trade wind inversions) so that the convection reaches into the upper troposphere. Sherwood (1999) and Raymond (2001)

conclude that the most important variable for tropical DMC is the amount of low-level moisture. Increasing the low-level moisture increases the buoyancy of air parcels, which increases the updraft strength sufficiently to ascend to the tropopause.

Deep moist convection can be classified according to its intensity. Deep moist convection that culminates in rain showers is assumed to be of weaker intensity. Deep moist convection that culminates in thunderstorms is assumed to be of stronger intensity. Barnes (2001, p. 384) has shown that lightning is an indicator of when a system has more vigorous updrafts. Additionally, stratiform-type precipitation (hereafter simply called rain) can occur towards the end of the life cycle of DMC.

Deep moist convection occurs in many horizontal configurations and scales. The smallest unit of DMC is an isolated cumulonimbus, which may have a diameter on the order of a few kilometers. Multiple cumulonimbi caused by the same forcing mechanism can be organized into larger units called mesoscale convective systems (MCSs). The term MCS has been applied to phenomena across a broad range of spatial scales from aggregates of a few cumulonimbi to well-organized, small tropical cyclones (Fritsch and Forbes 2001). Deep moist convection can also be organized on synoptic scales. The largest organization of DMC is a synoptic-scale feature called a monsoon gyre (Lander 1994), which is unique to the tropical western North Pacific. It should be noted that the synoptic-scale environment (temperature, moisture, and wind distribution) often determines how the DMC will develop and organize.

An individual convective element (cell) often has a life cycle on the order of an hour or less (Kodama and Businger 1998). However, an MCS may last several days if the system is able to generate new cells as it propagates. Despite the longevity of some MCSs, they can still be reasonably classified as mesoscale in nature.

In the middle of the MCS size continuum are the phenomena of squall lines. Generally, the term squall line describes a group of thunderstorms organized into a line whose length is much greater than its width. Squall lines are of particular interest to forecasters due to the relative frequency of their occurrence and the associated sensible weather. Doswell (2001) states a linear organization is the most common form of DMC

organization. Oceanic squall lines can produce surface winds that approach the severe (= 50 kt) threshold (Barnes 2001).

Squall lines in the tropics and mid-latitudes are caused by a combination of factors. As a subset of both DMC and MCSs, squall lines are caused by release of instability throughout the depth of the troposphere. Additionally, squall lines require certain amounts of environmental vertical wind shear and dry mid-level air. The wind shear helps to initiate downdrafts of dry mid-level air, which forms a cold pool near the surface and forces subsequent convection along its leading edge. Convective cells are likely to become squall lines wherever a moist lower troposphere is overlain be a relatively dry middle troposphere (Ramage 1995). Houze (1977) and Zipser (1977) present excellent conceptual models of tropical squall lines (Figure 3).

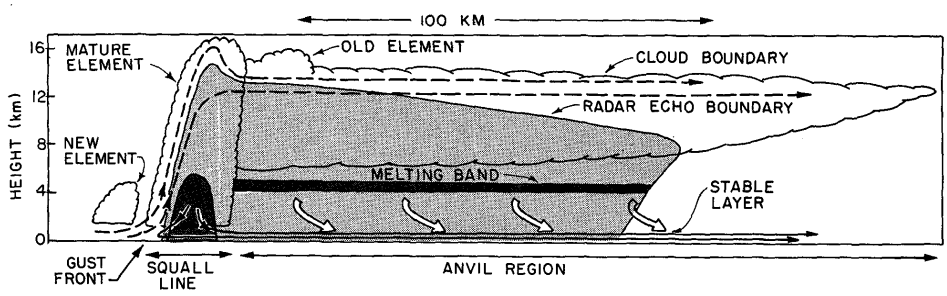

Figure 3. Tropical squall line cross section (after Houze 1977).

B. CLIMATOLOGY OF MESOSCALE TROPICAL CONVECTION

The environment in the tropics is often favorable for convection. Because the earth surface absorbs large amounts of solar energy over tropical latitudes where large expanses of the tropics are oceanic, heat and moisture fluxes from the surface to the overlying atmospheric boundary layer increase the buoyancy of the air.

However, the tropical atmosphere is neither static nor homogeneous. A wide range of tropical environments exist due to annual variability, semi-permanent features associated with surface types, and synoptic-scale phenomena (Barnes 2001) (Figure 4).

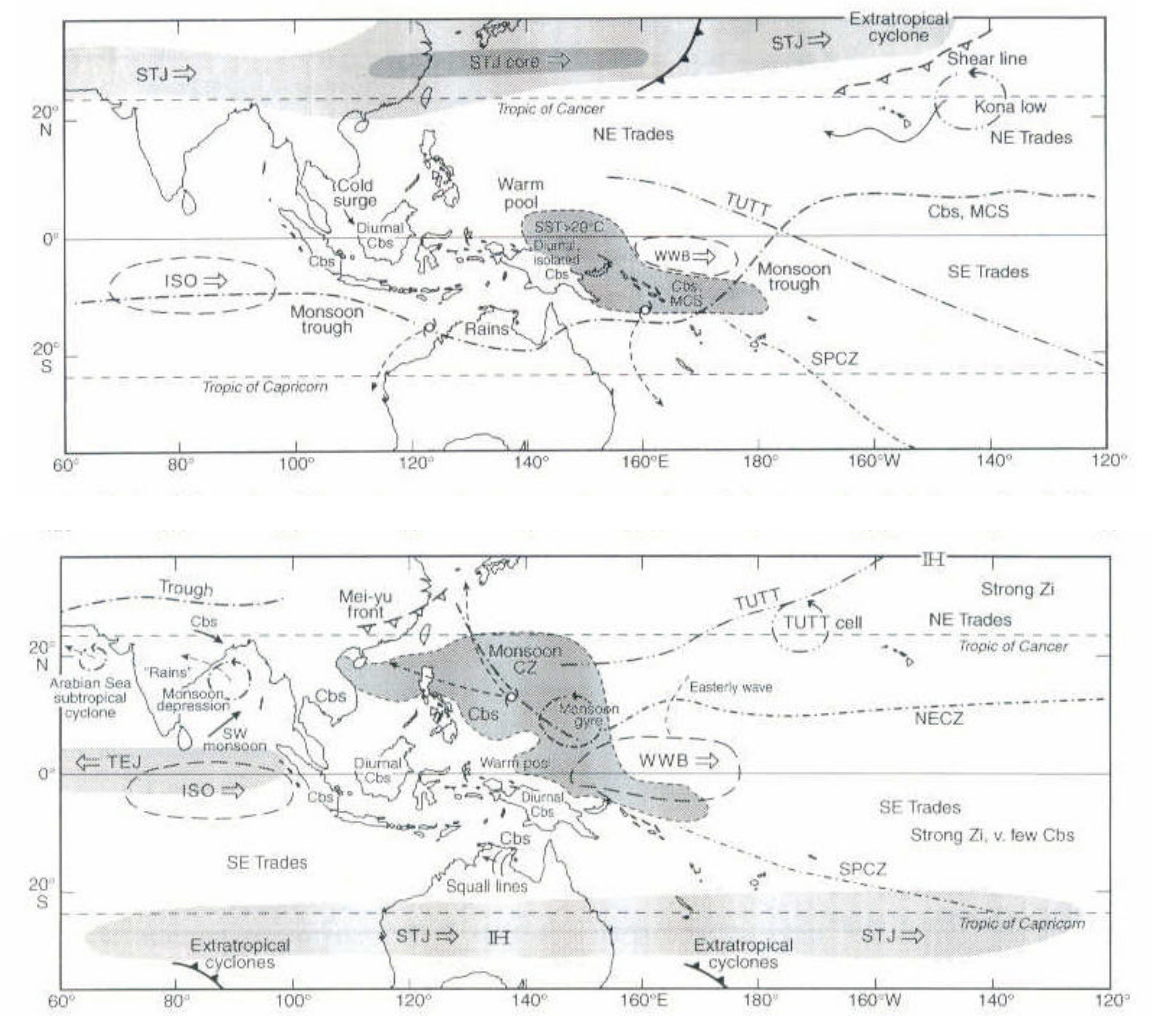

Figure 4. Semi-permanent synoptic-scale phenomena in the tropical Pacific for January (top) and July (bottom) (after Barnes 2001).

The position and strength of the subtropical highs (Figure 5) and resulting trade wind inversions have a major influence on convection in the tropics. On the western side of ocean basins, the influence of the subtropical highs is diminished and more substantial convective clouds increase in frequency (Barnes 2001).

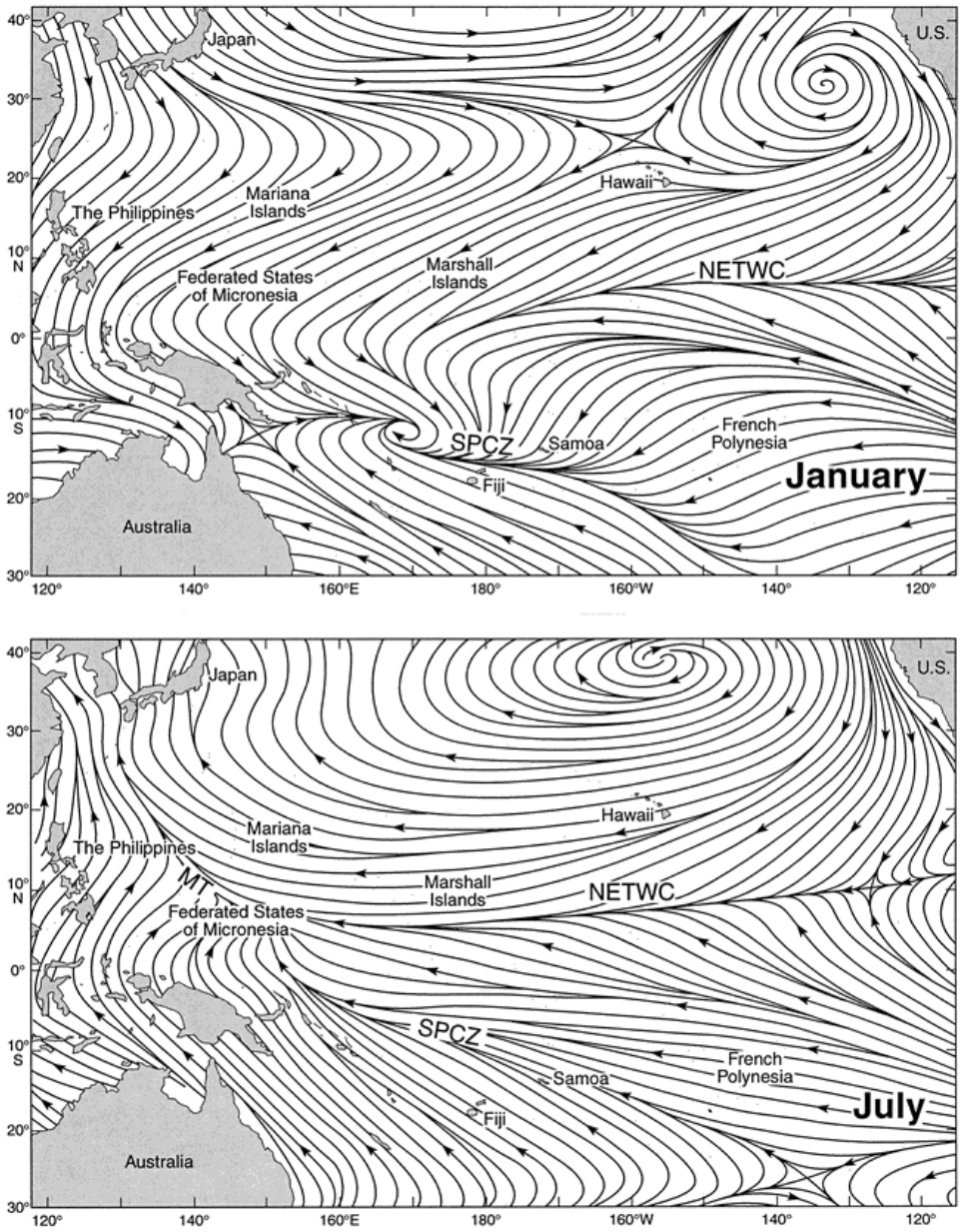

Figure 5. Streamlines over the Pacific for January (top) and July (bottom). Subtropical highs are centered in the middle of anticyclonic circulations (after Sadler et al. 1987).

Two main types of tropical convection climatology are available: i) outgoing longwave radiation (OLR), and ii) lightning (Figure 6). Both types are detected by meteorological satellites and yield similar results.

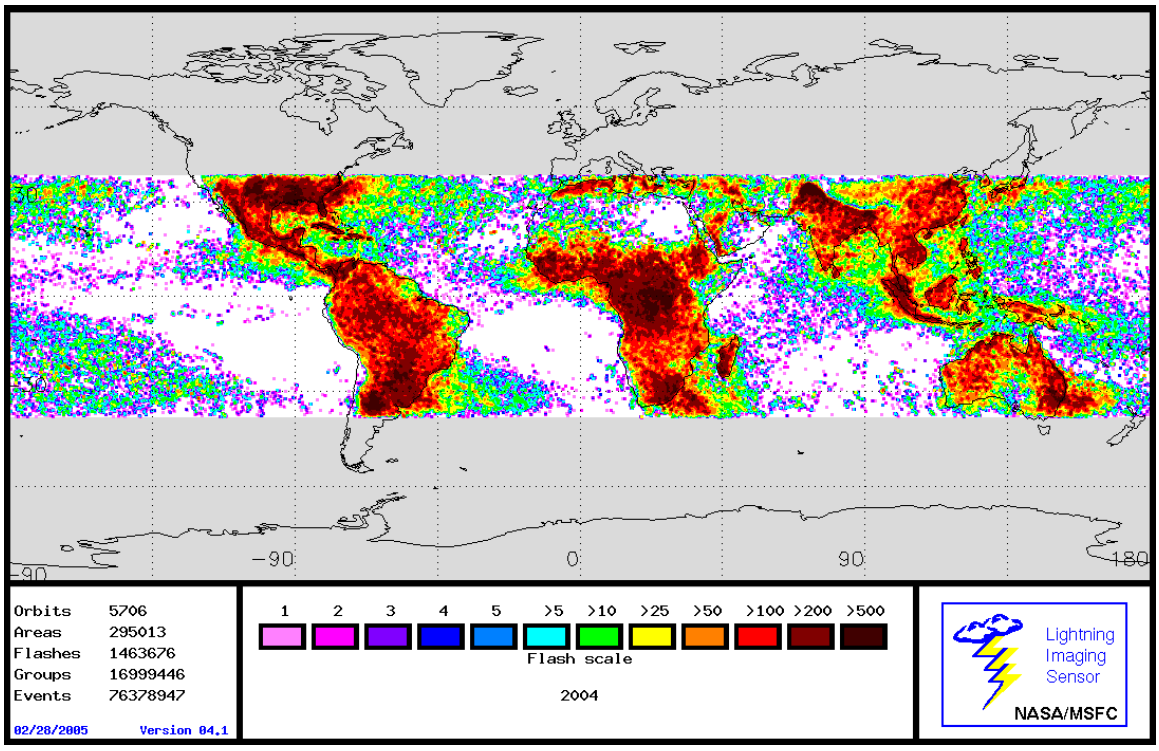

Figure 6. Lightning strikes detected by Tropical Rainfall Measuring Mission (TRMM) Lightning Imaging Sensor (LIS) for the period January 2004 to December 2004 (from NASA/MSFC, http://thunder.msfc.nasa.gov/data/query/distributions.html).

Convection in the tropics occurs much more frequently over land than over ocean. Presumably, this is because of greater surface heat fluxes, which leads to increased instability over land. Still, there is a general lack of mesoscale severe weather (winds = 50 kt, hail = ¾ inch, tornadoes, or funnel clouds) in the tropics (Barnes 2001).

Over tropical oceans, convection occurs less frequently. However, the ocean accounts for a much larger area of the tropics and most military bases in the tropics are on islands in primarily oceanic environments. Fortunately, Barnes (2001) suggests only the Near Equatorial Convergence Zone (NECZ) supports a thunderstorm frequency of more than 20 days per year.

C. OBSERVING MESOSCALE TROPICAL CONVECTION

To detect and analyze tropical DMC, observations are required on specific time and spatial resolutions. Observations must be taken at least hourly to detect single isolated cells with life cycles on the order of an hour. Spatially, the observations must

resolve the diameter of a cumulonimbus, which is only a few kilometers. Due to their greater size, MCSs can be resolved by coarser resolution observations.

Tropical DMC is manifest in several meteorological parameters. First, the convective overturning of the atmosphere causes vertical motion, horizontal motion, and turbulence. Adiabatic or pseudo-adiabatic cooling during ascent leads to condensation, latent heat release, and precipitation. During field experiments, microphysical processes may be observed by various non-operational methods.

1. Surface-Based Observations

Opportunities to observe convection in the tropics from the surface are limited at best. Large expanses of the tropics are ocean, with only a few widely-spaced islands from which to make observations. A small fraction of those islands report surface weather observations and even fewer conduct weather radar surveillance. Likewise, surface-based lightning detection systems are sparse in the tropics. Over the open ocean far from island-based sensors, surface observations are often simply not possible. Fine-scale surface meso-networks such as those in the midlatitudes are not practical over the ocean. With these limitations, perhaps the best means of observing tropical convection is via remote sensing techniques and meteorological satellites in particular.

2. Conventional Remote Sensing

Sensors onboard meteorological satellites (hereafter referred to as satellites) have capabilities uniquely suited for observing the tropical environment. Satellite sensors can monitor much larger areas than surface-based sensors. Satellite sensors are also less hindered by cloud and precipitation obscurations through use of multi-spectral techniques. Additionally, multiple satellites in various orbits provide complete coverage of the earth's surface with a wide range of time and spatial resolutions. All areas, even sparsely populated tropical regions, are routinely observed by satellites.

Despite the many different types of satellite sensors, the majority collect data as passive receivers of electromagnetic radiance emanating from the earth/atmosphere-system. Most geostationary satellites possess sensors for visible and infrared (IR) wavelengths. Satellites in low-earth-orbit (LEO) often possess additional sensors for microwave wavelengths. A few LEO satellites have been equipped with lightning detection capabilities (Christiansen et al. 1999), but their sampling is too short and

infrequent to be of operational use. The National Oceanic and Atmospheric Administration (NOAA) is planning future geostationary satellites that will have lightning detection capabilities, but the technology is not yet mature. Therefore, operational forecasters currently rely primarily on visible, IR, and microwave data.

Visible and IR satellite sensors provide information on cloud brightness, shape, opacity, temperature, and height, which can then be used to deduce additional information about the cloud (Barnes 2001). Microwave sensors, which better detect emission by precipitation, can provide more direct information on liquid and ice water content. Used together, data from all three wavelengths provide useful--but incomplete--information about tropical convection.

A problem central to observing and classifying convection is how to measure it. Satellite sensors cannot directly measure the vertical motion in convection. Therefore, convection must be inferred from sensible weather accompanying it. At operational military weather units, techniques of observing and classifying convection are often limited to interpreting visible and IR images. Unfortunately, manual interpretation can lead to misidentification and misclassification, especially by less-experienced personnel. Visual determinations of what is a rain shower and what is a thunderstorm are subjective, even using IR enhancement curves. For critical operational decisions, a more objective technique is needed.

3. NRL Blended Rainrate Technique

A possible solution for observing tropical DMC has recently been developed. The Naval Research Laboratory (NRL) Blended Rainrate Technique (Turk et al. 2003) creates a rain accumulation product (Figure 7) that could serve as a reliable, quantifiable proxy for convection. The Blended Rainrate Technique is a three-step process that uses data from both geostationary and LEO satellite sensors. First, rainrates are determined using geostationary IR data with a lookup table that is based on the assumption that rainrates are inversely proportional to cloud-top temperatures. Second, these rainrates are calibrated with available LEO passive microwave data. Finally, adjustments are made for growth, decay, and orographic effects.

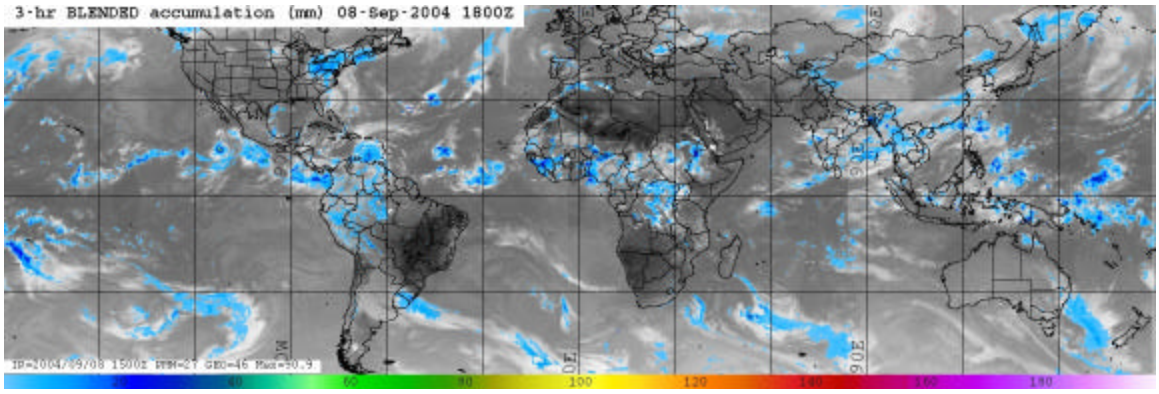

Figure 7. Sample NRL Blended Rainrate 3-hr accumulation product (from NRL, http://www.nrlmry.navy.mil/training-bin/training.cgi).

The NRL Blended Rainrate Technique has many advantages for observing tropical convection. The geostationary IR data provides at least half-hourly sampling, which allows frequent, timely measurements. Additionally, the use of LEO microwave data improves accuracy by calibrating lookup tables on a 2-degree lat./long. outer mesh and ¼-degree lat./long. inner mesh. This technique surpasses the inaccurate, traditional geostationary rainrate method of applying the same lookup table across the full disk regardless of differences in regions, seasons, and weather regimes. Thus, the NRL Blended Rainrate Technique leverages the best qualities of both geostationary and LEO remote sensing sources while minimizing the deficiencies of each.

A major limitation of the technique is the assumption that colder cloud tops have greater rainrates. Sometimes, heavy precipitation falls beneath warm cloud tops, or no precipitation falls beneath cold cloud tops (i.e., thick cirrus clouds). However, that key assumption is more likely to be true in the tropics (Turk et al. 2003) and thus the Blended Rainrate Technique may be effective for tropical convection. Other drawbacks to the technique are difficulty in estimating orographic precipitation and the uncertain relation between convective intensity and rainrate. While it is assumed that more intense convection has stronger updrafts that produce higher rainrates, discriminating thunderstorms from heavy rain showers may be difficult.

D. FORECASTING MESOSCALE TROPICAL CONVECTION

1. Persistence

Because of the relative rarity of tropical oceanic convection mentioned above, a possible forecasting method is to assume persistence of the current conditions. Forecasting "no convection" when there is currently no convection will verify correctly the majority of the time. However, this technique is guaranteed to never correctly forecast the onset or the termination of convection, which are both significant events for military operations. Whereas the persistence forecast may positively influence verification scores, it does nothing to aid the goal of risk management.

2. "Progging"

A second method of forecasting tropical convection is "progging," or timing arrival based on current movement. This method hinges on the premise that mesoscale convection will maintain its intensity and course, which allows a prediction based on advection over a location. Progging has an advantage over persistence in that progging allows a change to be forecast when convection exists upstream. Unfortunately, progging will not be accurate during situations of convective initiation or dissipation. To deal with situations in which convection forms or decays close to a location, another method is necessary.

3. Nowcasting

A third possibility is to develop very short-range (0-2 hours) forecasts, or "nowcasts," using multiple data sources. By combining radar, satellite, and surface weather observations, forecasters can detect and track boundary layer convergence lines and thus predict where they may interact to initiate convection (Wilson et al. 2001). Some researchers (Fox et al. 2004) have attempted to make nowcasting predictions more objective by using complex automated tracking algorithms. For the vast majority of tropical locations, observations are too scarce to effectively nowcast convection.

4. Numerical Weather Prediction (NWP)

A fourth option is to rely on numerical weather predictions (model forecasts) of convection. While this may seem attractive at first, several problems occur in using model forecasts of mesoscale convection. First, most models covering the central and western North Pacific are synoptic-scale global models. Whereas Global model

resolution may be adequate for forecasting aspects of synoptic-scale features (i.e., tropical cyclones), it is not optimal for resolving mesoscale convective weather systems. Even higher-resolution mesoscale models, such as the Air Force Weather Agency (AFWA) Mesoscale Model, version 5 (MM5) model with 45 km or 15 km resolution must parameterize convection.

Second, the parameterizations techniques are inflexible. The model parameterization of convection is used over the entire model domain, with no adjustments for individual locations. This "broad-brush" approach neglects important local factors that can affect mesoscale convection.

Finally, some model (e.g., AFWA's MM5) forecasts of convection rely heavily on a few mid-latitude convective indices and thresholds that are unproven in the tropics, which often cause the model to over-forecast areas of convection and leads to false alarms. Rather than tying the forecast of convection to a single index or limited set of indices implied in the parameterization technique, perhaps a better method would be to let the model calculate many indices and let operational forecasters use the most applicable one for a given time and location.

5. Convective Indices

Convective indices are a widely used method of quickly and easily diagnosing convection (Doswell 1996). Operationally, they help to focus attention on places and times that convection is likely to occur. Additionally, some indices attempt to diagnose the intensity of the convection.

Convective indices can be broadly classified into three groups. Thermodynamic indices measure buoyancy, as determined by moisture and/or conditional instability. Kinematic indices relate to vertical motion, as determined by parcel speed or direction. Combined indices measure both buoyancy and motion. Common indices for thermodynamic, kinematic, and combined indices are the lifted index, helicity, and the SWEAT index (see Appendix A for definitions).

Thermodynamics and kinematics each play a part in tropical convection. According to Raymond (2001), thermodynamic processes act to develop instability, which is then released by mechanical (kinematic) processes. In other words,

thermodynamics prime the atmosphere and then kinematics initiate convection. Kodama and Businger (1998) elaborate that the thermodynamics operate primarily on the synoptic scale, while the kinematics operate primarily on the mesoscale.

While convective indices can certainly be useful, they must be used with caution. Applicability of a convective index depends on specific conditions being satisfied. First, an index should be physically related to the process causing the convection. Second, an index should be used for the situation (geographic, synoptic, etc.) for which it was designed. Finally, an index should include as much relevant information as possible from the upper-air data and not just the mandatory levels of rawinsondes.

Field studies have been organized to quantify the important physical processes for certain situations. In the tropical western Pacific, low-level moisture was shown to have the strongest correlation (out of 10 environmental variables) to subsequent convection (Sherwood 1999). Also in the tropical Pacific, Barnes (2001) found strong low-level wind shear allows development of squall lines with wind speeds approaching 50 kt. Lucas et al. (1994) hypothesized that the shape of the Convective Available Potential Energy (CAPE) determines updraft intensity. This idea was extended by Blanchard (1998).

E. OWS FORECASTS OF MESOSCALE TROPICAL CONVECTION

1. Tools and Techniques

Currently, the 17th OWS and 20th OWS, who are responsible for forecasting in the central and western North Pacific, do not use a single, documented technique to forecast convection. Instead, duty forecasters are given sparse guidance and thus have permission to choose a method they think works best. Often, the forecasters rely upon past experience, although this experience is often limited to three years or less. The standard operating procedures (SOPs) suggest two methods as a starting point.

a) K Index

The Standard Operating Procedures (SOPs) of the 17th OWS (2005) describe a method used to forecast thunderstorms over the central and southwestern Pacific and Indian oceans. This method is a combination of K index and upper-level divergence. Using Global Forecast System (GFS) model data, a forecaster outlines potential areas of thunderstorms where the K index is greater than 30°C and the 200 mb

winds are divergent. Additional factors that forecasters consider are satellite imagery, surface weather observations, and observed/forecast skew-Ts, as well as the Joint Typhoon Warning Center (JTWC) and other regional military weather forecasts.

The K Index/Divergence method is likely to identify areas that are "primed" for convection by synoptic-scale processes. The K Index takes into account instability and low-level moisture. The 200 mb (upper-level) divergence takes into account areas favored for synoptic-scale ascent with the assumption of mass continuity. However, the method will not identify specific locations where cells will form within that area, because mesoscale lifting features cannot be resolved by the GFS. Therefore, the method will over-forecast areas of thunderstorms. These broad areas of forecast thunderstorms are likely to be of minimal utility to operations personnel.

b) Moisture Convergence

The method utilized by the 20th OWS (S. Kammerer, personal communication, 2005) is a combination of low-level streamlines, upper-level divergence, and low-level moisture convergence. Data are from the Navy Operational Global Atmospheric Prediction System (NOGAPS) (winds) and MM5 (moisture convergence) models. Additional factors that forecasters consider are satellite imagery, 500 mb vorticity, forecast skew-Ts, low-level wind speeds (= 15 kt) and coincidence of four stability indices (see appendix A for definitions): TT = 47, LI = 0, CAPE = 1000, and SSI = 0.

The 20th OWS moisture convergence method may work because moisture flux convergence is directly proportional to the horizontal mass convergence field (Banacos and Schultz 2005), which helps identify boundaries between different air masses. This is of questionable utility to the deep tropics, but could have some utility closer to the subtropical highs especially in winter.

2. Products and Verification

Verification of OWS products (TAFs, charts, etc.) that are based on these two convective forecasting methods is quite limited. No verification is conducted for the convection forecast in the TAFs. The FITL thunderstorm chart verification is conducted subjectively for only a fraction of the Area of Responsibility (AOR) at only one forecast hour and at extremely coarse spatial resolution. Specifically, one chart for one time per

day is verified manually. The forecast is verified as correct, if convection is forecast anywhere in a 10° lat. by 10° long. box and indications of convection are observed anywhere in the box (not necessarily at the same locations).

Central to any discussion of forecasting capability is the subject of predictability, i.e., what is the theoretical limit for forecasting convection? In an excellent discussion of the predictability of mesoscale phenomena, Anthes (1986) states that that mesoscale weather systems have considerably less predictability than synoptic-scale systems. Also, the type of convection (forcing mechanism) affects predictability. The MCSs forced by surface inhomogeneities (squall lines, etc.) may be more predictable than an isolated thunderstorm in a region of instability. Anthes optimistically hypothesizes that some mesoscale phenomena forced by large-scale flows and surface inhomogeneities may be skillfully forecast up to 1-3 days. However, that hypothesis assumes synoptic-scale features and surface inhomogeneities are perfectly predicted—neither of which is true for the current state of forecasting or modeling.

3. Areas for Improvements

Although not ideal, the use of convective indices to forecast tropical convection has many advantages. Indices are easily calculated from both observed and forecast upper-air data. Since such indices have been used for many decades, forecasters readily understand them. Perhaps most importantly, convective indices help forecasters eliminate situations unfavorable for convection and thereby focus their attention on more favorable situations. This helps to reduce the amount of information overload—a serious problem in today's operational weather centers.

Some problems exist with how the indices are currently used. Kodama and Businger (1998) and Ramage (1995) claim wholesale that conventional indices do not perform well in the tropics. Forecasting documents for tropical locations such as 17 OWS FRNs, etc., do not cite many verification studies. It is clear that an objective study is needed to help forecasters use the best index, if any, in a given situation. Additionally, verifications are needed using both surface weather observations (for point forecasts) and NRL Blended Rainrate data (for area forecasts). The following verification study was performed in an effort to meet those needs.

THIS PAGE INTENTIONALLY LEFT BLANK

III. METHODOLOGY

A. GOAL OF STUDY

The goal of this study is to find the convective index that best predicts initiation of deep convection in the central and western tropical Pacific for a given situation. Situations are classified by geographic location and time, with the assumption that similar situations will support convection within similar environments. Also, classifications of location and time may partially account for local mesoscale effects that can significantly affect development of convection.

B. STUDY PARAMETERS

1. Geographic Locations

Five island locations (Figure 8) in the tropical Pacific were chosen for this study—three in the western Pacific and two in the central Pacific. The western Pacific locations were Naha (ROAH) on the island of Okinawa, Agana (PGUM) on the island of Guam, and Kwajalein (PKWA) on Kwajalein Atoll. The central Pacific locations were Lihue (PHLI) on the Hawaiian island of Kauai and Hilo (PHTO) on the Hawaiian island of Hawaii (the "big island").

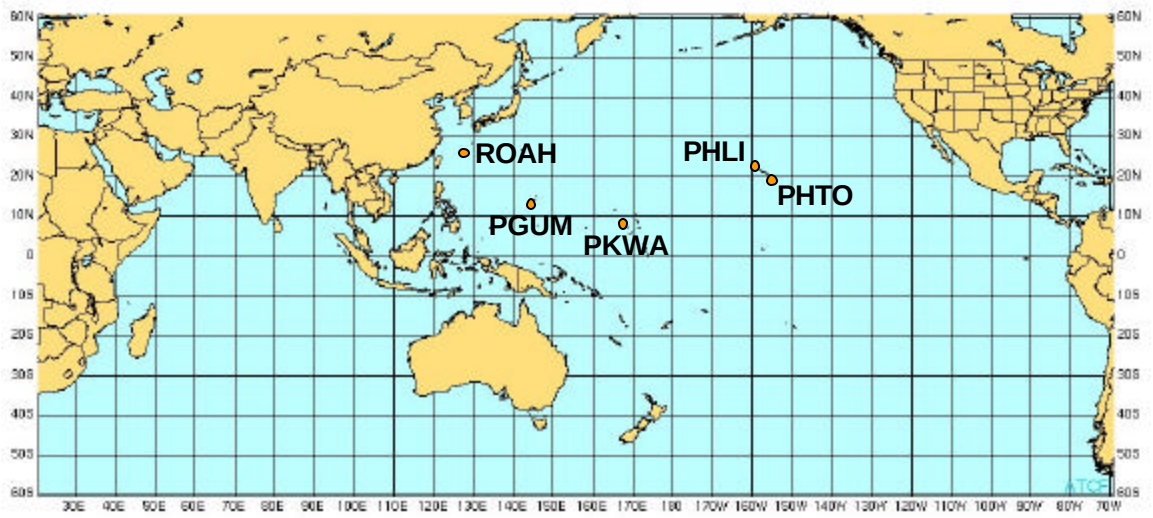

Figure 8. Geographic locations included in this study.

Table 1. Summary of location information.

	ROAH	PGUM	PKWA	PHLI	PHTO
Region:	WPAC	WPAC	WPAC	CPAC	CPAC
Lat./Long.:	26.20N 127.65E	13.47N 144.77E	8.72N 167.72E	21.97N 159.32W	19.72N 155.05W
Elevation (ft):	20	246	26	105	33
Island Size:	Medium	Medium	Small	Medium	Medium
Summer:	1 Apr-30 Sep	1 Jul-30 Nov	1 Jun-31 Dec	1 May-30 Sep	1 May-30 Sep
Winter:	1 Oct-31 Mar	1 Dec-30 Jun	1 Jan-31 May	1 Oct-30 Apr	1 Oct-30 Apr
Day (UTC):	2100-0859	2100-0859	1800-0559	1800-0559	1800-0559
Night (UTC):	0900-2059	0900-2059	0600-1759	0600-1759	0600-1759

These five locations were chosen based upon several criteria. First, they are all within the 17th OWS and the 20th OWS areas of responsibility. Second, they all conduct rawinsonde (upper-air) and surface weather observations. Finally, all locations are within close proximity to U.S. military bases. While individual locations may experience their seasons at slightly different times of year (Table 1), they experience similar weather within the same season, particularly summer.

a. Agana

Agana/Guam International Airport (PGUM) was chosen for its proximity to Andersen Air Force Base. Agana is located on the island of Guam, which is approximately 35 miles long and 5-10 miles wide. Guam local time is ten hours ahead of Universal Coordinated Time (UTC). Guam experiences two seasons: Summer (wet season) from early July to late November and Winter (dry season) from early December to late June (17 OWS FRN 2005). For the purposes of this study, the following time segments were used to determine Guam classifications: i) Daytime from 2100 to 0859 UTC (0700-1859L); ii) Nighttime from 0900 to 2059 UTC (1900-0659L); iii) Summer from 1 July to 30 November; and iv) Winter from 1 December to 30 June.

b. Lihue

Lihue (PHLI) was chosen for its proximity to Hickam Air Force Base, which is approximately 60 miles away on the nearby island of Oahu. Lihue is on the island of Kauai, which is approximately 33 miles long and 25 miles wide. Hawaiian local time is ten hours behind UTC. Lihue experiences two seasons: Summer (dry season) from early May to late September and Winter (wet season) from early October to late April (17 OWS FRN, 2005). For the purposes of this study, the following time segments were used to determine Lihue classifications: i) Daytime from 1800 to 0559 UTC (0800-1959L); ii) Night Time from 0600 to 1759 UTC (2000-0759L); iii) Summer from 1 May to 30 September; and iv) Winter from 1 October to 30 April.

c. Hilo

Hilo (PHTO) was chosen for its proximity to Bradshaw Army Air Field. Hilo is on the island of Hawaii, which is approximately 93 miles long and 76 miles wide. Local times and seasons are the same as Lihue.

d. Kwajalein

Kwajalein (PKWA) was chosen for its location within the Ronald Reagan Ballistic Missile Defense Test Site. Kwajalein is on Kwajalein Island, which is approximately four miles long and one mile wide. Kwajalein local time is 12 hours ahead of UTC. Kwajalein experiences two seasons: Summer (wet season) from early June to late December and Winter (dry season) from early January to late May (RTS website 2005). For the purposes of this study, the following time segments were used to determine Kwajalein classifications: i) Day Time from 1800 to 0559 UTC (0600-1759L); ii) Night Time from 0600 to 1759 UTC (1800-0559L); iii) Summer from 1 June to 31 December; and iv) Winter from 1 January to 31 May.

e. Naha

Naha (ROAH) was chosen for its proximity to Kadena Air Base. Naha is on the island of Okinawa, which is approximately 65 miles long and 2-15 miles wide. Naha local time is nine hours ahead of UTC. Naha experiences two seasons: Summer (wet season) from early April to late September and Winter (dry season) from early October to late March (AFCCC summary 1999). For the purposes of this study, the following time segments were used to determine Naha classifications: i) Daytime from

2100 to 0859 UTC (0600-1759L); ii) Nighttime from 0900 to 2059 UTC (1800-0559L); iii) Summer from 1 April to 30 September; and iv) Winter from 1 October to 31 March.

2. Period of Study

Data from August 2004 to July 2005 were used for this study. The starting and ending times were chosen primarily to coincide with available data archives. The use of an entire year of data accounted for seasonal variations in convection. Within the year, data were categorized by season (summer or winter) and time of day (day or night). While some data from the time period were missing, the vast majority were available and utilized.

August 2004 to July 2005 was classified by the Climate Prediction Center as a weak El Nino episode. In general, El Nino acts to increase convection in the central Pacific and decrease convection in the western Pacific. Although interannual effects might be considered with a longer record, any changes in the observed amount of convection due to El Nino should also be reflected in the environmental predictor data.

C. HYPOTHESIS AND STRUCTURE OF STUDY

1. Hypothesis

In keeping with the goal of this study, various predictors were chosen to test for skill in predicting the initiation of convection. Following Haklander and Van Delden (2003) and Sherwood (1999), several indices were chosen as predictors of convection (see Appendix A). The hypothesis is that the components of the index (moisture, wind speed, etc.) will determine the forecast skill, and that one component will have more skill than the others.

Although Haklander and Van Delden (2005) evaluated convective events in the mid-latitudes, the basic structure of their study could be applied to tropical data. The predictors (indices) were calculated from rawinsonde data. It is assumed that the sampling error of the rawinsondes is negligible compared to the range of index values. The predictands (whether or not convection occurred) were determined from subsequent observations. Although this study was focused on convective initiation, observations were also used to establish the convective state prior to the rawinsonde.

Several differences distinguish this study from that of Haklander and Van Delden (2005). First, the number of predictors investigated is different. This study evaluated 18 predictors at five separate locations, compared to the 32 predictors at only one location used by Haklander and Van Delden (2005). Second, the predictands (ground truth) are significantly different. Whereas Haklander and Van Delden utilized synoptic (6-hourly) weather observations as their predictands, this study utilizes hourly surface weather observations. The advantages of surface weather observations are that they are obtained at a finer time resolution and they contain more detailed descriptions of weather parameters.

While Haklander and Van Delden only utilized one predictand, this study utilizes a second predictand, which is the NRL Blended Rainrate data. Ground truth of tropical convection is difficult to determine because of the limited surface observing network. In areas where there are no surface observations, NRL blended rainrate data can serve as a proxy for convection. This second predictand will be necessary in the future for verification of area forecasts over data-sparse areas.

2. First Predictand: Surface Weather Observations

To use surface weather observations as a predictand of convection, it is assumed that the majority of the precipitation in the tropics results from convection. Although precipitation does fall from stratiform clouds in the tropics, these stratiform clouds are often remnants of convective cells at the end of their life cycle (Houze 1997). Therefore, most precipitation in the tropics may be broadly generalized as convective precipitation, which allows precipitation to be used as an indicator of convection.

It was also assumed that thunderstorms are a special subset of convective precipitation. In particular, updraft speeds must be strong enough to support mixed-phase water that permits electrification that leads to lightning. Observational studies (Rutledge et al. 1992, Williams et al. 1992) have demonstrated that lightning increases with updraft speeds, although no single threshold value will perfectly discriminate thunderstorms from rain showers. However, it can be assumed that thunderstorm updrafts are relatively stronger than rain shower updrafts, which in turn are stronger than ascent in stratiform clouds. In other words, convective intensity increases from (stratiform) rain to showers to thunderstorms.

The highly-variable time resolution of surface weather observations made their use challenging. While surface weather observations could theoretically be taken as often as once per minute in fast-changing conditions, observation frequency is usually a few times per hour. At a minimum, surface weather observations are taken hourly (FMH-1 2005). With the minimum frequency of an hour as a guide, surface observations were binned into 1-hour time blocks.

Within each hour, all observations were examined and the hour was classified according to the weather reported in the present weather or remarks (on station or vicinity). If at least one observation reported thunderstorms or lightning (TS or LTG), the hour block was coded with a 3. If at least one observation reported showers (SH), the hour block was coded with at 2. If at least one observation reported rain (RA), the hour block was coded with a 1. If none of the above conditions were met, the hour block was coded with a 0.

After each 1-hour block was coded, the information from individual hour blocks was combined into eight 3-hour blocks: 0000-0259 UTC, 0300-0559 UTC, 0600-0859 UTC, 0900-1159 UTC, 1200-1459 UTC, 1500-1759 UTC, 1800-2059 UTC, and 2100-2359 UTC. Within each 3-hour block, the 1-hour blocks were examined to determine the maximum code of the three (ranging from 0 to 3) and the 3-hour sum of the one hour blocks (ranging from 0 to 9). These codes could then be used to quickly and efficiently describe convective intensity, duration, and cumulative effects. For example, an hour of showers followed by an hour of thunderstorms followed by an hour of rain would have hour blocks coded 2/3/1, a maximum convective type of 3, and a 3-hour sum of 6. By contrast, three straight hours of showers would also have a 3-hour sum of 6, but hour blocks would be coded 2/2/2 with a maximum convective type of 2.

3. Second Predictand: Rainrate Data

In addition to the surface observations, the NRL Blended Rainrate 3-hour accumulations were also examined for signs of convection. These data were available as accumulation amounts (mm h^{-1}) at ¼ degree spatial and 3-hour time resolutions, and were related to, but significantly different from, the surface weather observations. For each of the five locations, the ¼ degree box containing the location was examined, as well as the eight surrounding boxes for a total area of nine boxes. The nine-box area was used so

that rainrate could be more easily compared to surface weather observations, which sometimes report distant convection (beyond the 7.5 nautical miles from the center of a ¼ degree box). The maximum rainrate value and the average over the nine-box area were calculated for each 3-hour time bin.

More information than precipitation accumulation amounts was required. Convection type, as coded in the surface weather observations, was also desired information. To determine what rainrates from the Blended Rainrate data were representative of rain, showers, and thunderstorms, rainrates were thresholded and compared with surface weather observations during the same 3-hour period.

It was assumed that rainrates were a function of both convection intensity and duration. Therefore, a boxplot was created for different categories of intensity and duration, as determined by the maximum convective type and 3-hour sum from the surface observations (Figure 9). By using the median values for no convection cases (0/0), convective rain or showers cases (1:3/1:2 and 4:6/1:2), and thunderstorm cases (3/3, 4:6/3, and 7+/3), thresholds of >0 and >2.3 were determined for convective precipitation and thunderstorms, respectively.

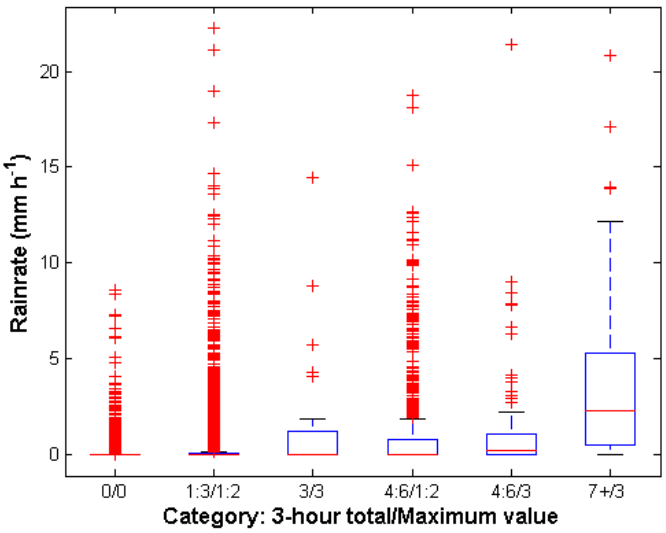

Figure 9. Box plots of NRL Blended Rainrate values as a function of convective duration and intensity. The box defines the middle 50% of the data (interquantile range, IQR). Whiskers are defined as 1.5 times the IQR or the maximum or minimum value. Extreme points are defined by plus signs outside the whiskers.

4. Predictors: Indices

All indices were calculated from rawinsonde (upper-air) observations. It was assumed that the rawinsonde sampled the environment at the reporting time, although some flexibility is allowed in rawinsonde operations (FCM-H3-1997). It was also assumed that the environment measured by the rawinsonde did not significantly change within 3 hours. This assumption is aided by the restriction that no convection could be occurring during or prior to the rawinsonde.

Originally, 36 indices were considered for evaluation. Due to concerns of overfitting and practicality, the list was reduced to 18 indices (see Appendix A). For example, the Thompson Index was considered but eventually discarded as its components of the K Index and Lifted Index were already selected.

Several criteria guided the selection of the indices. Some were chosen due to their ongoing use by the 17th and 20th OWSs (K Index, Total Totals Index, etc.). Others were chosen due to their physical relation to convective processes (CAPE, CIN, etc., see Appendix A). Yet others were chosen based on their established performance in the mid-latitudes (SWEAT, wind shear, etc.) for comparison purposes in the tropics. A few indices that utilized layer averages (low-level temperature, mid-level relative humidity, etc.) were chosen due to the previous work of Sherwood (1999). For those layer averages, low-level was defined to be surface to 850 mb, mid-level was defined to be 700 to 500 mb, and high-level was defined to be 300 to 200 mb.

Indices were categorized into one of three groups: thermodynamic, kinematic, or combined. Thermodynamic indices were those indices that measured a parcel's potential energy state, such as the Lifted Index. Kinematic indices were those indices that measured a parcel's kinetic energy state, such as the wind speed. Combined indices were those indices that measure both potential and kinetic energy, such as the SWEAT index.

Indices were also be categorized by the influence of their components. Indices with similar components should perform similarly. For example, both low-level relative humidity and mid-level relative humidity share the component of moisture. If moisture is responsible for convection, both indices should be good predictors and exhibit forecast

skill as compared to indices with other components. For indices with multiple types of components, one was chosen as the primary influence.

D. DATA SOURCES AND FORMATS

The three data types came from three sources in three formats. First, rawinsonde data were obtained from the University of Wyoming web site in decoded tables. Surface weather observations were obtained from the Air Force Combat Climatology Center (AFCCC) in raw form. Finally, blended rainrate data was obtained from NRL in binary format.

E. DATA PROCESSING

Three FORTRAN programs were utilized to read the data and create output files. The sonde-reader program was downloaded from the website http://ocw.mit.edu/OcwWeb/Earth--Atmospheric--and-Planetary-Sciences/12-811Spring-2005/Tools/index.htm and subsequently edited to meet the needs of this study. The observation-reader program was written by Dr. Patrick Harr for the purposes of this study. The rainrate-reader program was written by Dr. Joe Turk of NRL-Monterey and subsequently edited to meet the needs of this study. Each program contained rudimentary error-checking procedures for unrealistic or missing data. All programs created output text files of predictor or predictand information. The text was then quality-controlled.

F. QUALITY CONTROL

Quality control was performed in three ways. First, incomplete data (resulting from abbreviated rawinsondes, only mandatory levels, etc.) were removed. Next, erroneous data (resulting from unrealistic temperatures, winds, etc.) were removed. Finally, garbled information (missing a "Z" after the time, etc.) was corrected and evaluated, if possible. Data were then input into a Microsoft Access database for easy manipulation.

G. DATA ORGANIZATION

To compare the predictors and predictands, time sequencing and establishment of time coincidence was required. Complicating matters, all three data types (rawinsondes, surface observations, and rainrate data) were collected at different time resolutions. By assuming that the rawinsondes were instantaneous measurements at the reporting times, predictor information was set to 00 UTC or 12 UTC (or 06 UTC, 18 UTC, or other times,

if available). Predictand (surface observations and rainrate) information was then examined for 3 hours before and 3 hours after the rawinsonde.

The environment type of each rawinsonde was determined from the observations 3 hours before and 3 hours after the rawinsonde reporting time. If no convection occurred 3 hours before or after the sonde report time, the environment was classified "non-convective." If no convection occurred within 3 hours before but some occurred within 3 hours after, the environment was classified "pre-convective." Pre-convective was further be subdivided into pre-rain and pre-thunderstorms. If convection occurred both within 3 hours before and within 3 hours after the sonde report time, the environment was classified "continuing convection." If convection occurred within 3 hours before but no convection occurred within 3 hours after, the environment was classified "ending convection." If the environment could not be determined due to missing data, the environment was classified "unknown/missing." Because the two predictands reported convection independently, there were two environment classifications for each 3-hour period: one by surface observations and one by rainrate.

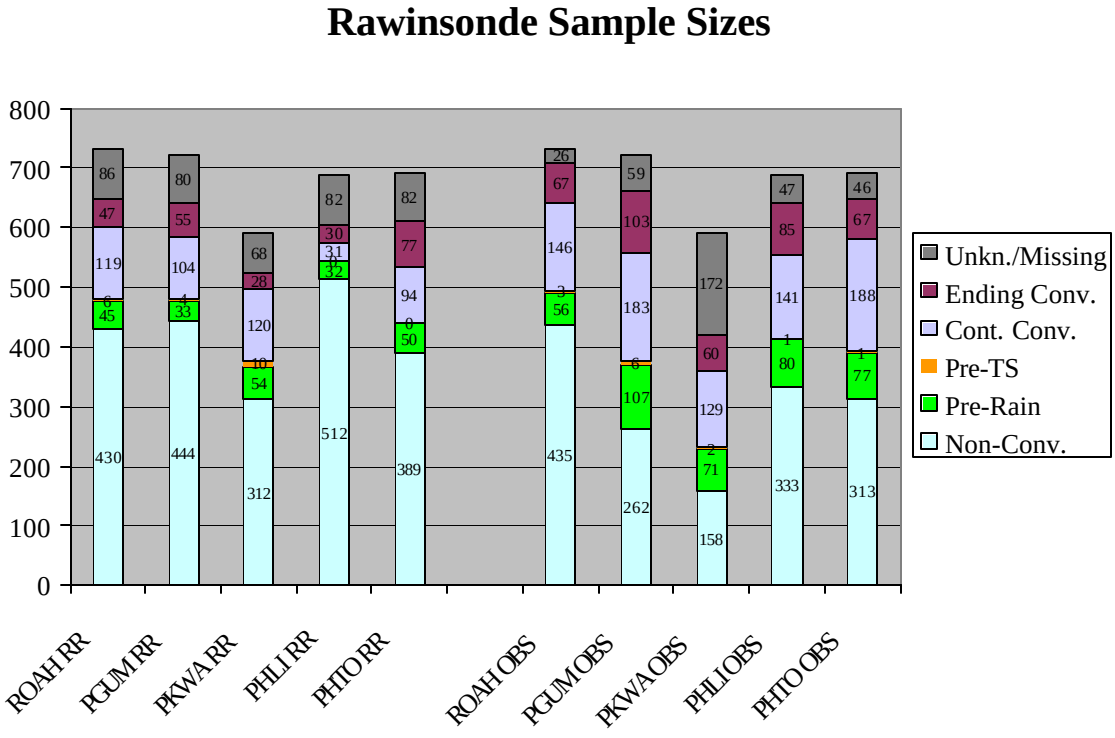

Figure 10. Rawinsonde sample sizes categorized by location and environment type

H. SAMPLE SIZES

The final rawinsonde sample sizes, which are used in the analysis and results, are displayed above (Figure 10).

Several problems became apparent with the predictand data sets. First, there were very few thunderstorm cases within 3 hours following rawinsondes (Figure 11). Additionally a strong bias appeared as to how precipitation was reported in surface weather observations. It is unlikely that three locations (PGUM, PHLI, and PHTO) nearly always receive stratiform rain while the two other locations (ROAH and PKWA) overwhelmingly receive convective rain showers. Instead, a human bias may exist in reporting precipitation, possibly caused by training differences. Finally, a delay appeared in the satellite-derived rainrate detection of convection. Pre-convective rainrate assessments were confirmed by surface observations only 18% of the time (Table 2); more often (33% of the time) the surface observations assessed continuing convection.

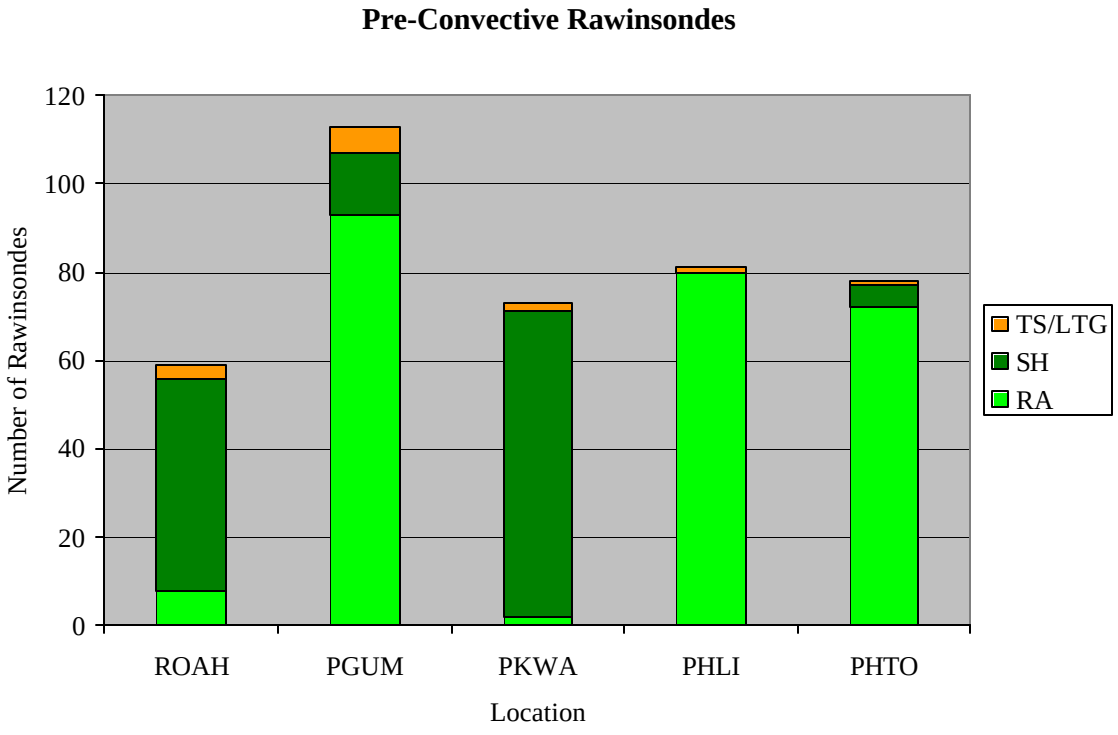

Figure 11. The frequency of pre-convective rawinsondes reported by max convection type in surface weather observations. In the legend, TS indicates thunderstorms, LTG indicates lightning, SH indicates showers, and RA indicates rain.

Table 2. Comparison of rainrate (RR) environment assessments to surface weather observation environment assessments.

Agreement Between RR and Sfc Obs

Environment determined by RR \ Environment determined by Surface Obs	Unkn	Non-Conv	Pre-Conv	Ending Conv	Cont Conv
Unkn	.15	.47	.09	.12	.16
Non-Conv	.09	.52	.12	.11	.16
Pre-Conv	.12	.27	.18	.11	.33
Ending Conv	.11	.36	.11	.14	.28
Cont Conv	.10	.15	.11	.10	.54

To overcome these dataset problems, two adjustments were made. First, all cases of pre-convective rain, showers, and thunderstorms were counted together as one phenomenon: convective precipitation (CP). This term will be used throughout the remainder of this study. In light of the disagreement between the two predictands, the surface weather observation predictand was given preference for the remainder of the study due to its higher spatial and time resolution.

IV. ANALYSIS AND RESULTS

A. SCATTER PLOTS

1. Scatter Plot Analysis Technique

Analysis of the predictand and predictor data began with the creation of 90 scatter plots (see Appendix B): one for each of 18 indices at five locations using surface weather observations as the predictand. Index values from the non-convective and pre-convective soundings at each location's were plotted as a function of Julian date. Because of the focus on predicting convective initiation, continuing convection, ending convection, and unknown soundings were not included. Index values were labeled by convection event type (none, convective precipitation, and thunderstorm) and time of day (day or night). An additional 90 scatter plots using rainrate data as the predictand were not included.

These scatter plots were subjectively analyzed to determine if an index discriminated between non-convective (none) and pre-convective events. The analysis addressed three questions:

i) For which range of values do most of the non-convective events occur?

ii) For which range of values do most of the convective precipitation events occur?

and iii) For which range of values do most of the thunderstorm events occur?

Besides comparing event type to index value, event types were also compared to season and time-of-day. After scatter plots were examined individually, they were viewed as a group of the same index at the five locations.

2. Scatter Plot Results

Results of the subjective analysis were mixed because no discrimination was apparent for many of the indices. Instead, non-convective and pre-convective events were well-mixed throughout the ranges of values (e.g., Figure 12). In particular, CAPE, CIN, depth of negative buoyancy, depth of positive buoyancy, Lifted Index, normalized CAPE, low-to-mid-level wind shear, low-level wind speed, high-level temperature, and Vertical Totals Index did not indicate discrimination at any of the locations. Therefore, both thermodynamic- and kinematic-based indices are represented among the poorly-discriminating indices.

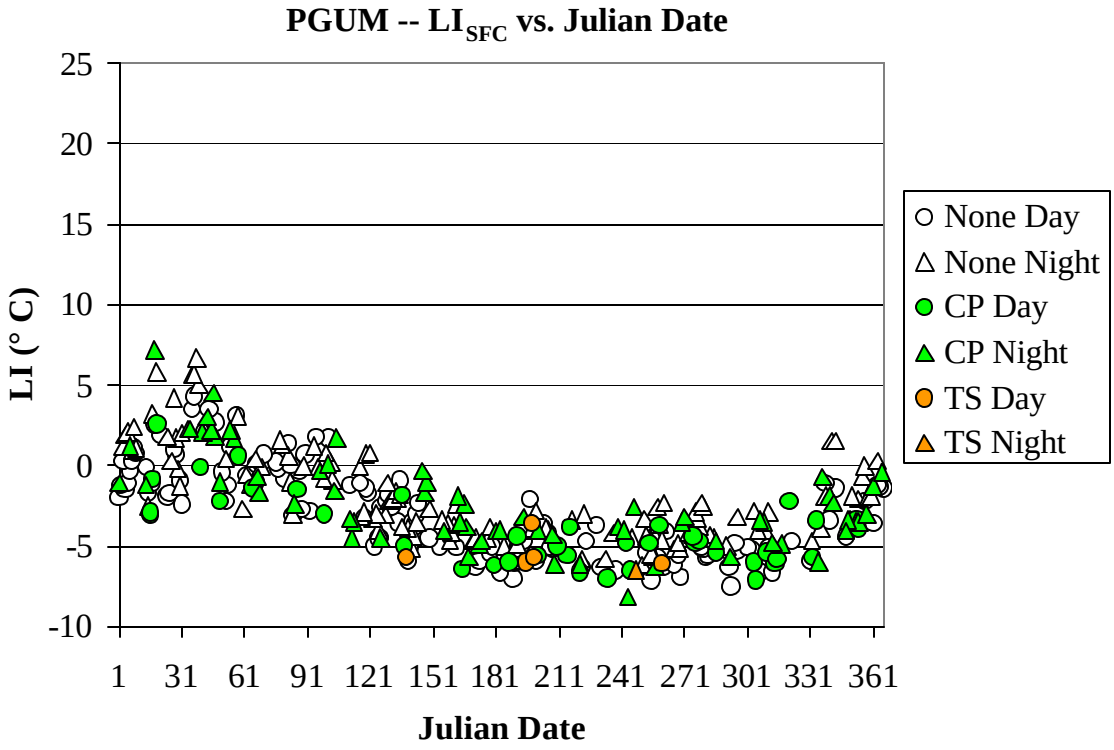

Figure 12. Example of a scatter plot of Lifted Index of a surface parcel at Agana, Guam, with poor discrimination between non-convective and pre-convective events.

However, some indices did appear to discriminate between non-convective and pre-convective events with respect to a threshold value. The Cross Totals Index appeared to be a discriminator of non-convective and pre-convective events at Naha (Figure 13). Similarly, other indices appeared to discriminate among environment types at other locations: the K Index at Naha and Kwajalein; the low-level relative humidity at Naha, Guam, Lihue, and Hilo; the mid-level relative humidity at Naha; the Showalter Index at Naha; the SWEAT Index at all locations; the low-level temperature at Naha; and the Total Totals Index at Naha and Kwajalein. Clearly, the capability to discriminate among convective events varies widely from location to location and index to index. Among the indices displaying significant discrimination, the combined index of SWEAT appeared to perform best.

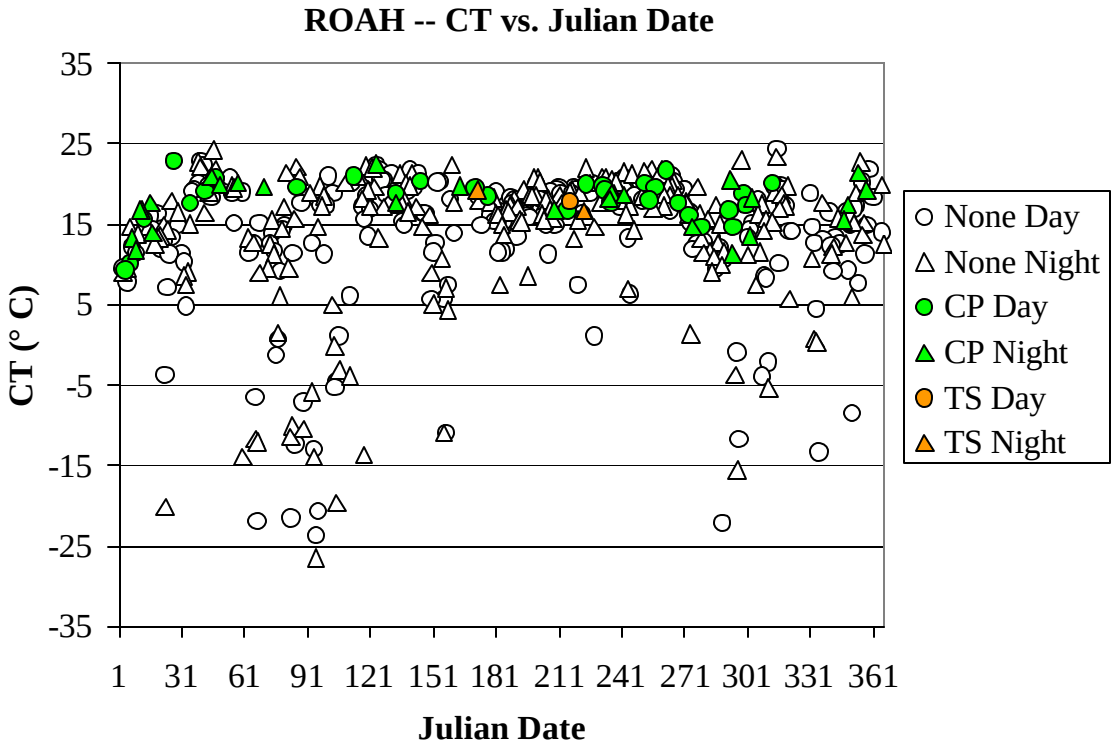

Figure 13. Example of a scatter plot of the Cross Total Index at Naha, Okinawa that exhibits good discrimination between non-convective and pre-convective events.

Additionally, some indices appeared to discriminate better in a specific season. The Cross Totals Index, K Index, low-level relative humidity, mid-level relative humidity, Showalter Index, low-level temperature, and Total Totals Index all seemed to discriminate better in the winter, when there was a wider range of index values. Only SWEAT seemed to discriminate well in both summer and winter.

Close examination of the indices (see Appendix A) revealed that none of the components of the indices are likely to experience large diurnal variations in tropical oceanic regions. Therefore, day/night classifications were not examined further and the focus was only on seasonal classifications.

B. HEIDKE SKILL SCORES (HSS)

1. HSS Analysis Technique

Following the subjective analysis of the scatter plots, a more objective method was used to assess predictor performance. First, the data were subdivided into 10 distinct classifications based on location (ROAH, PGUM, PKWA, PHLI, and PHTO) and season

(Summer or Winter). This subdivision was done because subjective analysis of the scatter plots identified the influence of location and season on predictor performance. Next, the 18 indices were evaluated individually by a threshold test for each of the 10 classifications for a total of 180 tests for each of the two predictands.

For each classification, a range of values was defined by the difference between the minimum and maximum index value. This range was divided into 1% increments that were used as a base to calculate discrete threshold values. For each of the 100 threshold index values, convection was forecast when the index exceeded the threshold and no convection was forecast if the index was below the threshold. The prediction for each threshold was verified for the two predictands.

A 2x2 contingency table was formed for each threshold value using the forecast and verification information. Forecast skill for that threshold value was then determined by the Heidke Skill Score (HSS), which is defined as

$$HSS = \frac{2(ad - bc)}{(a+c)(c+d) + (a+b)(b+d)}. \tag{3}$$

Variables a, b, c, and d correspond to the hits, false alarms, misses, and correct negative cases recorded in the contingency table positions (Table 3). Consequently, a perfect forecast receives a Heidke score of one, a forecast equivalent to a random forecast receives a zero score, and a forecast worse than random receives a negative score.

The maximum Heidke Skill Score (Max HSS) was then determined for all 100 threshold index values. The index value that corresponded to the maximum HSS was chosen as the threshold value for defining a pre-convective or non-convective environment. This process was repeated for each combination of predictor (index), classification (location and season), and predictand (surface observation or rainrate).

Table 3. The 2 by 2 contingency table used to evaluate forecast skill.

	Observed	Not observed
Forecast	a	b
Not forecast	c	d

2. HSS Results

In all, 360 plots and maximum HSSs were created for all combinations of predictors, situations, and predictands. Two are presented below as case studies.

a) Case Study #1: K Index at PKWA During Summer

At Kwajalein in the summer, K Index values ranged from -2.5 to 41.4. Using surface observations, the HSS was calculated for 100 values between -2.5 and 41.4. The maximum HSS was 0.248 at a K Index threshold value of 34.4 (Figure 14a). Using rainrate data, HSSs were again calculated and the maximum HSS was determined to be 0.209 at a K Index threshold value of 34.8 (Figure 14b). Both positive HSSs indicate the predictor is better than random forecasts.

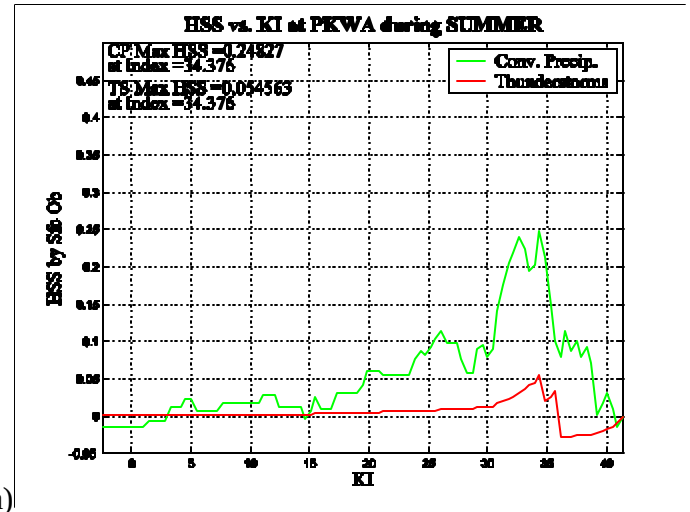

(a)

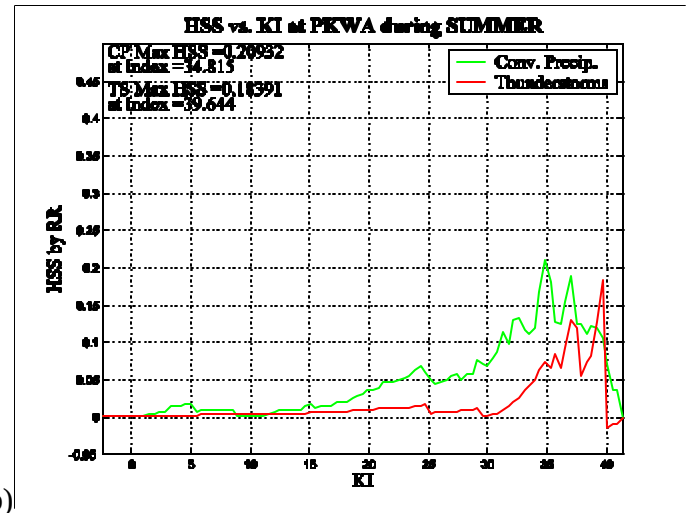

(b)

Figure 14. Heidke Skill Scores for K Index values at Kwajalein during Summer using (a) surface observations as the predictand; and (b) rainrate data as the predictand.

b) Case Study # 2: Convective Inhibition at PHTO During Winter

At Hilo in the winter, convective inhibition values ranged from -608.09 to 0. Using surface observations, the HSS was calculated for each of the 100 values between -608.09 and 0. The maximum HSS was 0.012 at a convective inhibition of -437.8 (Figure 15a). Using rainrate data, HSSs were again calculated and the maximum HSS was 0.010 at a convective inhibition of -121.6 (Figure 15b). Both HSSs approximately equal to zero indicate the predictor is no better than random forecasts.

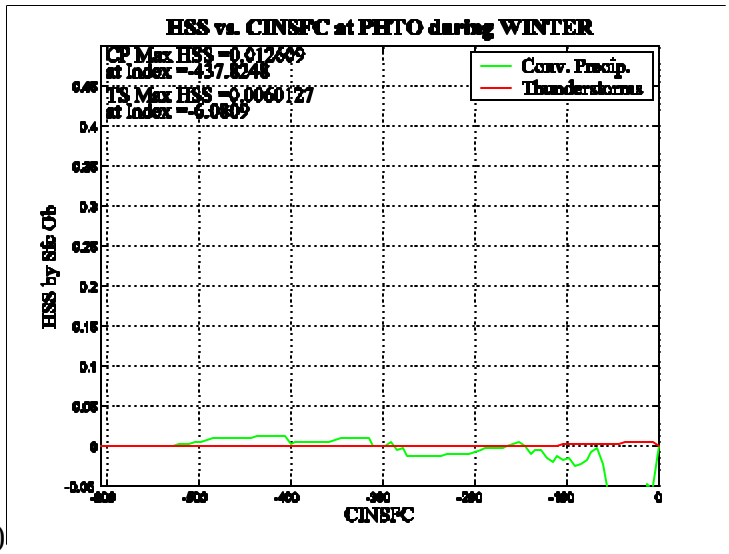

(a)

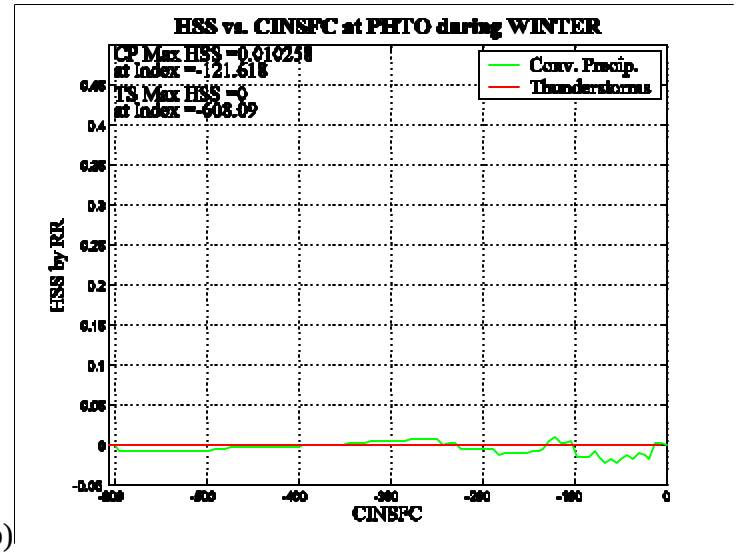

(b)

Figure 15. Heidke Skill Scores for convective inhibition values at Hilo during Winter using (a) surface observations as the predictand, and (b) rainrate data as the predictand.

C. RANKINGS OF INDICES

The maximum HSS for each combination of classification, predictor, and predictand was assembled into four seasonal tables (see appendix C). These maximum HSS values were then used to rank all 18 indices from best (1) to worst (18) for each location and season (Tables 4 through 7). Finally, indices were color-coded based upon their primary component influence (see right side of Tables 4 through 7).

In addition to rankings based on HSS at each location, regional rankings were also created. In the summer, index rankings for Naha, Guam, and Kwajalein tended to be similar. Likewise, index rankings for Lihue and Hilo tended to be similar in the summer. This supported grouping locations into two summertime areas: Naha, Guam, and Kwajalein composed the western Pacific (WPAC) group, while Lihue and Hilo composed the central Pacific (CPAC) group.

In the winter, index rankings for Guam and Kwajalein remained similar, while Naha differed significantly from Guam and Kwajalein. This difference at Naha was likely due to mid-latitude influences of polar fronts and continental polar air masses. Index rankings for Lihue and Hilo remained similar to each other in the winter. This supported grouping locations into three wintertime areas: Naha was by itself, Guam and Kwajalein were the WPAC group, and Lihue and Hilo were the CPAC group.

1. Surface Observations as Predictand

In summer, moisture-related indices were ranked highest at all locations (Table 4). Buoyancy-related indices ranked higher at western Pacific locations and lower at central Pacific locations. Latent-instability- related indices ranked low at all locations.

In keeping with the goal of the study, the highest-ranked index for each season and location was identified. Highest-ranked indices, hereafter referred to as "best-ranking" indices, were singled out for closer examination. Among the five locations, three indices individually qualified as best in the summer: Low-level relative humidity, SWEAT, and K Index. All three were previously identified as good discriminators via visual inspection of the scatter plots in Appendix B. However, their performance varied considerably from location to location (Figure 16).

Table 4. Rankings of indices for summer convective precipitation using surface observations as the predictand. All are colored by index type as defined by the key at the far right.

Rank	ROAH	PGUM	PKWA	PHLI	PHTO	WPAC	CPAC
1	RHL	SWEAT	KI	SWEAT	RHL	SWEAT	SWEAT
2	KI	SPDL	RHM	RHL	SWEAT	RHM	RHL
3	RHM	RHL	DPTHpos	SPDL	DPTHneg	KI	CT
4	SPDL	CINsfc	SWEAT	CT	CT	RHL	SPDL
5	SWEAT	DPTHpos	CAPEsfc	RHM	LIsfc	DPTHpos	TT
6	TEMPH	CAPEsfc	TT	KI	TT	SPDL	KI
7	DPTHpos	RHM	NCAPEsfc	TT	SPDL	CAPEsfc	DPTHneg
8	CT	TEMPH	CT	SHRLM	KI	CT	LIsfc
9	CAPEsfc	SHRLM	RHL	LIsfc	VT	CINsfc	RHM
10	TEMPL	KI	CINsfc	TEMPH	RHM	NCAPEsfc	SHRLM
11	SHRLM	CT	SPDL	DPTHneg	TEMPH	SHRLM	TEMPH
12	NCAPEsfc	NCAPEsfc	SHRLM	TEMPL	SHRLM	TEMPH	DPTHpos
13	TT	TEMPL	VT	DPTHpos	DPTHpos	TT	VT
14	CINsfc	TT	DPTHneg	CAPEsfc	CAPEsfc	TEMPL	TEMPL
15	DPTHneg	DPTHneg	LIsfc	NCAPEsfc	TEMPL	DPTHneg	CAPEsfc
16	LIsfc	LIsfc	TEMPL	SSI	CINsfc	LIsfc	NCAPEsfc
17	SSI	VT	SSI	VT	NCAPEsfc	VT	CINsfc
18	VT	SSI	TEMPH	CINsfc	SSI	SSI	SSI

Primary Influence
Moisture
Pos Buoyancy
Neg Buoyancy
Latent Instability
Kinematic

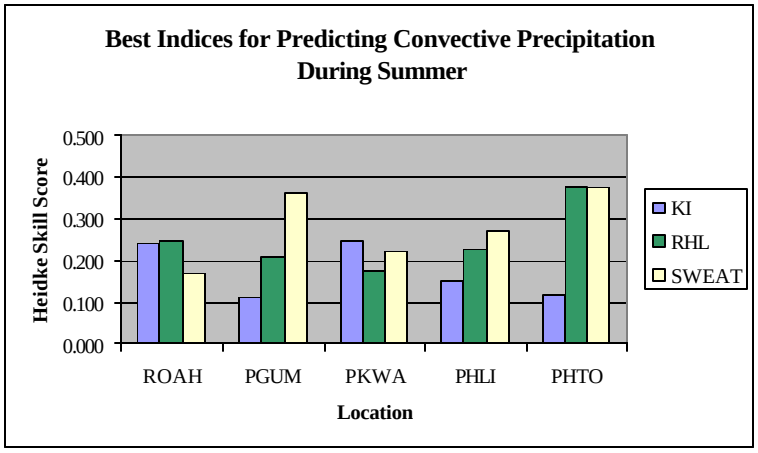

Figure 16. Best-ranking indices for predicting convective precipitation during summer using surface observations as the predictand.

In winter, moisture-related indices ranked highest at western Pacific locations and Naha (Table 5). However, buoyancy-related indices were ranked highest at central Pacific locations. In particular, depth of the positive buoyancy and depth of the negative buoyancy moved to first and second in the rankings. Latent-instability-related indices continued to be ranked low at western and central Pacific locations and slightly higher at Naha.

Among the five locations, four indices qualified individually as best in the winter: mid-level relative humidity, SWEAT, depth of positive buoyancy and depth of the negative buoyancy. Two of the four (mid-level relative humidity and SWEAT) were previously identified as good discriminators via visual inspection of the scatter plots in Appendix B. Index performance varied considerably from location to location (Figure 17).

Table 5. Rankings of indices for winter convective precipitation using surface observations as the predictand.

Rank	ROAH	PGUM	PKWA	PHLI	PHTO
1	RHM	SWEAT	SWEAT	DPTHpos	DPTHneg
2	SWEAT	RHL	CT	RHM	RHL
3	CT	CT	TT	SWEAT	CT
4	RHL	TT	KI	CAPEsfc	TT
5	KI	SPDL	SPDL	SPDL	DPTHpos
6	TEMPL	KI	RHL	DPTHneg	RHM
7	TEMPH	RHM	CAPEsfc	CT	KI
8	TT	DPTHpos	NCAPEsfc	RHL	SWEAT
9	SHRLM	CAPEsfc	RHM	TEMPL	CAPEsfc
10	DPTHpos	TEMPL	DPTHpos	NCAPEsfc	NCAPEsfc
11	CAPEsfc	NCAPEsfc	TEMPL	KI	VT
12	SPDL	DPTHneg	CINsfc	TT	SHRLM
13	NCAPEsfc	CINsfc	SHRLM	SHRLM	SPDL
14	DPTHneg	VT	VT	CINsfc	CINsfc
15	VT	TEMPH	TEMPH	VT	TEMPL
16	SSI	LIsfc	LIsfc	TEMPH	TEMPH
17	LIsfc	SHRLM	DPTHneg	SSI	SSI
18	CINsfc	SSI	SSI	LIsfc	LIsfc

ROAH	WPAC	CPAC
RHM	SWEAT	DPTHpos
SWEAT	CT	DPTHneg
CT	TT	RHM
RHL	RHL	CT
KI	KI	RHL
TEMPL	SPDL	SWEAT
TEMPH	CAPEsfc	CAPEsfc
TT	RHM	TT
SHRLM	DPTHpos	KI
DPTHpos	NCAPEsfc	SPDL
CAPEsfc	TEMPL	NCAPEsfc
SPDL	CINsfc	TEMPL
NCAPEsfc	VT	SHRLM
DPTHneg	DPTHneg	VT
VT	SHRLM	CINsfc
SSI	TEMPH	TEMPH
LIsfc	LIsfc	SSI
CINsfc	SSI	LIsfc

Primary Influence
Moisture
Pos Buoyancy
Neg Buoyancy
Latent Instability
Kinematic

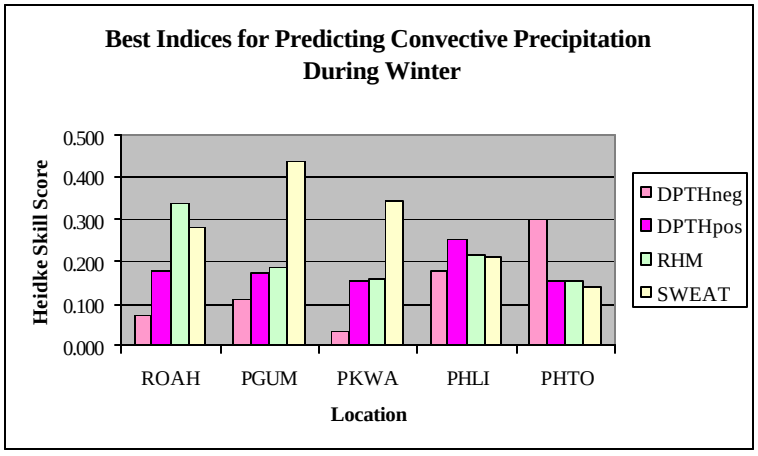

Figure 17. Best-ranking indices for predicting convective precipitation during winter using surface observations as the predictand.

2. Rainrate as Predictand

For comparison purposes and completeness, seasonal rankings and best-ranking indices were determined using rainrate data. In summer, moisture-related indices were still ranked high in the western Pacific, but less so in the central Pacific (Table 6). Low-level relative humidity, SWEAT, and K Index were best-ranked indices, in addition to depth of the negative buoyancy and Lifted Index. Index performance varied considerably from location to location (Figure 18).

Table 6. Rankings of indices for summer convective precipitation using rainrates as the predictand.

Rank	ROAH	PGUM	PKWA	PHLI	PHTO	WPAC	CPAC
1	SWEAT	RHL	KI	DPTHneg	LIsfc	KI	LIsfc
2	SPDL	KI	SWEAT	LIsfc	SWEAT	RHM	SWEAT
3	RHM	RHM	CT	RHM	SPDL	SWEAT	SPDL
4	TEMPH	LIsfc	RHM	SPDL	NCAPEsfc	RHL	DPTHneg
5	KI	NCAPEsfc	RHL	SWEAT	CAPEsfc	SPDL	NCAPEsfc
6	SHRLM	CAPEsfc	TT	VT	DPTHpos	TEMPH	RHL
7	TEMPL	SWEAT	CAPEsfc	CT	SHRLM	CT	CAPEsfc
8	DPTHneg	DPTHpos	DPTHpos	TT	RHL	DPTHpos	CT
9	RHL	SHRLM	NCAPEsfc	KI	DPTHneg	SHRLM	DPTHpos
10	DPTHpos	TEMPH	TEMPH	RHL	SSI	CAPEsfc	RHM
11	CT	SPDL	SPDL	TEMPL	TEMPH	TT	VT
12	TT	CT	TEMPL	NCAPEsfc	TEMPL	NCAPEsfc	TT
13	LIsfc	TT	SHRLM	CAPEsfc	CT	LIsfc	SHRLM
14	VT	VT	VT	DPTHpos	TT	TEMPL	TEMPL
15	SSI	CINsfc	DPTHneg	TEMPH	VT	DPTHneg	KI
16	CINsfc	SSI	CINsfc	SHRLM	KI	VT	TEMPH
17	CAPEsfc	TEMPL	LIsfc	SSI	CINsfc	CINsfc	SSI
18	NCAPEsfc	DPTHneg	SSI	CINsfc	RHM	SSI	CINsfc

Primary Influence
Moisture
Pos Buoyancy
Neg Buoyancy
Latent Instability
Kinematic

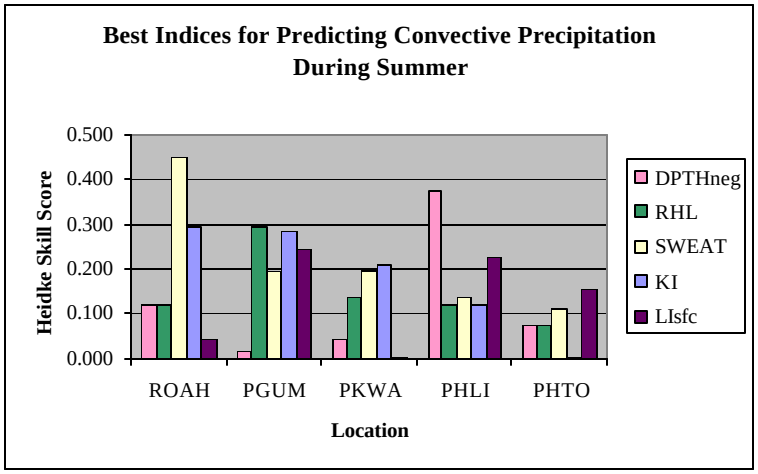

Figure 18. Best-ranking indices for predicting convective precipitation during summer using rainrates as the predictand.

In winter, moisture-related indices were still ranked highest at western Pacific locations (Table 7). However, moisture-related indices were ranked highest at central Pacific locations while a buoyancy-related index ranked highest at Naha. Latent-instability-related indices continued to be ranked low at all locations other than Hilo. The number of winter best-ranked indices decreased to two: depth of negative buoyancy and K Index. Index performance varied considerably from location to location (Figure 19).

Table 7. Rankings of indices for winter convective precipitation using rainrates as the predictand.

Rank	ROAH	PGUM	PKWA	PHLI	PHTO
1	DPTHneg	KI	KI	KI	DPTHneg
2	RHM	RHL	CT	RHL	LIsfc
3	CT	RHM	RHM	DPTHpos	SPDL
4	TT	SWEAT	TT	SHRLM	RHM
5	SWEAT	CT	RHL	RHM	SSI
6	KI	TT	SWEAT	CAPEsfc	TEMPH
7	SHRLM	SPDL	TEMPL	CT	SWEAT
8	RHL	DPTHpos	CAPEsfc	TEMPL	RHL
9	SPDL	CAPEsfc	NCAPEsfc	SWEAT	TEMPL
10	LIsfc	VT	DPTHpos	NCAPEsfc	SHRLM
11	VT	NCAPEsfc	SHRLM	TT	KI
12	DPTHpos	TEMPH	LIsfc	DPTHneg	TT
13	CAPEsfc	TEMPL	TEMPH	SPDL	CT
14	TEMPH	SSI	CINsfc	TEMPH	VT
15	NCAPEsfc	CINsfc	VT	VT	CINsfc
16	TEMPL	SHRLM	DPTHneg	CINsfc	DPTHpos
17	SSI	DPTHneg	SPDL	LIsfc	CAPEsfc
18	CINsfc	LIsfc	SSI	SSI	NCAPEsfc

ROAH	WPAC	CPAC
DPTHneg	KI	RHM
RHM	RHM	RHL
CT	CT	KI
TT	RHL	DPTHneg
SWEAT	TT	SHRLM
KI	SWEAT	SWEAT
SHRLM	CAPEsfc	SPDL
RHL	DPTHpos	TEMPL
SPDL	NCAPEsfc	DPTHpos
LIsfc	TEMPL	LIsfc
VT	SPDL	CT
DPTHpos	VT	TEMPH
CAPEsfc	TEMPH	TT
TEMPH	SHRLM	CAPEsfc
NCAPEsfc	CINsfc	SSI
TEMPL	LIsfc	NCAPEsfc
SSI	SSI	VT
CINsfc	DPTHneg	CINsfc

Primary Influence
Moisture
Pos Buoyancy
Neg Buoyancy
Latent Instability
Kinematic

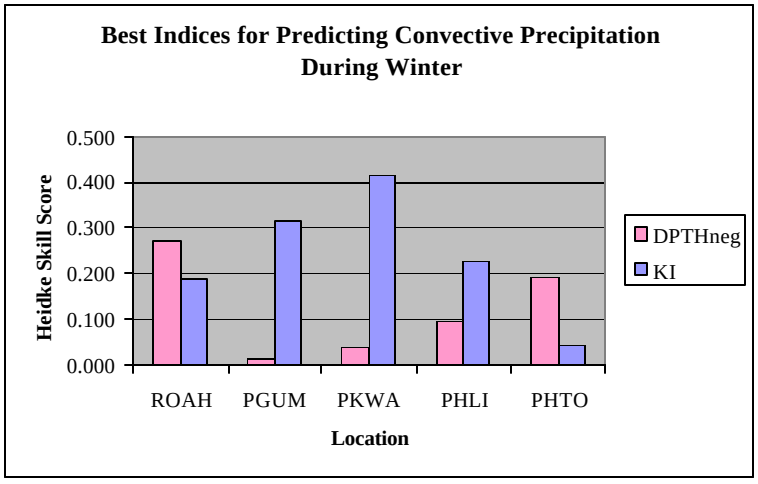

Figure 19. Best-ranking indices for predicting convective precipitation during winter using rainrates as the predictand.

D. DISCRIMINANT ANALYSIS

1. Discriminant Analysis Technique

In addition to evaluation of individual indices, combinations of multiple indices were also considered as predictors of convection through discriminant analysis (DA). Discriminant analysis (Wilks 2006) allows a single predictor to be constructed from a linear combination of indices similar to

$$Experimental\_Index = a * Index1 + b * Index2 + c * Index3 + \ldots . \quad (4)$$

Each index is weighted by its coefficient and the optimum weighting is determined by the DA. Because a regional dependency of each index had been previously established, the DA was accomplished for regional groupings.

Regional rankings from the surface observation-derived seasonal ranking tables were used to define the order of the indices input to the DA. To test the sensitivity to the HSS-based rankings of individual indices, a succession of DA steps were run. Initially, all 18 indices were included in the DA. Then the DA was re-run after the highest-ranking index was removed, and this was repeated until only the lowest ranking index remained. For a given region and season, indices were included and dropped according to their ranked order. The ability of each combination of indices to discriminate between convective and non-convective events was evaluated using the HSS.

2. Discriminant Analysis Results

a) DA for Summer

The DA applied to indices in the western Pacific during the summer revealed three key points. First, the ability to discriminate between environment types increased significantly when the depth of positive buoyancy and CAPE were added to the linear combination (Figure 20). Second, the ability to discriminate did not improve when indices ranked lower than CAPE (i.e., to the right of CPE on the abscissa in Figure 20) were added. Third, even when starting with the highest-ranked indices of SWEAT and mid-level relative humidity, Heidke Skill Scores peaked between 0.25 and 0.30, which is less than the HSS for some individual indices. To examine the reason for this decrease, multiple combinations of indices were input to the DA. Since depth of positive buoyancy and CAPE contributed most to the discriminant function (Figure 20), the DA using these

indices as input was examined (Figure 21). It is clear that for a wide range of CAPE and depth of positive buoyancy values, there is much overlap of environment types.

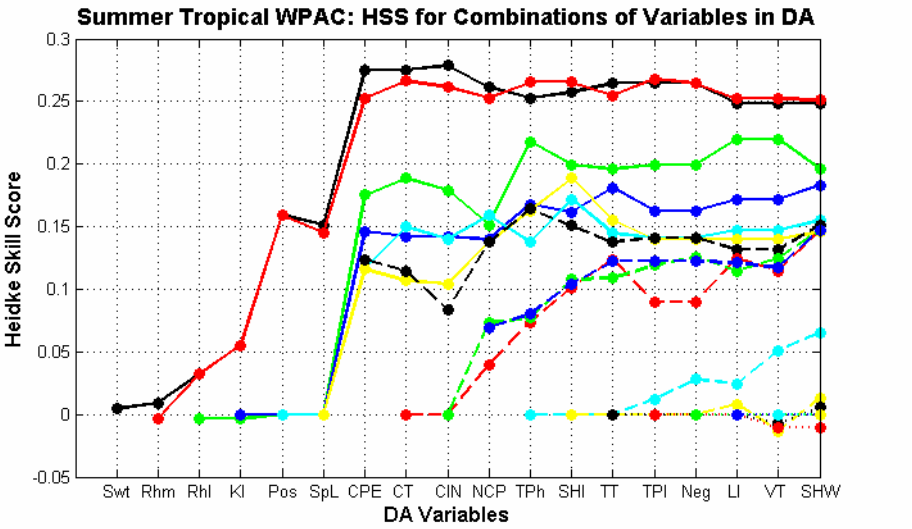

Figure 20. Heidke Skill Scores for combinations of indices in the DA for western Pacific locations during summer. Each colored line defines results of the classification from the DA starting with the index and adding lower-ranking indices to the DA at subsequent points. Each subsequent point defines the HSS associated with the addition of the respective index into the DA. New lines start one position (index) to the right of the preceding line as higher-ranking indices are excluded from the DA.

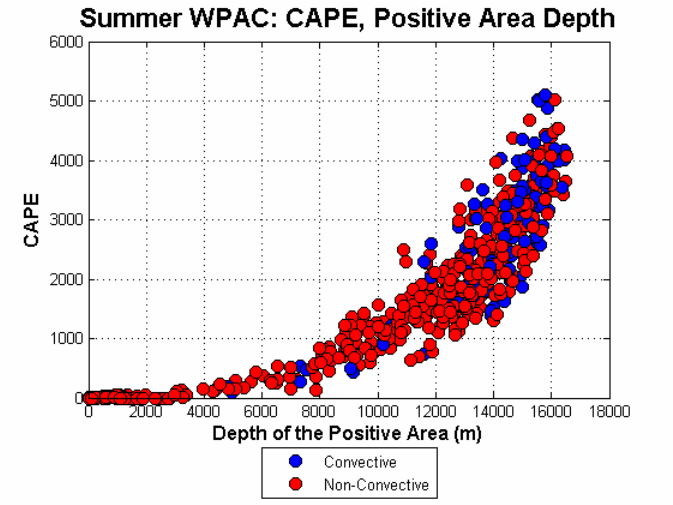

Figure 21. Scatter plot of CAPE versus depth of positive buoyancy for western Pacific locations during summer.

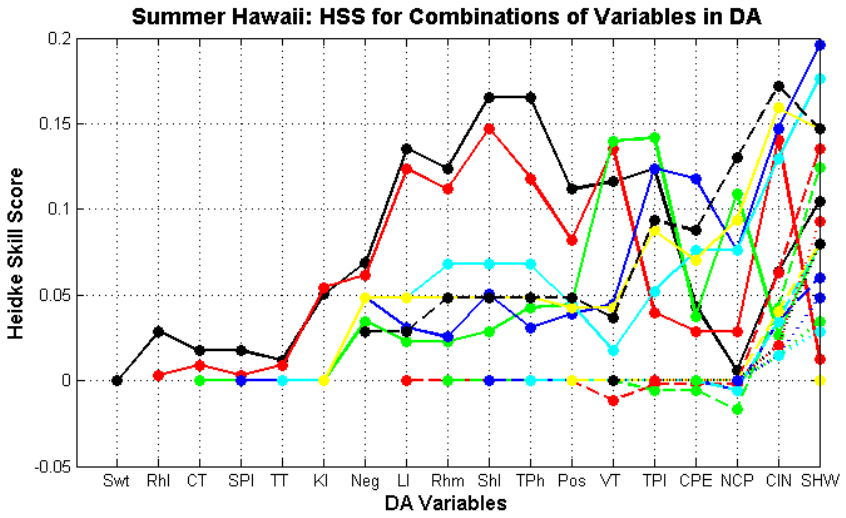

Figure 22. As in Figure 20, except for the Hawaii (central Pacific) stations during the summer.

Discriminant Analysis using indices in the central Pacific during the summer also revealed three key points. First, skill increased significantly when K Index and Lifted Index were added to the linear combination (Figure 22). Second, skill decreased significantly when depth of positive buoyancy and CAPE were added to the linear combination. Third, even when starting with the highest-ranked indices of SWEAT and low-level relative humidity, Heidke Skill Scores peaked between 0.15 and 0.20, which is less than the HSS for some individual indices and less than the western Pacific in summer. Similar results with respect to subsets for indices as input to the DA for western Pacific stations were identified for various combinations of indices for central Pacific locations.

b) DA for Winter

Discriminant Analysis of indices in the western Pacific during the winter revealed three key points. First, skill increased significantly when low-level relative humidity and Lifted Index was added to the linear combination (Figure 23). Second, forecast skill did not improve much when indices ranked lower than low-level relative humidity were added. Third, even when starting with the highest-ranked indices of SWEAT and Cross Totals Index, Heidke Skill Scores peaked around 0.20, which is less than the HSS for some individual indices. This HSS decrease can be explained by the inability of the two largest contributors (low-level relative humidity and Lifted Index) to

discriminate between non-convective and pre-convective events. Discrimination is poor throughout the range of Lifted Index values and for most relative humidity values (Figure 24).

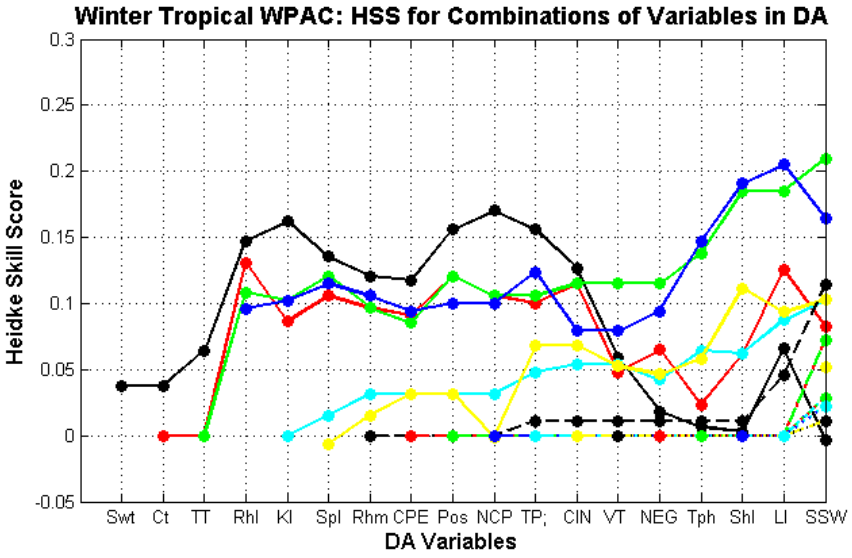

Figure 23. As in Figure 20, except for Guam and Kwajalein (western Pacific) during the winter.

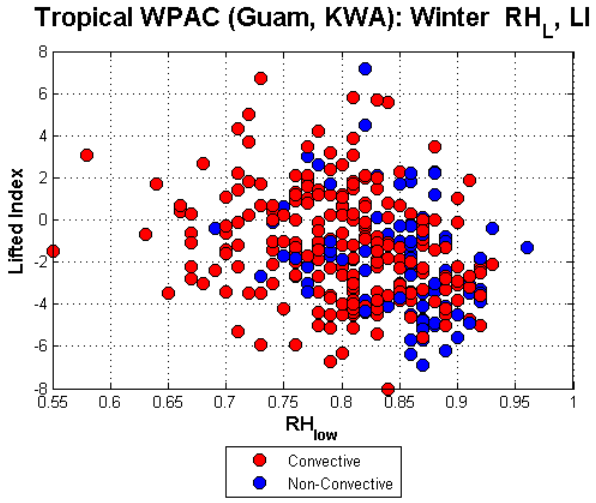

Figure 24. Scatter plot of Lifted Index vs. low-level relative humidity for Guam and Kwajalein during winter.

THIS PAGE INTENTIONALLY LEFT BLANK

V. CONCLUSIONS AND RECOMMENDATIONS

A. CONCLUSIONS

Several conclusions can be drawn from the results of this observational study.

1. Choice of Predictand

The choice of the predictand used as ground truth affected the skill scores of the indices. While the Heidke Skill Score of most indices differed by less than 0.1, nearly a quarter differed between 0.1 and 0.2 when calculated using different predictands. These differences are likely a result of the lower spatial and time resolution (1/4° lat./long. and 3 h accumulations) of the rainrate data. For instances of large differences, surface weather observations are the predictand of choice.

2. Overall Performance of Predictors

Few indices exhibited significant skill in forecasting initiation of convective precipitation. Using surface observations as the predictand, only three indices exhibited maximum Heidke Skill Scores greater than 0.3. The highest HSS value of all indices, which was 0.441 for the SWEAT Index at Agana during the winter, was well below the perfect score of one. It is likely that the indices account for some of the variability in convective initiation. However, factors such as mesoscale horizontal variability of an environment may not be adequately measured by rawinsondes. Despite these limitations, most convective indices performed better than random forecasts.

3. Moisture-related Predictors

Moisture-related indices are the best predictors of tropical convection. In particular, both low-level and mid-level relative humidity exhibit skill in predicting convective initiation. This is encouraging, as the importance of moisture to convective initiation has been previously documented by others (Sherwood 1999, Raymond 2001).

Surprisingly, SWEAT also exhibits skill in predicting tropical convection. Originally developed to forecast severe weather in the mid-latitudes, SWEAT ranks near the top of all locations in all seasons. This good ranking may be due to the components of SWEAT (see Appendix A), which includes several moisture-related, thermodynamic, and kinematic parameters. In essence, the SWEAT index is a simplified linear combination, similar to those created by the discriminant analysis.

4. Single Index Forecast

For all seasons and locations, individual indices outperformed linear combinations of multiple indices. That is, a threshold value for a single index had more skill than multiple indices combined in the DA. However, to utilize the single-index method, the right threshold value for the right location for the appropriate season had to be used. While this approach works well for point forecasts, the applicability to area forecasts is unknown at this time.

B. RECOMMENDATIONS

The following items are recommended for future research and operational implementation.

1. Future Research

While this study has addressed many problems related to observing and forecasting mesoscale tropical convection, several topics require additional research.

a) Differentiating between Thunderstorms and Convective Precip

Additional research would be useful in differentiating forecasts into Thunderstorms and Convective Precipitation. The ability to differentiate is important to military decision makers who must initiate protective actions for forecasts of thunderstorms and lightning. This research would require more years of predictor data to increase the number of thunderstorm cases.

b) Model Data Predictors

Additional research would be useful in using model-generated indices as predictors of convection. If model predictors have comparable skill to rawinsonde predictors, indices from model fields could be used to create: 1) area forecasts; and 2) forecasts several hours into the future.

c) Rainrate Predictands

Additional research would be useful in further evaluating NRL Blended Rainrate products for verification purposes. In particular, refined threshold values for convective precipitation and thunderstorms may yield better agreement with surface weather observations. Additionally, higher temporal and spatial resolution of Rainrate products may provide more useful as observations of mesoscale tropical convection.

2. Operational Implementation

a) Forecasting

Several aspects of the conclusions above could be implemented at operational weather units relatively easily. First, automated calculation of convective indices by weather unit computer systems should be expanded to include all of these best-ranked predictors from the tables. The best indices would then be available to forecasters, who would choose the best index as indicated by the seasonal tables (Chapter IV, Section C).

b) Verification

Additionally, forecast verification of both point forecasts and area forecasts of convection by the OWS should be enhanced. Satellite-derived rainrates and lightning detection provide objective sources of verification and should be used to the maximum extent possible. Point forecasts, including TAFs in particular, should be verified consistently to identify problem areas. This verification could easily be accomplished by 2x2 contingency tables. Area forecasts should also be verified more stringently. The best method to verify area forecasts would be threat scores, although this would require progressing from images (bmp, jpg, etc.) of FITL Thunderstorm charts to digitized file formats. With improved forecasts of mesoscale tropical convection and improved verifications, utility to military decision makers will be greatly enhanced.

THIS PAGE INTENTIONALLY LEFT BLANK

APPENDIX A – DESCRIPTIONS AND EQUATIONS OF INDICES

1. $CAPE_{SFC}$: CAPE of a surface parcel

$$CAPE_{SFC} = R_d \int_{LFC}^{EL} (T'_v - T_v) d(\ln p)$$

2. CIN_{SFC}: Convective Inhibition of a surface parcel

$$CIN_{SFC} = -R_d \int_{SFC}^{LFC} (T'_v - T_v) d(\ln p)$$

3. CT: Cross Totals Index (Miller 1967)

$$CT = T_d(850) - T(500)$$

4. $DPTH_{NEG}$: Depth of negative buoyancy for a surface parcel

$$DPTH_{NEG} = Z_{LFC} - Z_{SFC}$$

5. $DPTH_{POS}$: Depth of positive buoyancy for a surface parcel

$$DPTH_{POS} = Z_{EL} - Z_{LFC}$$

6. KI: K Index (George 1960)

$$KI = [T(850) - T(500)] + Td(850) - [T(700) - Td(700)]$$

7. LI_{SFC}: Lifted Index of a surface parcel (Galway 1956)

$$LI_{SFC} = T(500) - T'(SFC, 500)$$

8. $NCAPE_{SFC}$: Normalized CAPE of a surface parcel (Blanchard 1998)

$$NCAPE_{SFC} = \frac{CAPE_{SFC}}{(Z_{EL} - Z_{LFC})}$$

9. RH_L: Mean relative humidity in low-levels (surface to 850 mb)

10. RH_M: Mean relative humidity in mid-levels (700 mb to 500 mb)

11. SHR_{LM}: Magnitude of the wind shear between low-levels and mid-levels, as determined by the vector difference of the mean low-level winds and the mean mid-level winds

12. SPD_L: Mean wind speed in low-levels

13. SSI: Showalter Index (Showalter 1953)

$$SSI = T(500) - T'(850,500)$$

14. SWEAT: Severe Weather Threat Index (Miller 1972)

$$SWEAT = Term1 + Term2 + Term3 + Term4 + Term5$$

Set any negative terms equal to zero

$$Term1 = 12 * Td(850)$$

$$Term2 = 20 * (TT - 49)$$

$$Term3 = 2 * SPD(850)$$

$$Term4 = SPD(500)$$

$$Term5 = 125 * \{\sin[DIR(500) - DIR(850)] + 0.2\}$$

if and only if $210 \le DIR(500) \le 310$ and $130 \le DIR(850) \le 250$

and $DIR(500) > DIR(850)$ and $SPD(500) = 15$ and $SPD(850) = 15$

15. $TEMP_H$: Mean temperature of high-levels (300 mb to 200 mb)

16. $TEMP_L$: Mean temperature of high-levels (300 mb to 200 mb)

17. TT: Total Totals Index (Miller 1967)

$$TT = CT + VT = [T_d(850) - T(500)] + [T(850) - T(500)]$$

18. VT: Vertical Totals Index (Miller 1967)

$$VT = T(850) - T(500)$$

APPENDIX B – SCATTER PLOTS

The following scatter plots depict rawinsonde-derived index values (y-axis) versus the Julian dates (x-axis) on which the rawinsondes were launched. Hollow shapes designate non-convective events while colored shapes designate pre-convective events. Circles indicate rawinsondes launched during the day while triangle shapes indicate rawinsondes launched at night.

CAPE of Surface Parcel ($CAPE_{SFC}$)

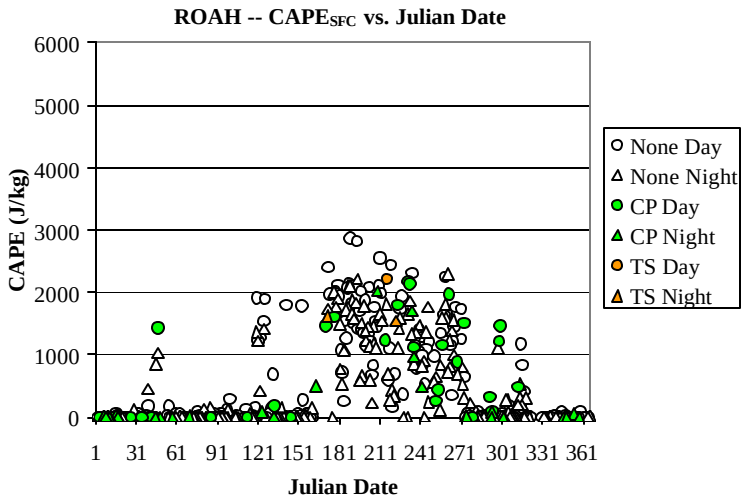

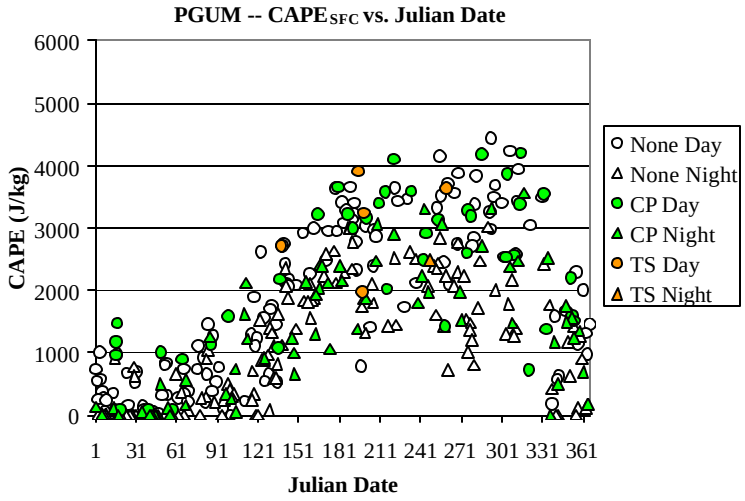

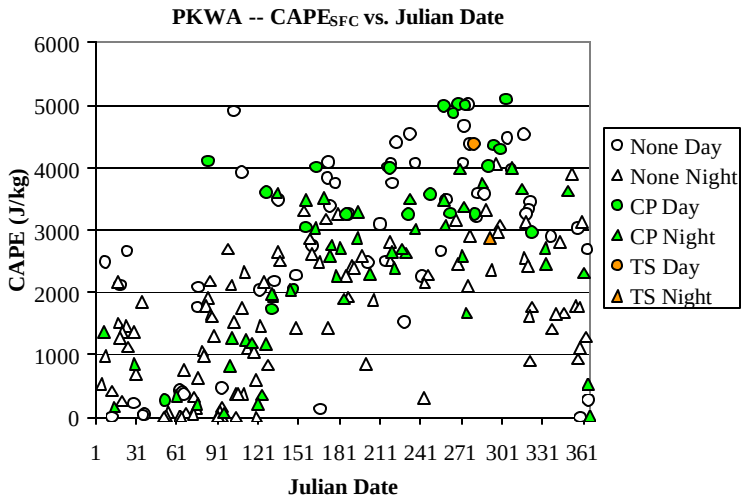
PKWA -- CAPE$_{SFC}$ vs. Julian Date
CAPE (J/kg)
0
1000
2000
3000
4000
5000
6000
1 31 61 91 121 151 181 211 241 271 301 331 361
Julian Date
None Day
None Night
CP Day
CP Night
TS Day
TS Night

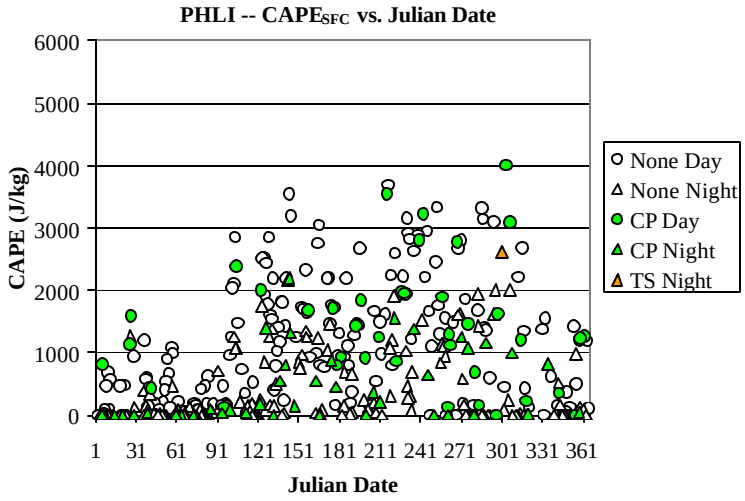
PHLI -- CAPE$_{SFC}$ vs. Julian Date
CAPE (J/kg)
0
1000
2000
3000
4000
5000
6000
1 31 61 91 121 151 181 211 241 271 301 331 361
Julian Date
None Day
None Night
CP Day
CP Night
TS Night

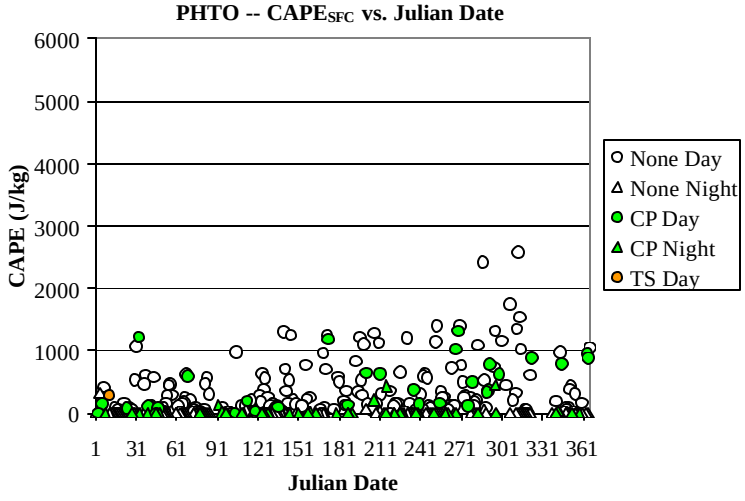
PHTO -- CAPE$_{SFC}$ vs. Julian Date
CAPE (J/kg)
0
1000
2000
3000
4000
5000
6000
1 31 61 91 121 151 181 211 241 271 301 331 361
Julian Date
None Day
None Night
CP Day
CP Night
TS Day

Convective Inhibition of Surface Parcel (CIN_{SFC})

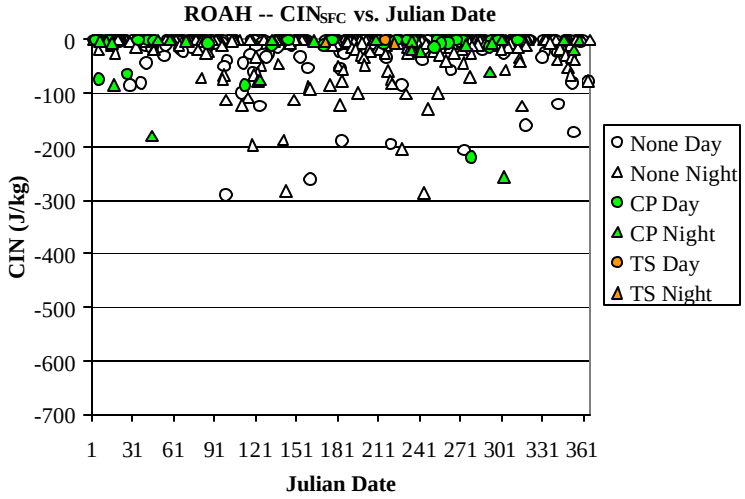

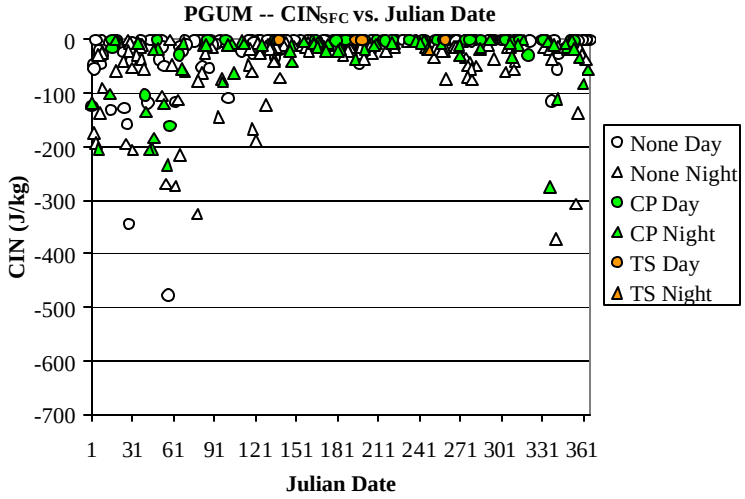

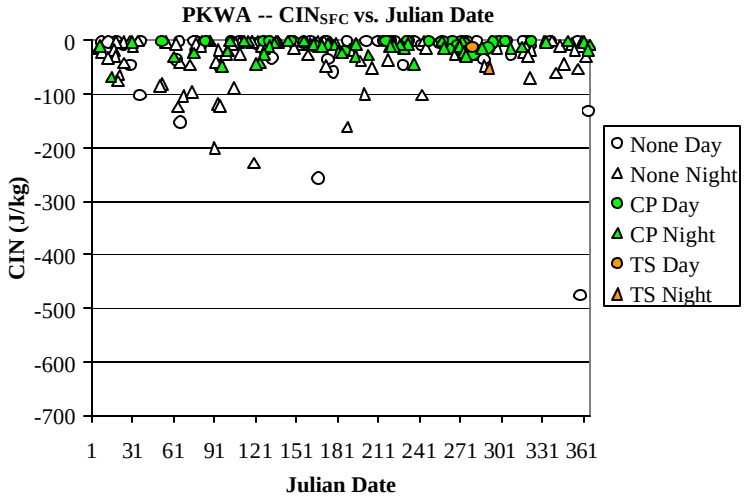

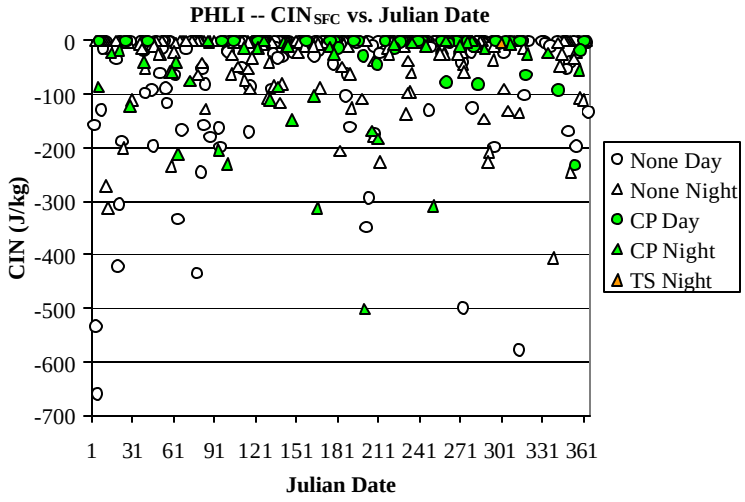
PHLI -- CIN SFC vs. Julian Date
CIN (J/kg)
0
-100
-200
-300
-400
-500
-600
-700
1 31 61 91 121 151 181 211 241 271 301 331 361
Julian Date
None Day
None Night
CP Day
CP Night
TS Night

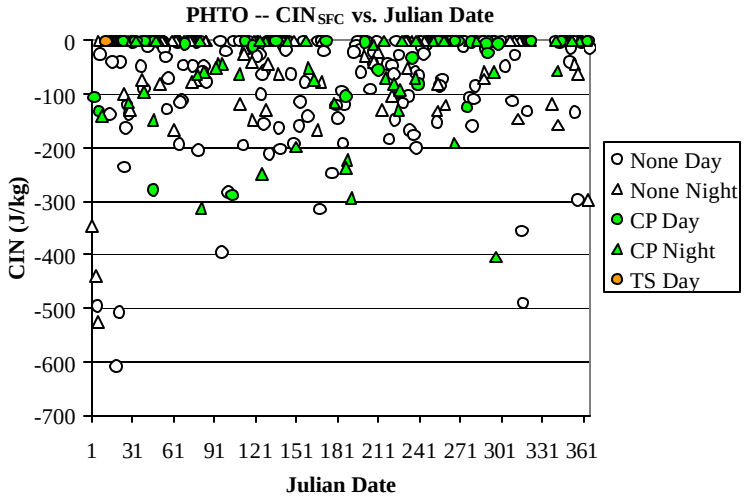
PHTO -- CIN SFC vs. Julian Date
CIN (J/kg)
0
-100
-200
-300
-400
-500
-600
-700
1 31 61 91 121 151 181 211 241 271 301 331 361
Julian Date
None Day
None Night
CP Day
CP Night
TS Day

Cross Totals Index (CT)

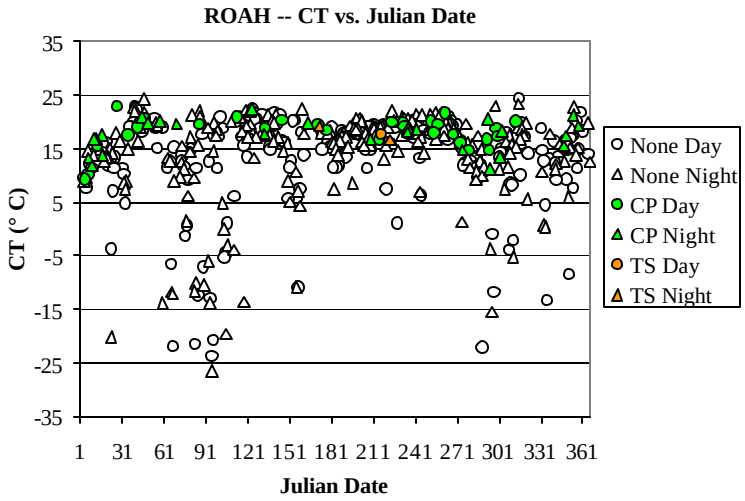

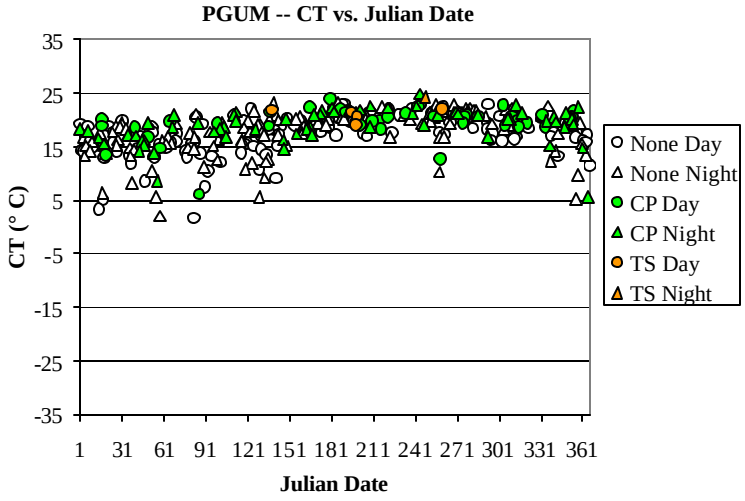

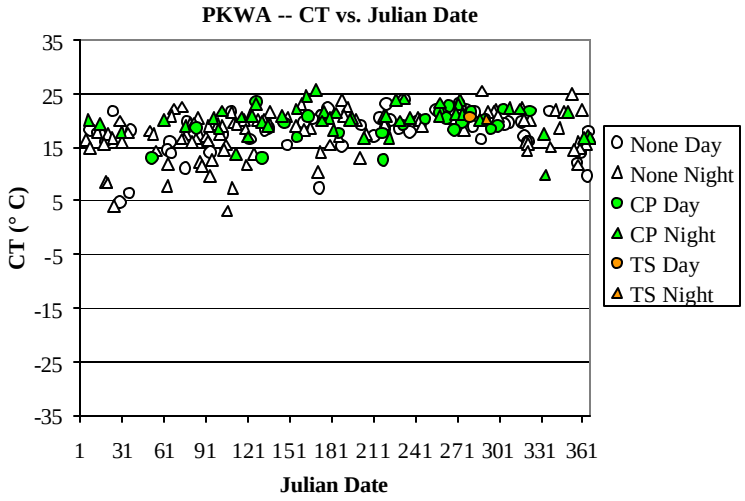

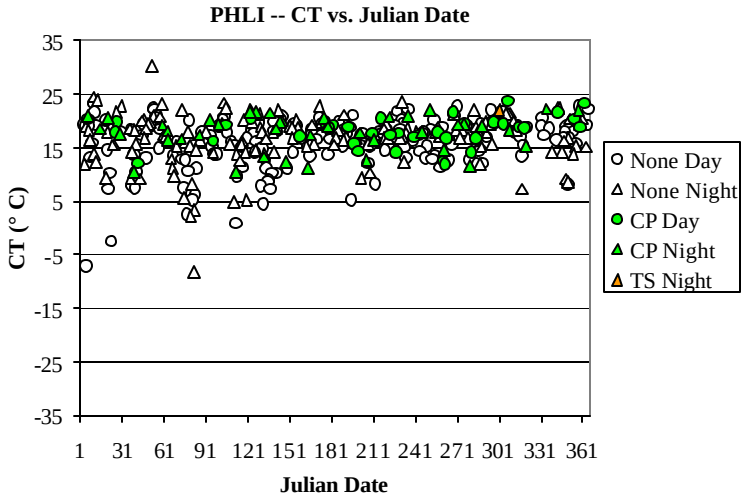
PHLI -- CT vs. Julian Date
CT (° C)
35
25
15
5
-5
-15
-25
-35
1 31 61 91 121 151 181 211 241 271 301 331 361
Julian Date
None Day
None Night
CP Day
CP Night
TS Night

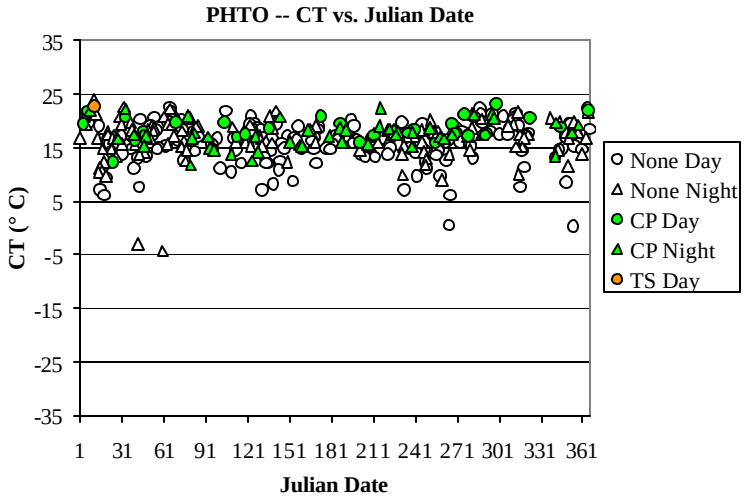
PHTO -- CT vs. Julian Date
CT (° C)
35
25
15
5
-5
-15
-25
-35
1 31 61 91 121 151 181 211 241 271 301 331 361
Julian Date
None Day
None Night
CP Day
CP Night
TS Day

K Index (KI)

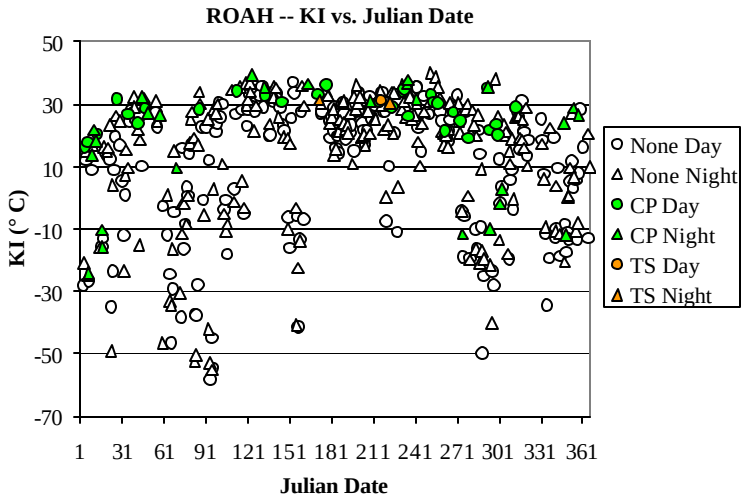
ROAH -- KI vs. Julian Date
KI (° C)
50
30
10
-10
-30
-50
-70
1 31 61 91 121 151 181 211 241 271 301 331 361
Julian Date
None Day
None Night
CP Day
CP Night
TS Day
TS Night

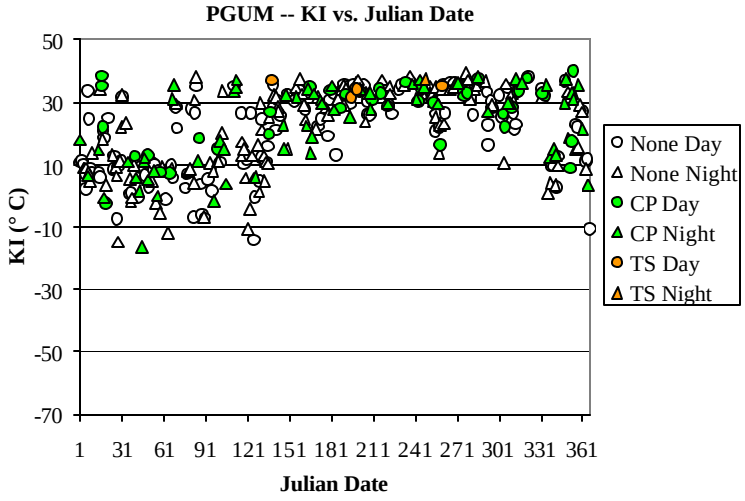
PGUM -- KI vs. Julian Date
KI (° C)
50
30
10
-10
-30
-50
-70
1 31 61 91 121 151 181 211 241 271 301 331 361
Julian Date
None Day
None Night
CP Day
CP Night
TS Day
TS Night

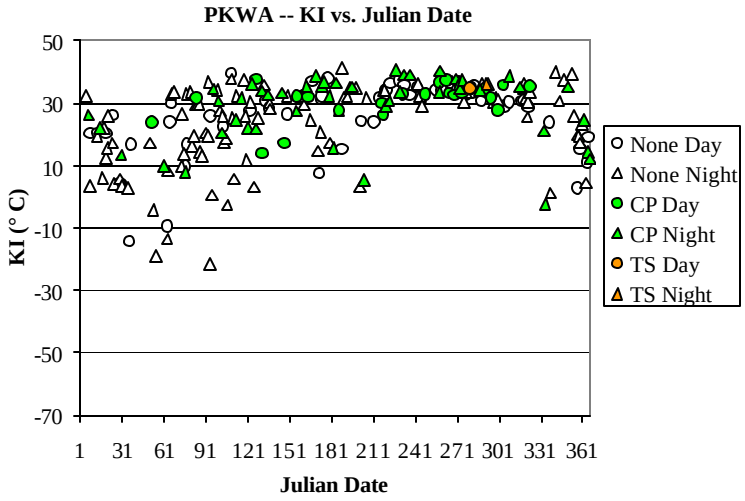
PKWA -- KI vs. Julian Date
KI (° C)
50
30
10
-10
-30
-50
-70
1 31 61 91 121 151 181 211 241 271 301 331 361
Julian Date
None Day
None Night
CP Day
CP Night
TS Day
TS Night

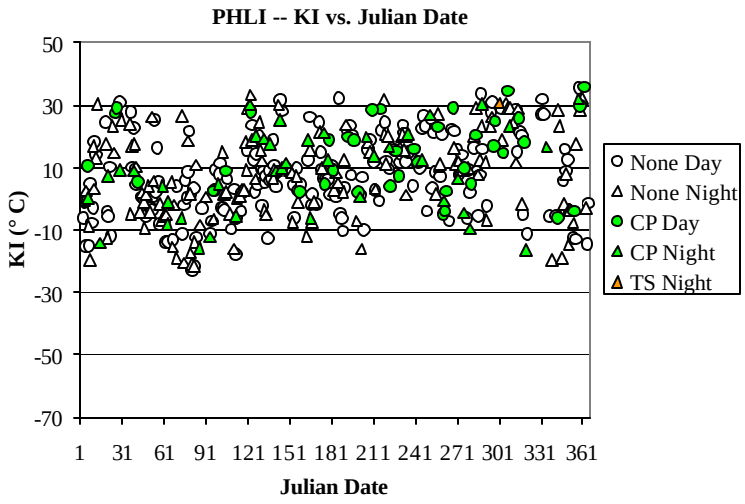
PHLI -- KI vs. Julian Date
KI (° C)
50
30
10
-10
-30
-50
-70
1 31 61 91 121 151 181 211 241 271 301 331 361
Julian Date
None Day
None Night
CP Day
CP Night
TS Night

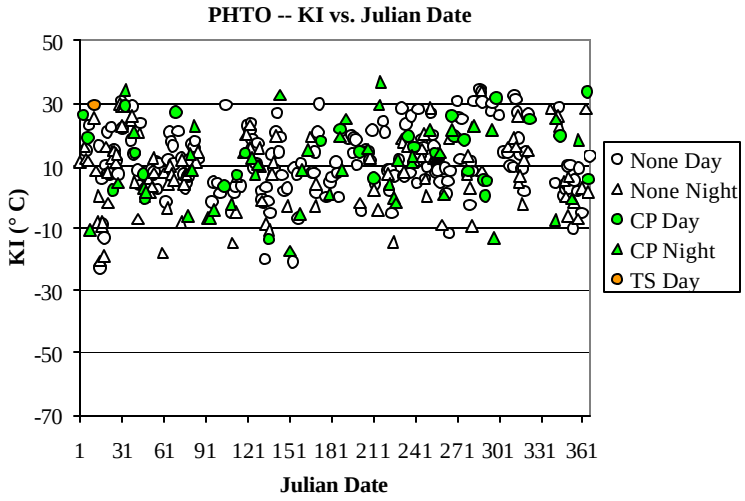
PHTO -- KI vs. Julian Date
KI (° C)
50
30
10
-10
-30
-50
-70
1 31 61 91 121 151 181 211 241 271 301 331 361
Julian Date
None Day
None Night
CP Day
CP Night
TS Day

Lifted Index of Surface Parcel (LI_{SFC})

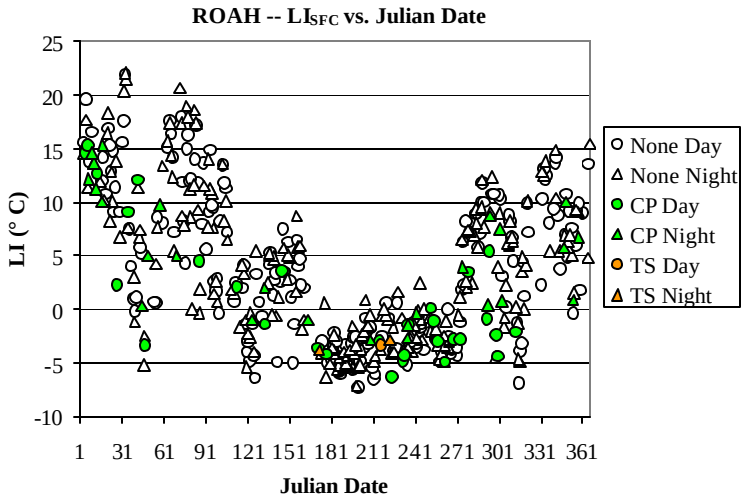

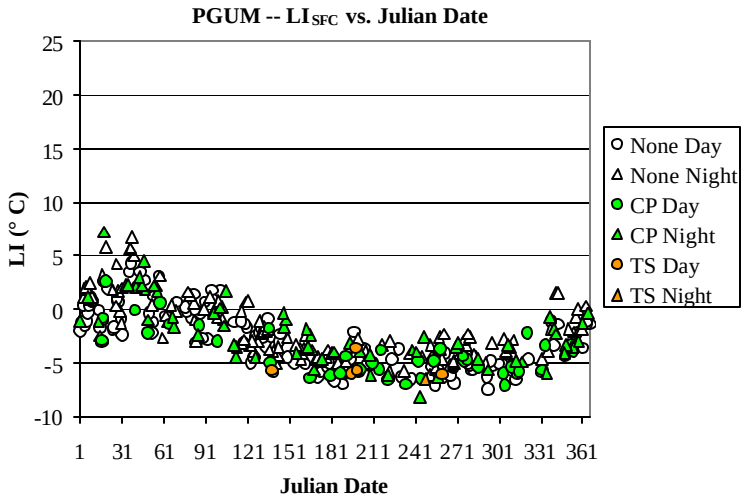

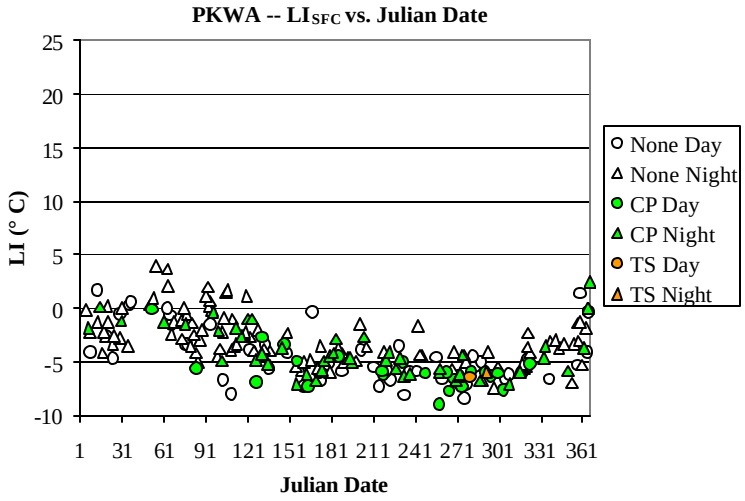

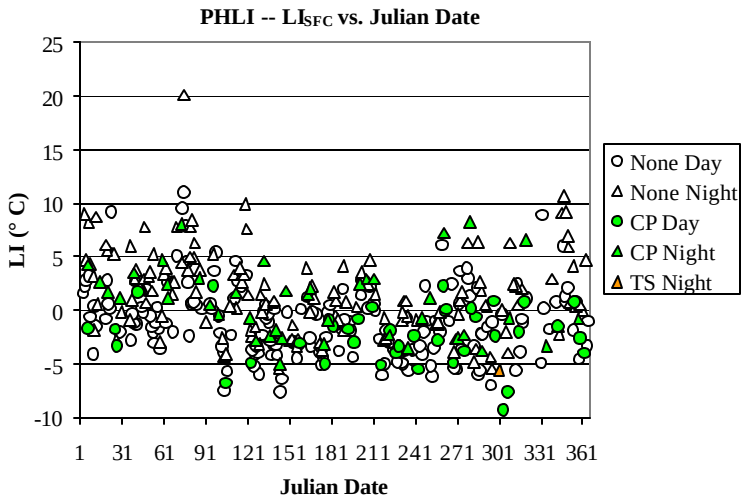
PHLI -- LISFC vs. Julian Date
LI (° C)
25
20
15
10
5
0
-5
-10
1 31 61 91 121 151 181 211 241 271 301 331 361
Julian Date
None Day
None Night
CP Day
CP Night
TS Night

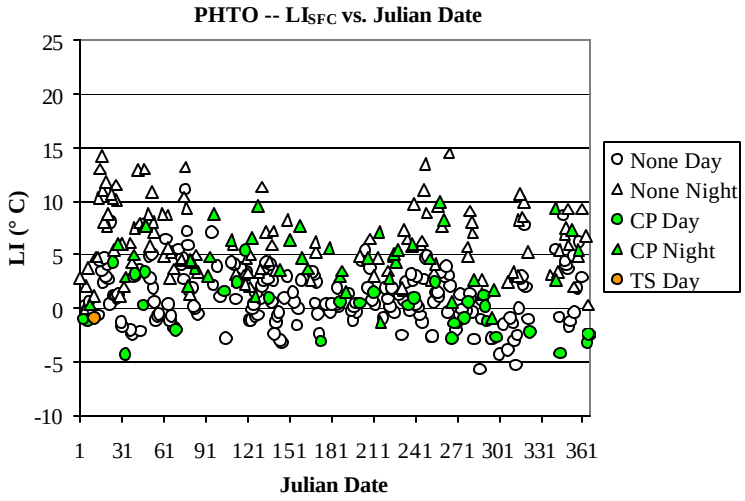
PHTO -- LISFC vs. Julian Date
LI (° C)
25
20
15
10
5
0
-5
-10
1 31 61 91 121 151 181 211 241 271 301 331 361
Julian Date
None Day
None Night
CP Day
CP Night
TS Day

Normalized CAPE of Surface Parcel ($NCAPE_{SFC}$)

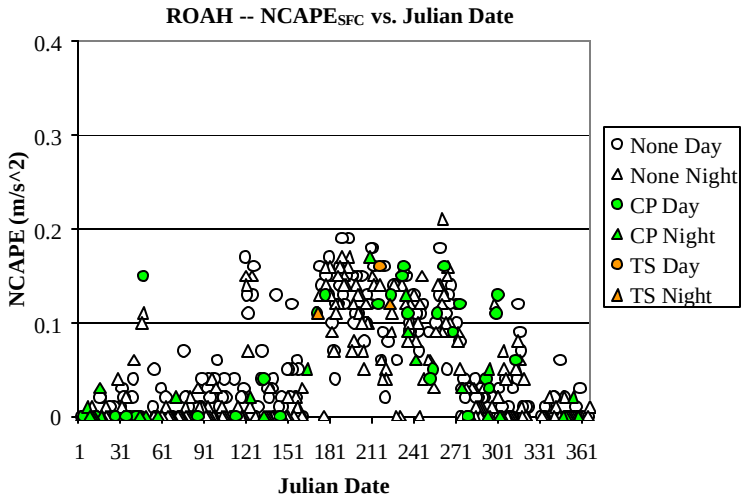

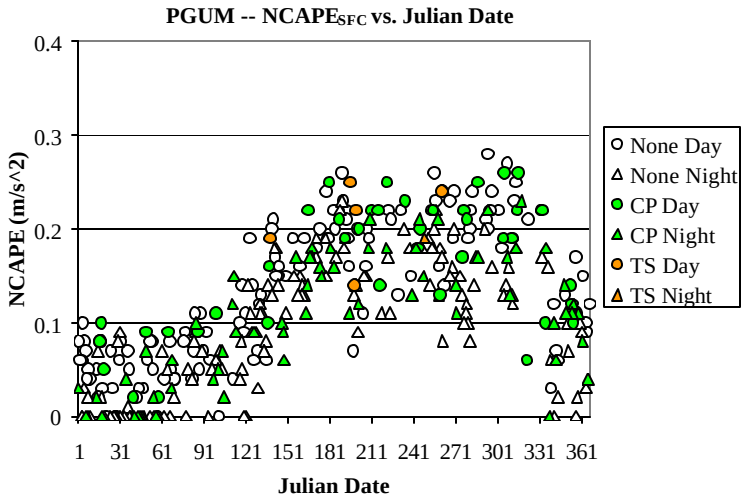

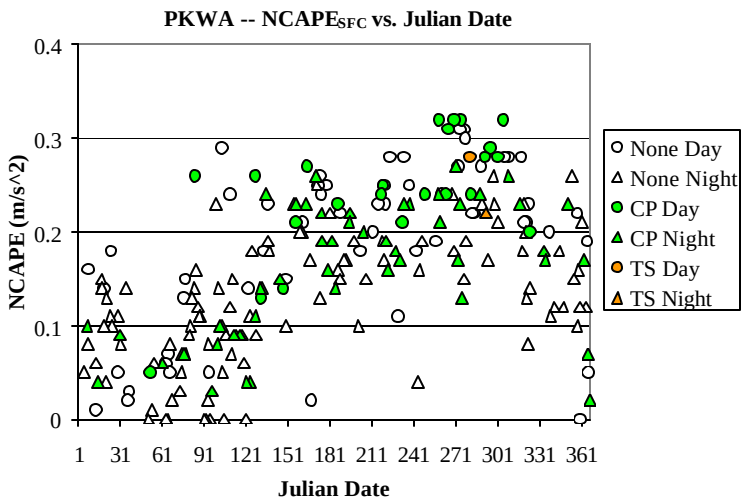

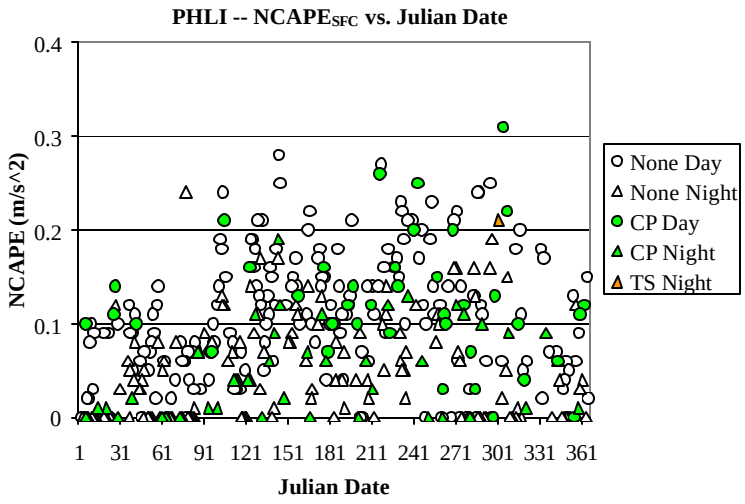
PHLI -- NCAPE$_{SFC}$ vs. Julian Date
NCAPE (m/s^2)
0.4
0.3
0.2
0.1
0
1 31 61 91 121 151 181 211 241 271 301 331 361
Julian Date
None Day
None Night
CP Day
CP Night
TS Night

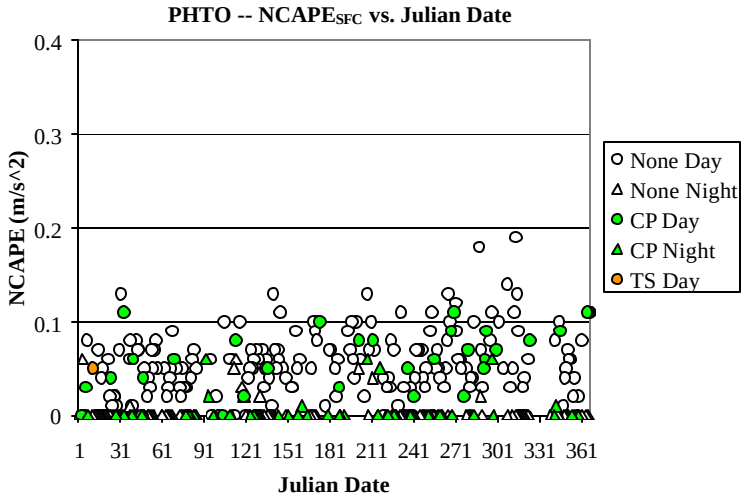
PHTO -- NCAPE$_{SFC}$ vs. Julian Date
NCAPE (m/s^2)
0.4
0.3
0.2
0.1
0
1 31 61 91 121 151 181 211 241 271 301 331 361
Julian Date
None Day
None Night
CP Day
CP Night
TS Day

Depth of Negative Buoyancy of Surface Parcel ($DPTH_{NEG}$)

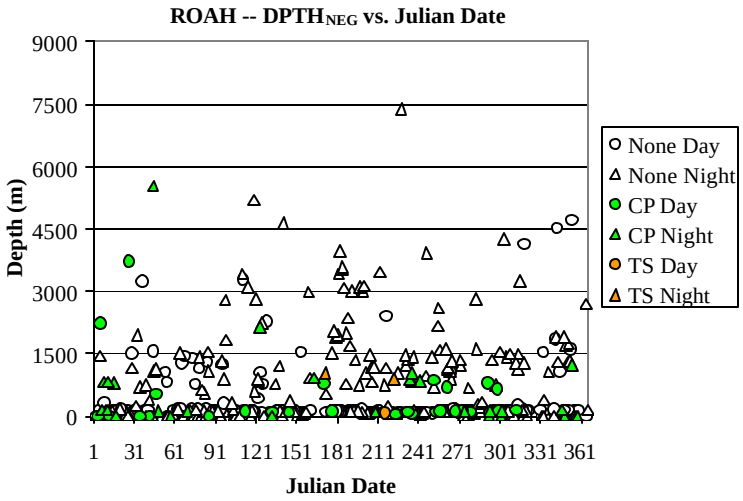

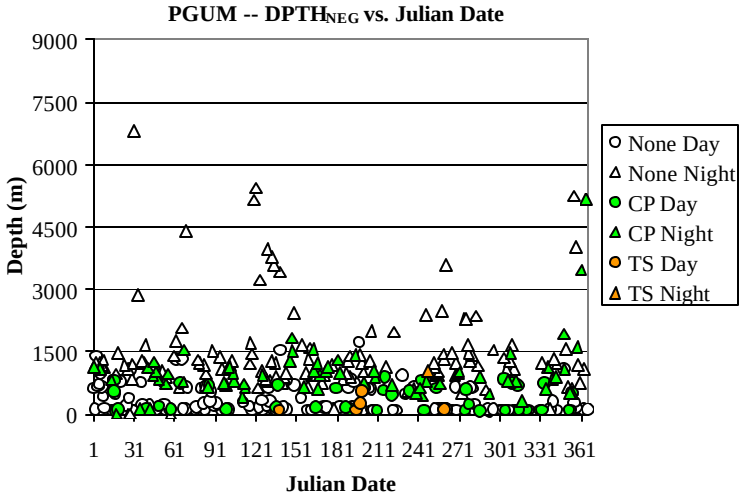

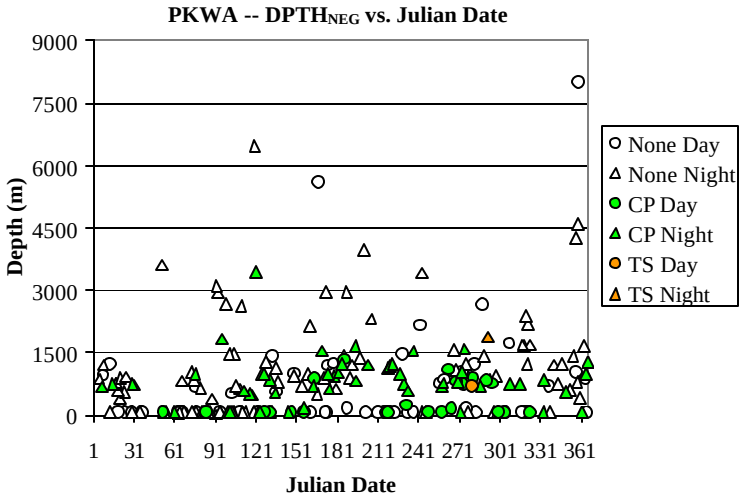

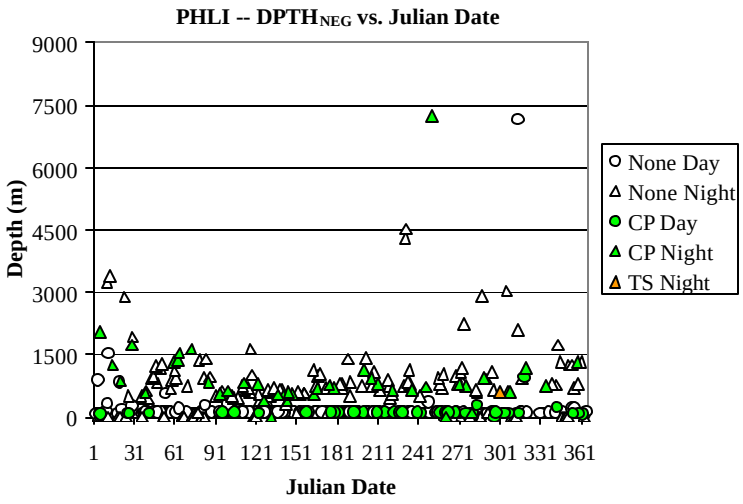
PHLI -- DPTH NEG vs. Julian Date
9000
7500
6000
4500
3000
1500
0
Depth (m)
1
31
61
91
121
151
181
211
241
271
301
331
361
Julian Date
None Day
None Night
CP Day
CP Night
TS Night

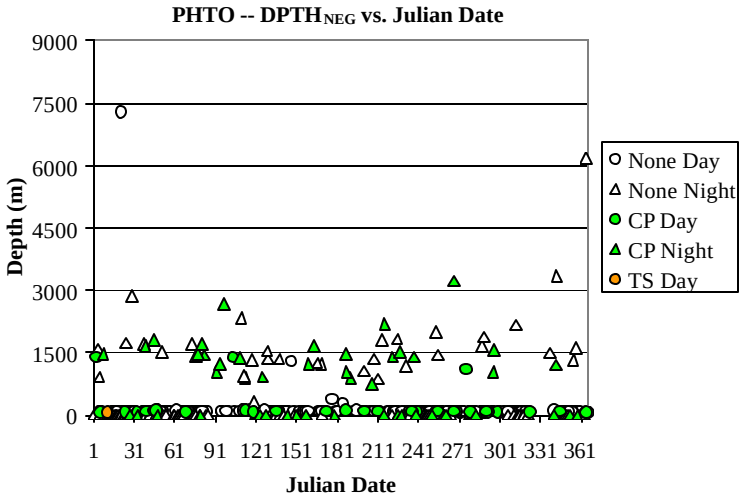
PHTO -- DPTH NEG vs. Julian Date
9000
7500
6000
4500
3000
1500
0
Depth (m)
1
31
61
91
121
151
181
211
241
271
301
331
361
Julian Date
None Day
None Night
CP Day
CP Night
TS Day

Depth of Positive Buoyancy of Surface Parcel ($DPTH_{POS}$)

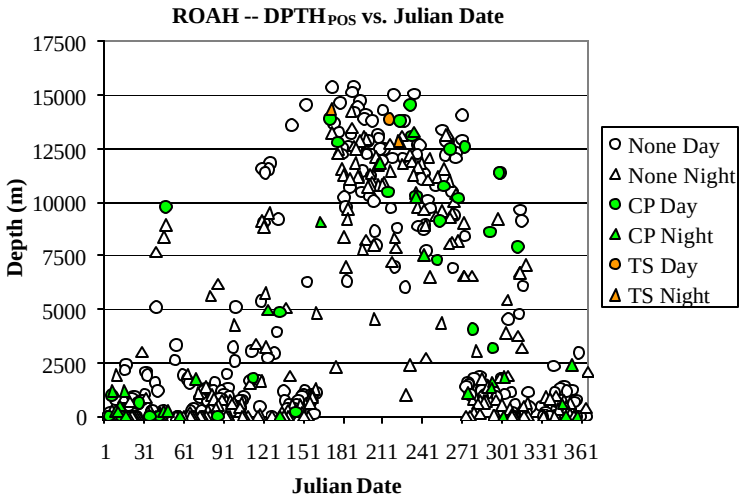

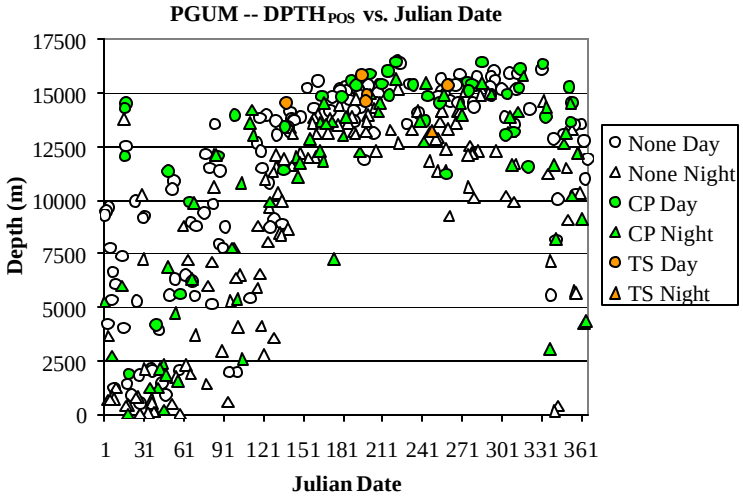

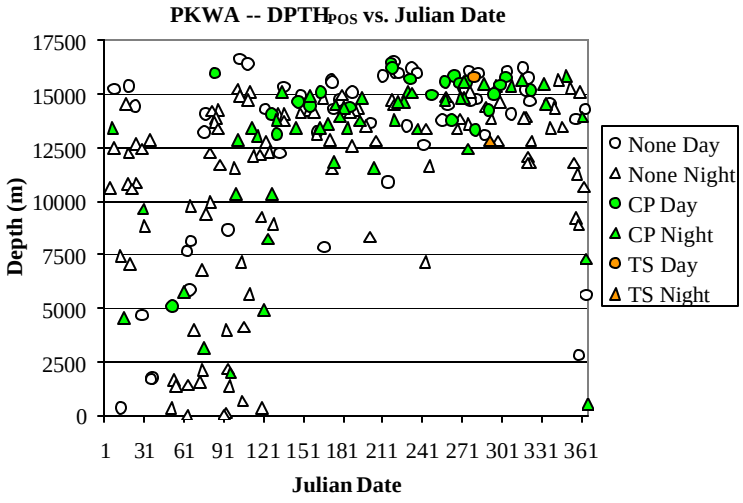

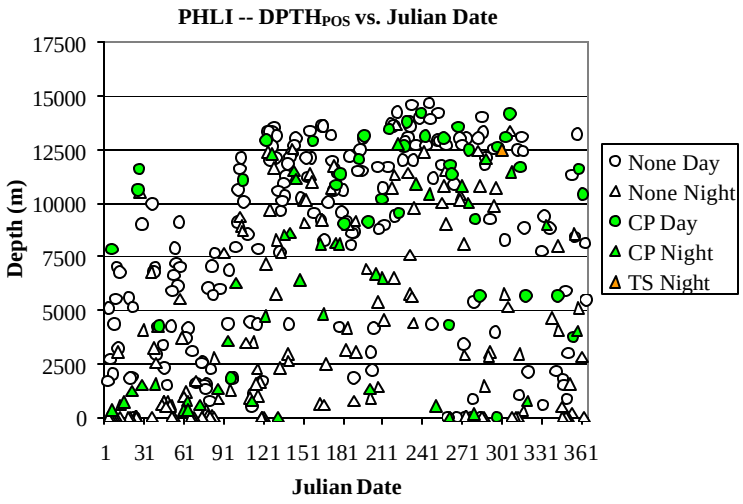
PHLI -- DPTHPOS vs. Julian Date
17500
15000
12500
10000
7500
5000
2500
0
Depth (m)
1 31 61 91 121 151 181 211 241 271 301 331 361
Julian Date
None Day
None Night
CP Day
CP Night
TS Night

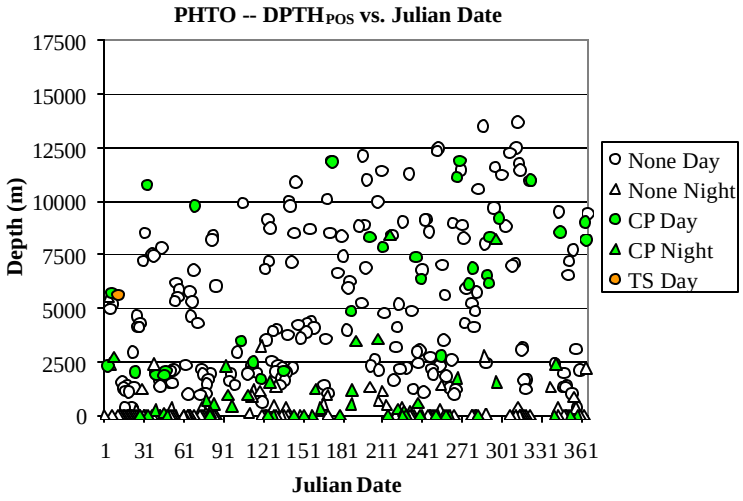
PHTO -- DPTHPOS vs. Julian Date
17500
15000
12500
10000
7500
5000
2500
0
Depth (m)
1 31 61 91 121 151 181 211 241 271 301 331 361
Julian Date
None Day
None Night
CP Day
CP Night
TS Day

Mean Relative Humidity of Low-Levels (RH_L)

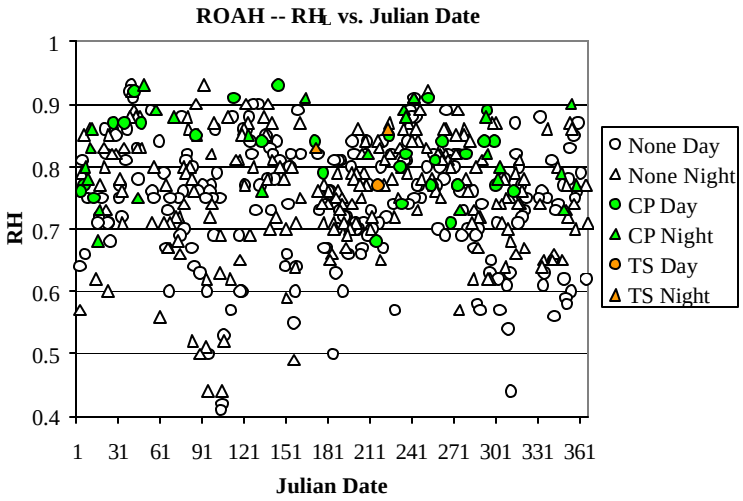

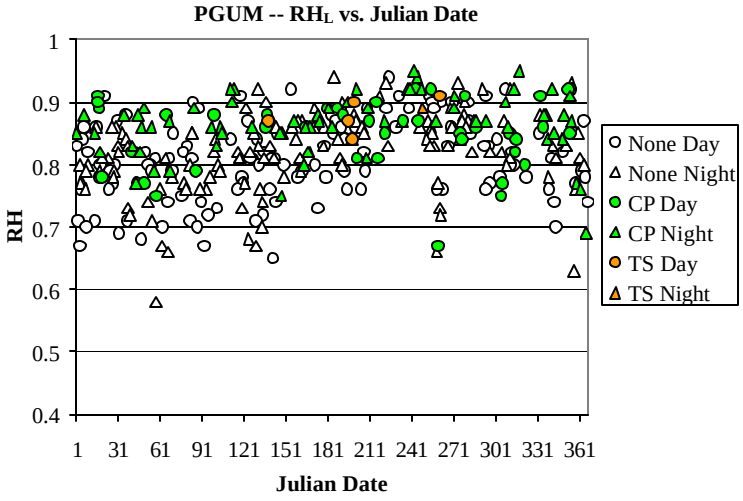

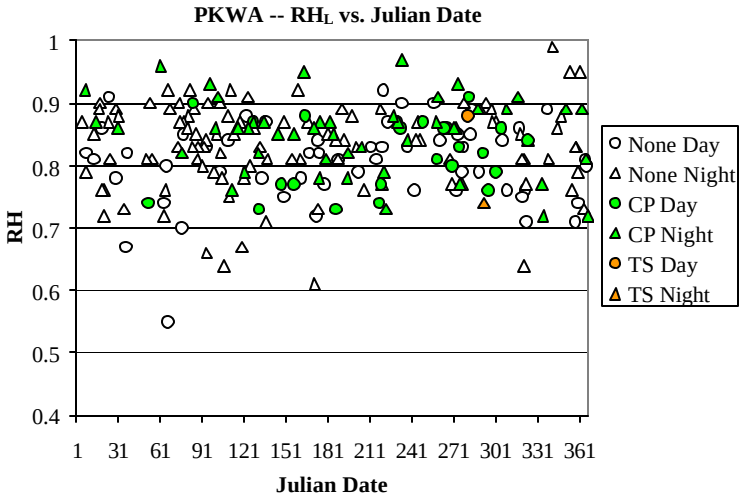

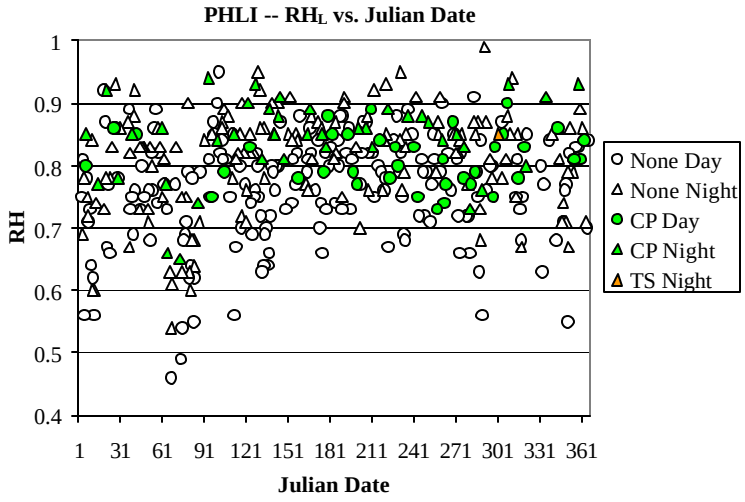
PHLI -- RH$_L$ vs. Julian Date
RH
1
0.9
0.8
0.7
0.6
0.5
0.4
1 31 61 91 121 151 181 211 241 271 301 331 361
Julian Date
None Day
None Night
CP Day
CP Night
TS Night

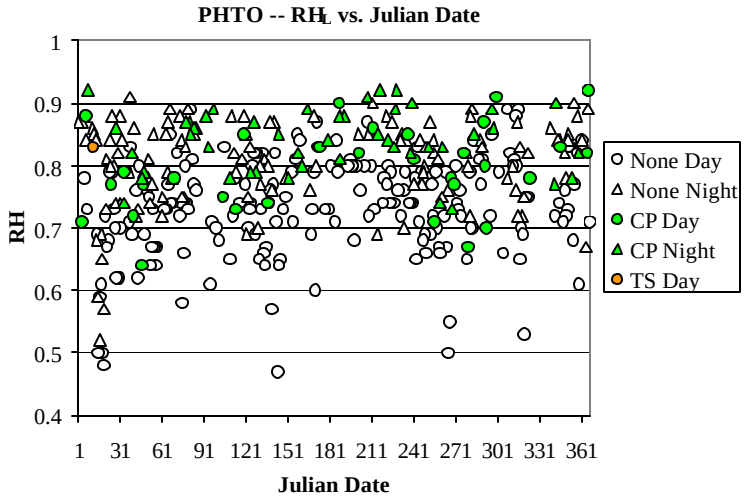
PHTO -- RH$_L$ vs. Julian Date
RH
1
0.9
0.8
0.7
0.6
0.5
0.4
1 31 61 91 121 151 181 211 241 271 301 331 361
Julian Date
None Day
None Night
CP Day
CP Night
TS Day

Mean Relative Humidity of Mid-Levels (RH_M)

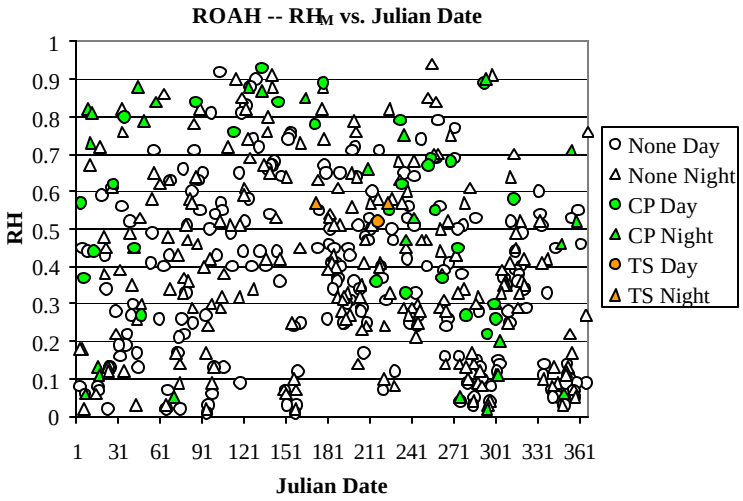

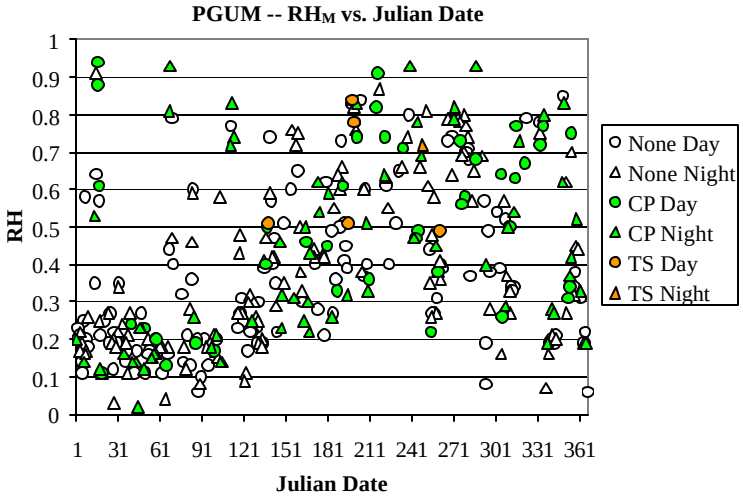

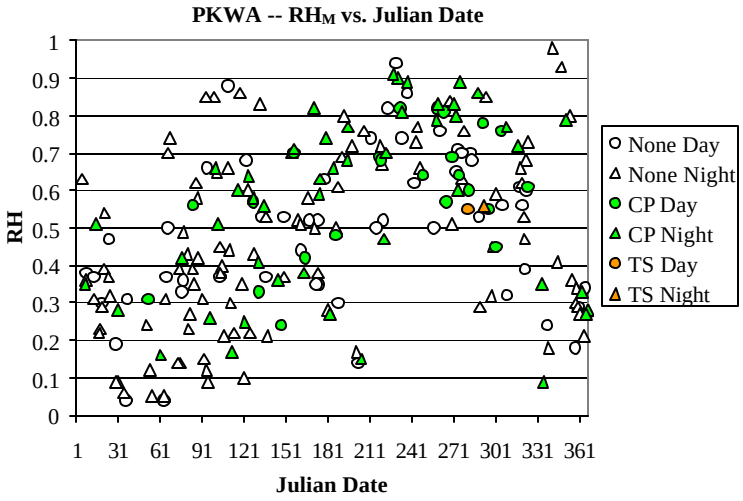

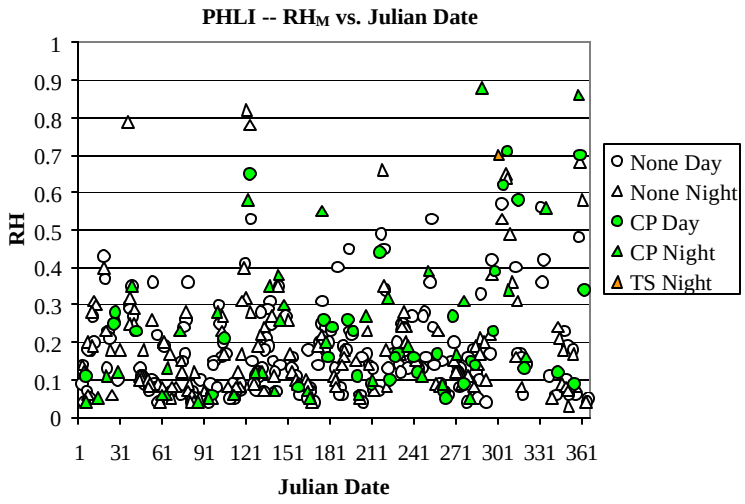
PHLI -- RHM vs. Julian Date
RH
Julian Date
None Day
None Night
CP Day
CP Night
TS Night

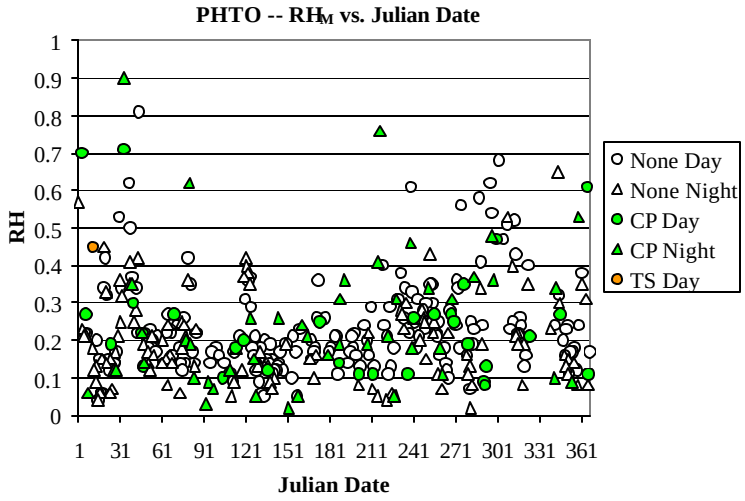
PHTO -- RHM vs. Julian Date
RH
Julian Date
None Day
None Night
CP Day
CP Night
TS Day

Wind Shear between Low- and Mid-Levels (SHR_{LM})

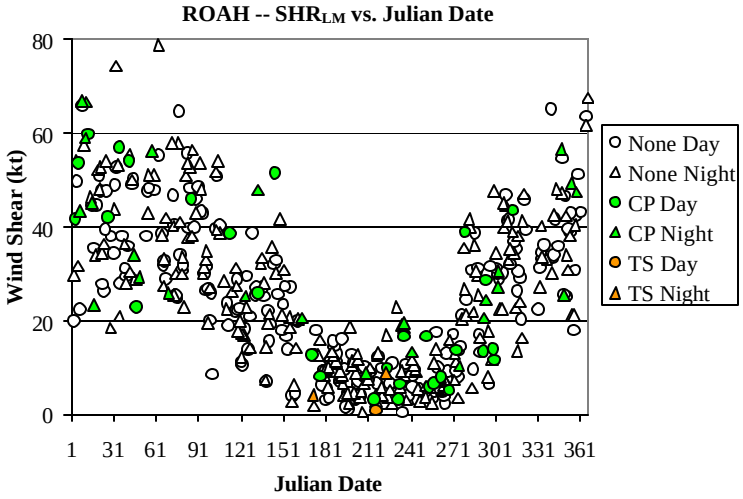

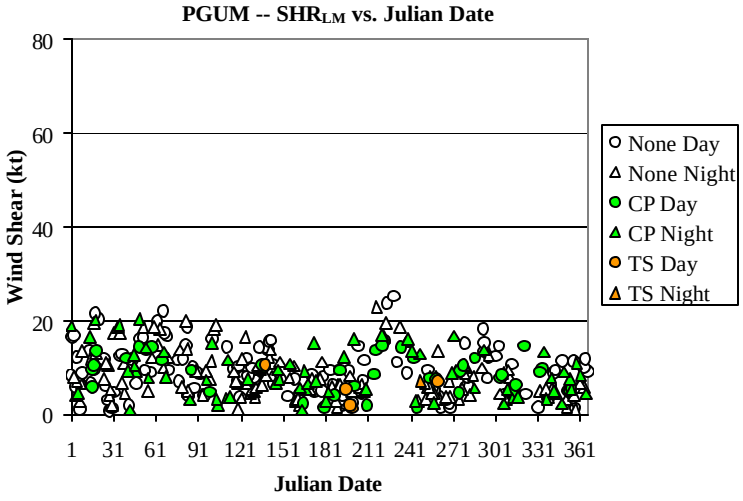

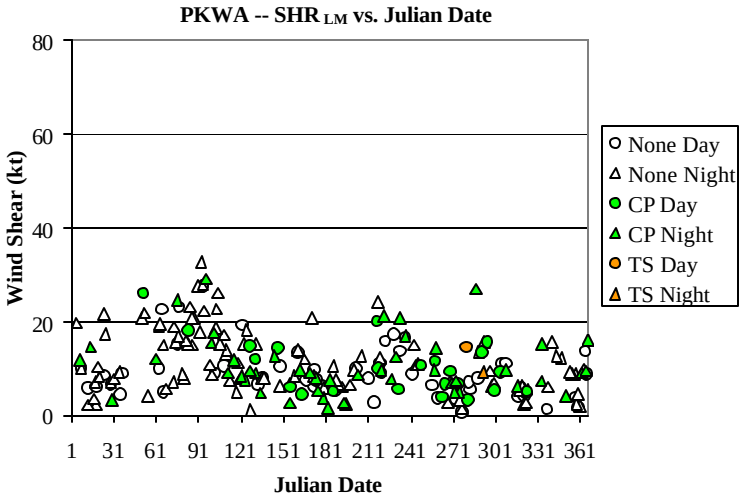

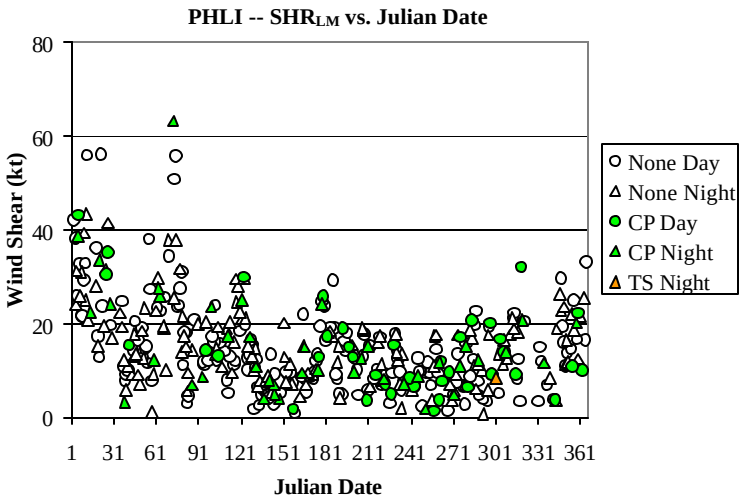
PHLI -- SHR$_{LM}$ vs. Julian Date
Wind Shear (kt)
0
20
40
60
80
1
31
61
91
121
151
181
211
241
271
301
331
361
Julian Date
None Day
None Night
CP Day
CP Night
TS Night

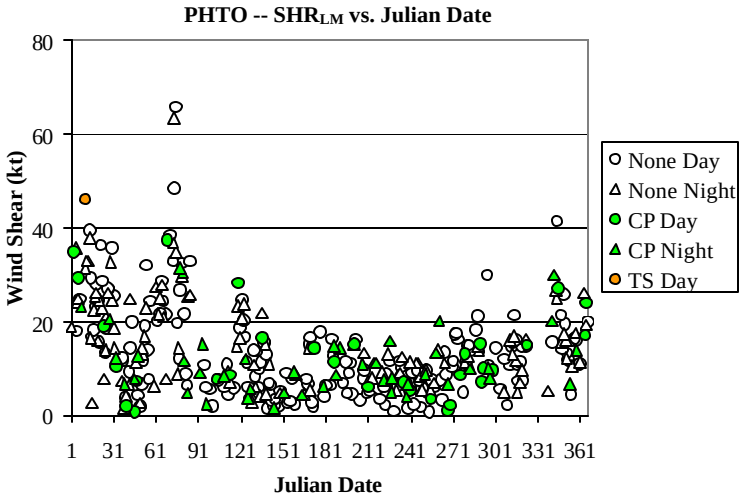
PHTO -- SHR$_{LM}$ vs. Julian Date
Wind Shear (kt)
0
20
40
60
80
1
31
61
91
121
151
181
211
241
271
301
331
361
Julian Date
None Day
None Night
CP Day
CP Night
TS Day

Mean Wind Speed of Low-Levels (SPD_L)

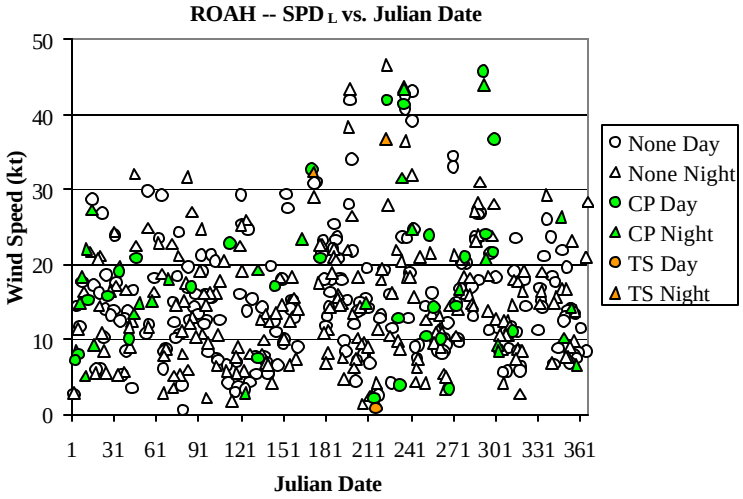

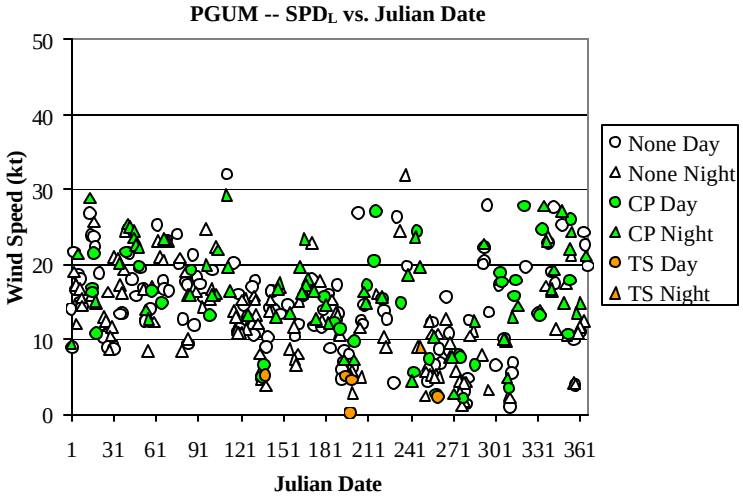

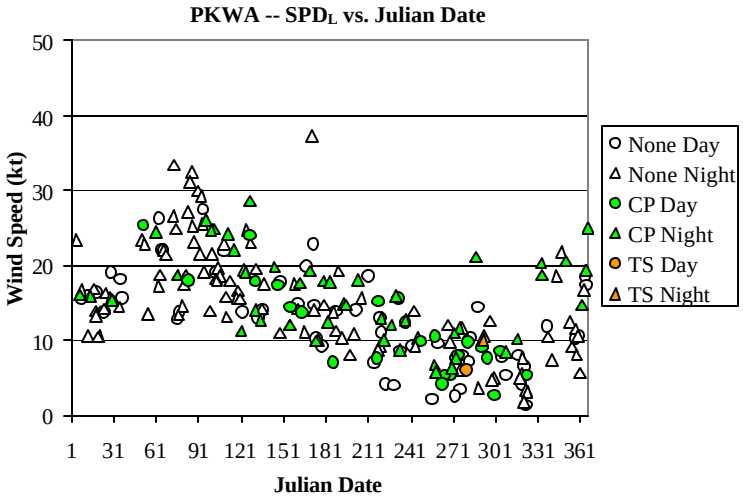

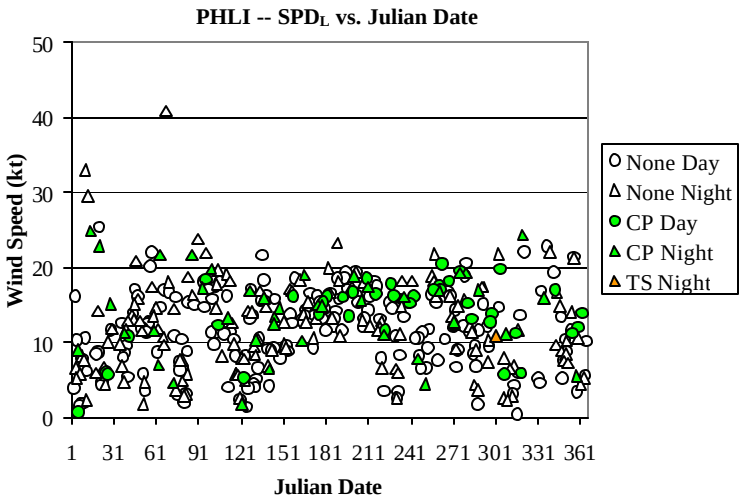
PHLI -- SPDL vs. Julian Date
Wind Speed (kt)
0
10
20
30
40
50
1
31
61
91
121
151
181
211
241
271
301
331
361
Julian Date
None Day
None Night
CP Day
CP Night
TS Night

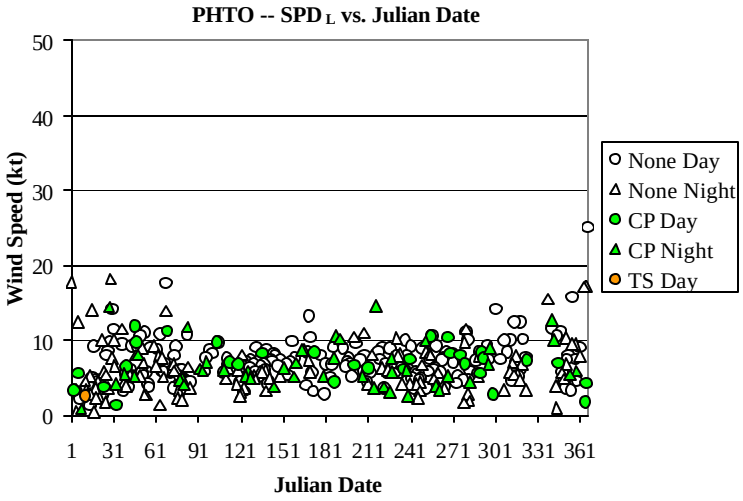
PHTO -- SPD L vs. Julian Date
Wind Speed (kt)
0
10
20
30
40
50
1
31
61
91
121
151
181
211
241
271
301
331
361
Julian Date
None Day
None Night
CP Day
CP Night
TS Day

Showalter Index (SSI)

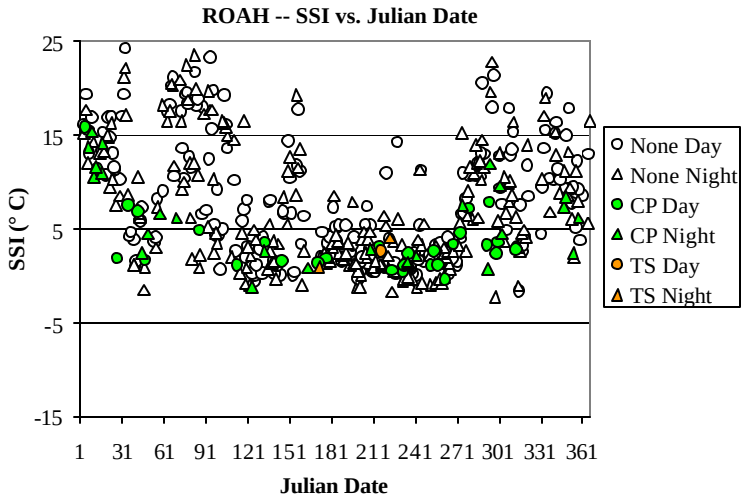

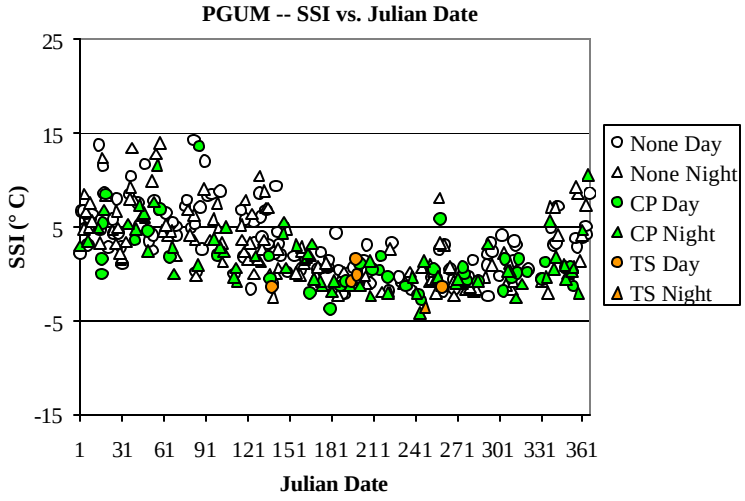

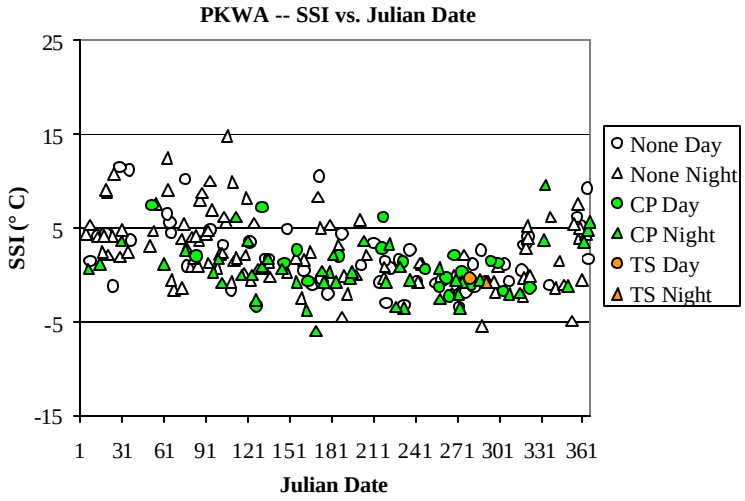

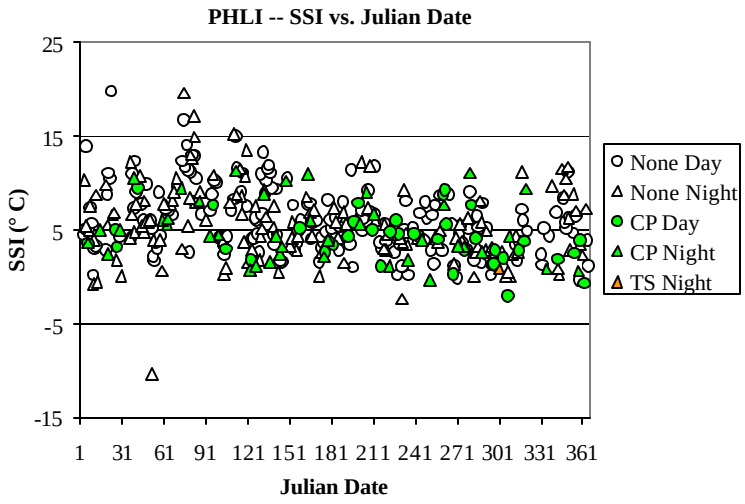
PHLI -- SSI vs. Julian Date
SSI (° C)
25
15
5
-5
-15
1 31 61 91 121 151 181 211 241 271 301 331 361
Julian Date
None Day
None Night
CP Day
CP Night
TS Night

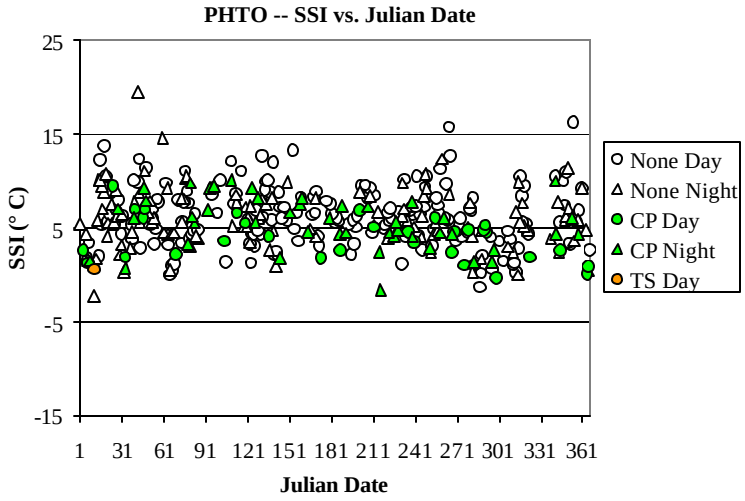
PHTO -- SSI vs. Julian Date
SSI (° C)
25
15
5
-5
-15
1 31 61 91 121 151 181 211 241 271 301 331 361
Julian Date
None Day
None Night
CP Day
CP Night
TS Day

Severe Weather Threat Index (SWEAT)

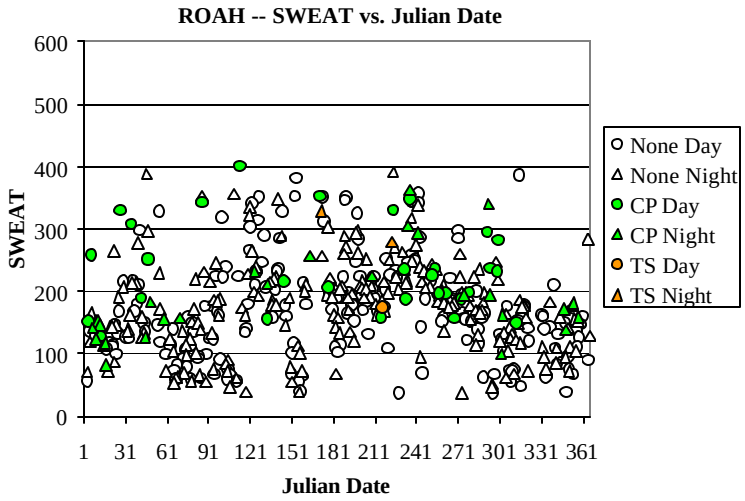

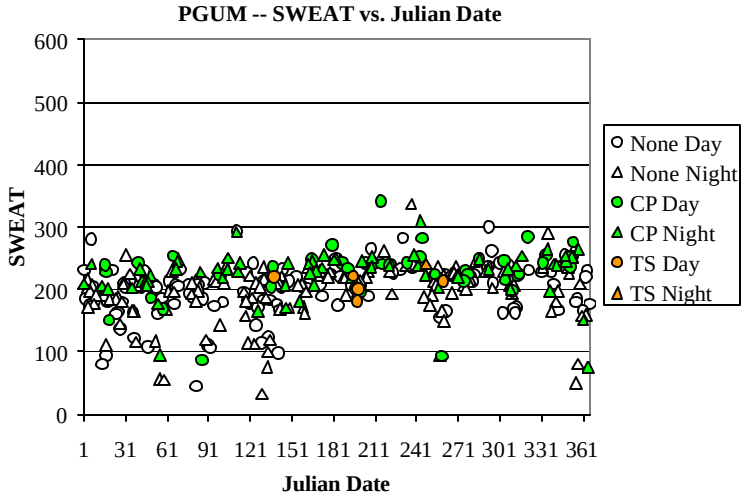

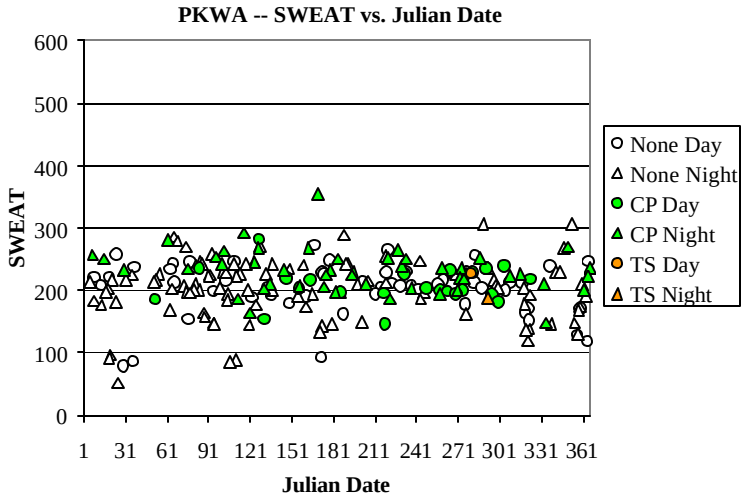

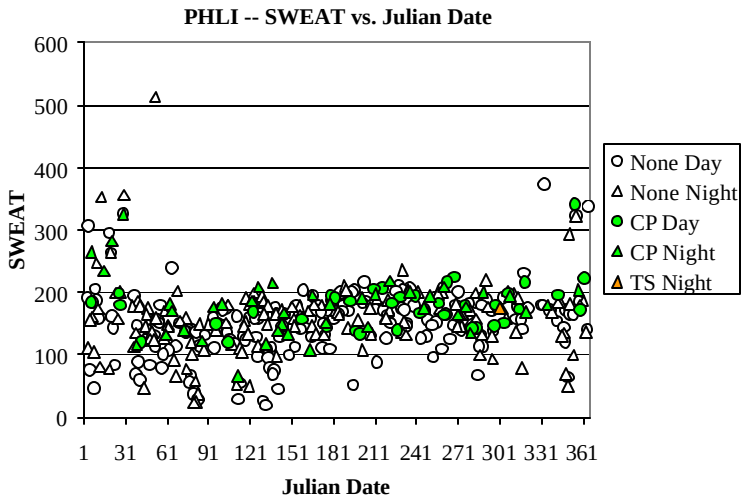
PHLI -- SWEAT vs. Julian Date
SWEAT
600
500
400
300
200
100
0
1 31 61 91 121 151 181 211 241 271 301 331 361
Julian Date
None Day
None Night
CP Day
CP Night
TS Night

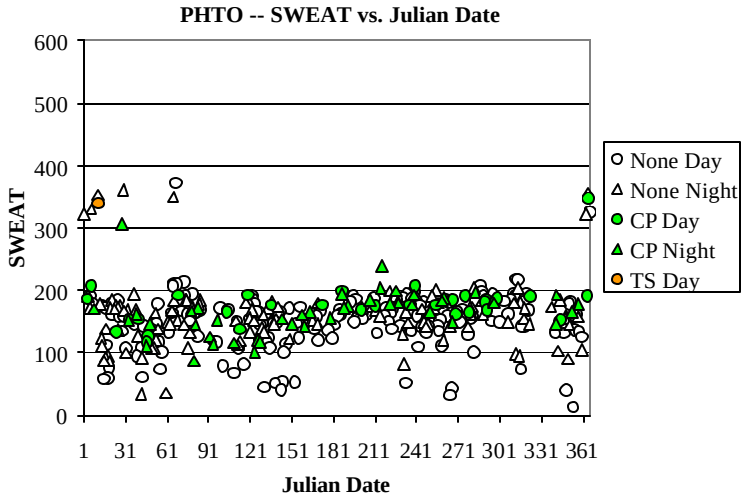
PHTO -- SWEAT vs. Julian Date
SWEAT
600
500
400
300
200
100
0
1 31 61 91 121 151 181 211 241 271 301 331 361
Julian Date
None Day
None Night
CP Day
CP Night
TS Day

Mean Temperature of High-Levels ($TEMP_H$)

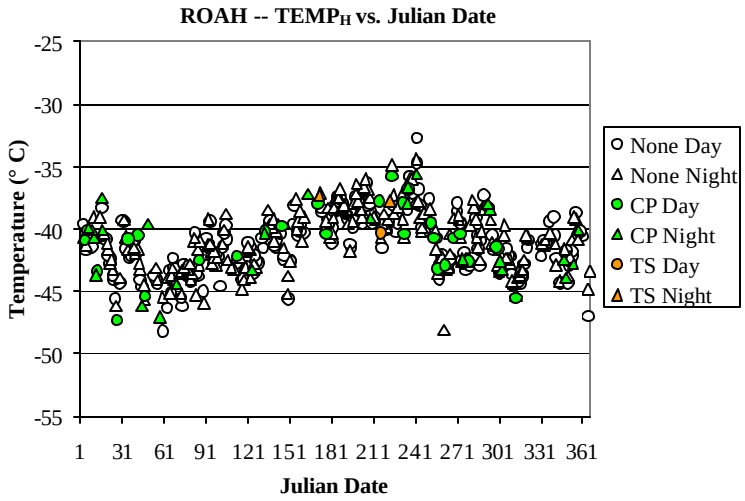

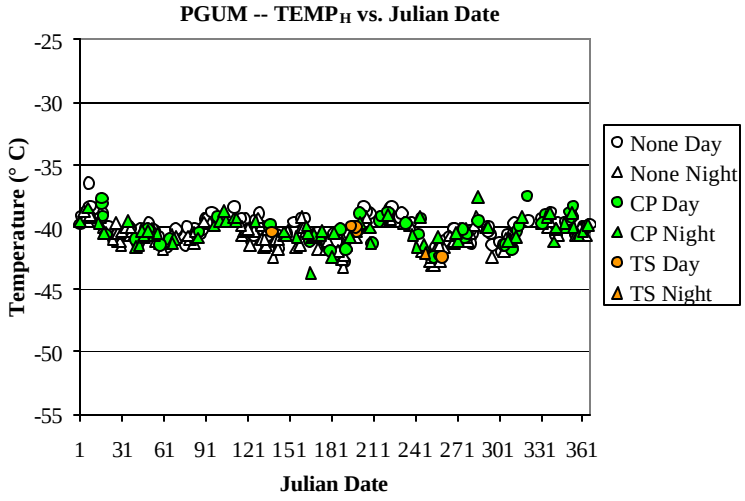

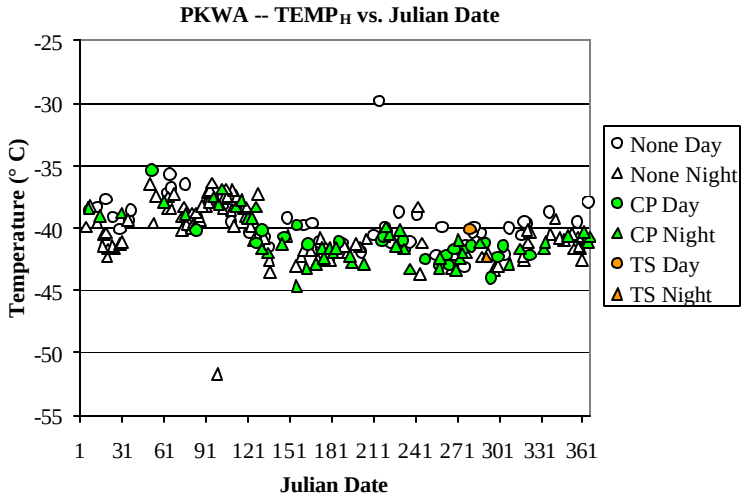

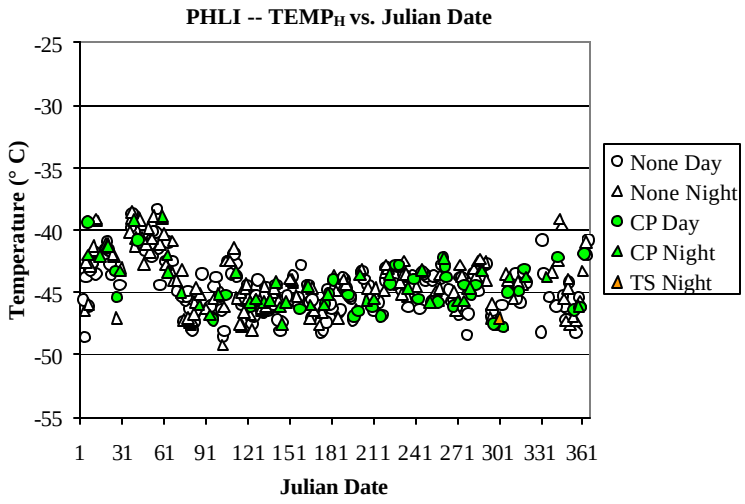
PHLI -- TEMPH vs. Julian Date
-25
-30
-35
-40
-45
-50
-55
Temperature (° C)
1 31 61 91 121 151 181 211 241 271 301 331 361
Julian Date
None Day
None Night
CP Day
CP Night
TS Night

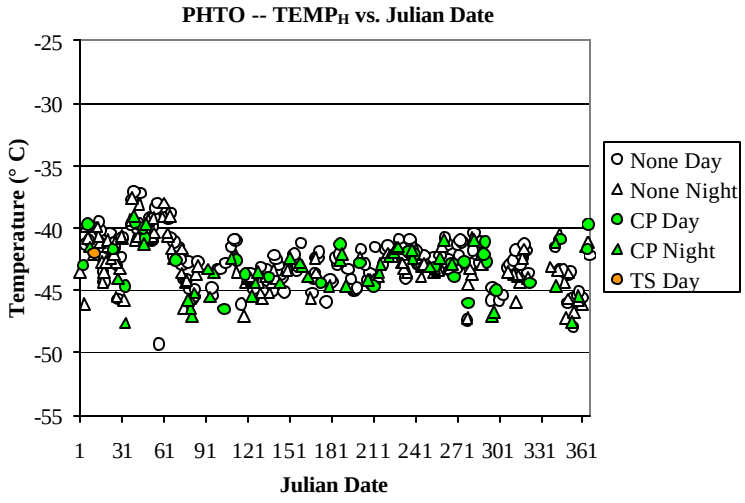
PHTO -- TEMPH vs. Julian Date
-25
-30
-35
-40
-45
-50
-55
Temperature (° C)
1 31 61 91 121 151 181 211 241 271 301 331 361
Julian Date
None Day
None Night
CP Day
CP Night
TS Day

Mean Temperature of Low-Levels ($TEMP_L$)

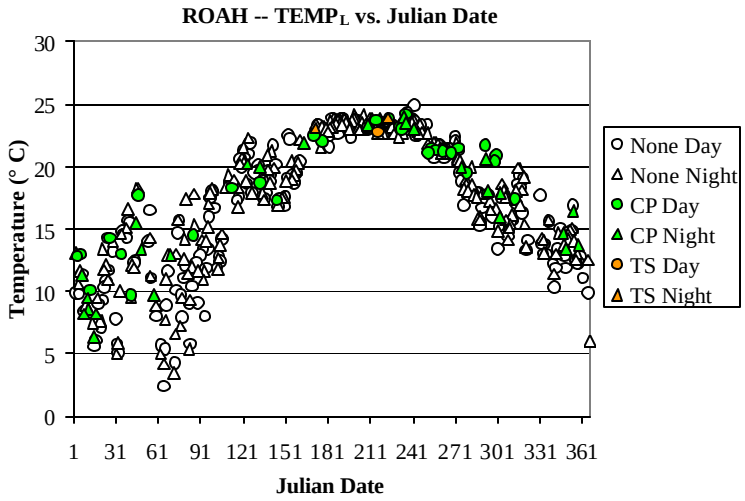

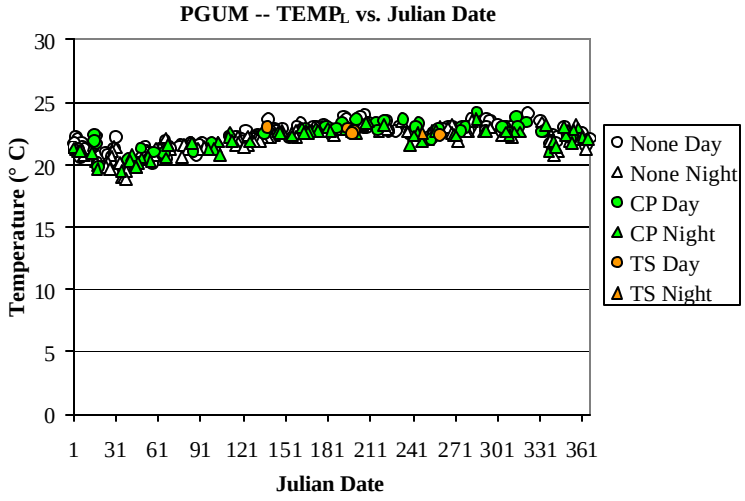

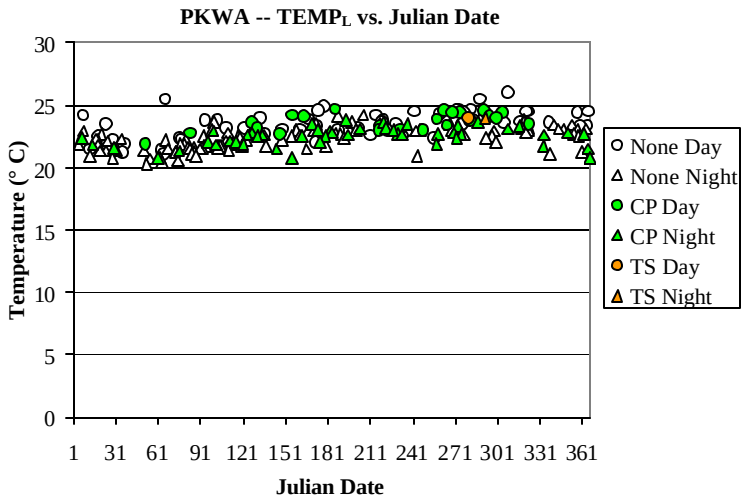

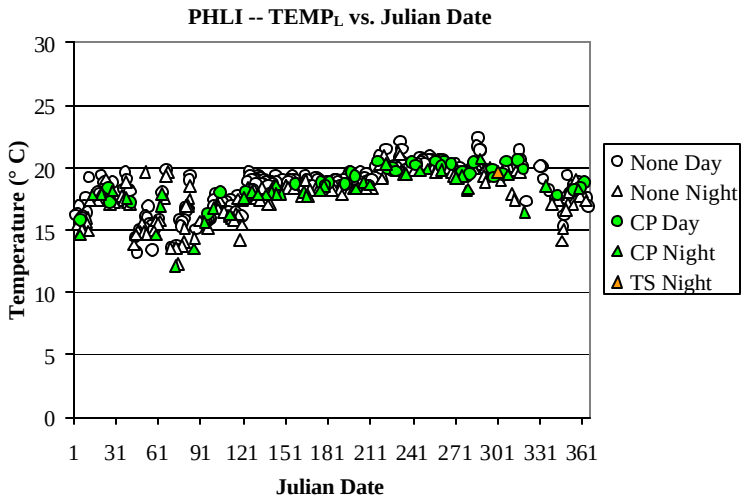
PHLI -- TEMP$_L$ vs. Julian Date
Temperature (° C)
30
25
20
15
10
5
0
1 31 61 91 121 151 181 211 241 271 301 331 361
Julian Date
None Day
None Night
CP Day
CP Night
TS Night

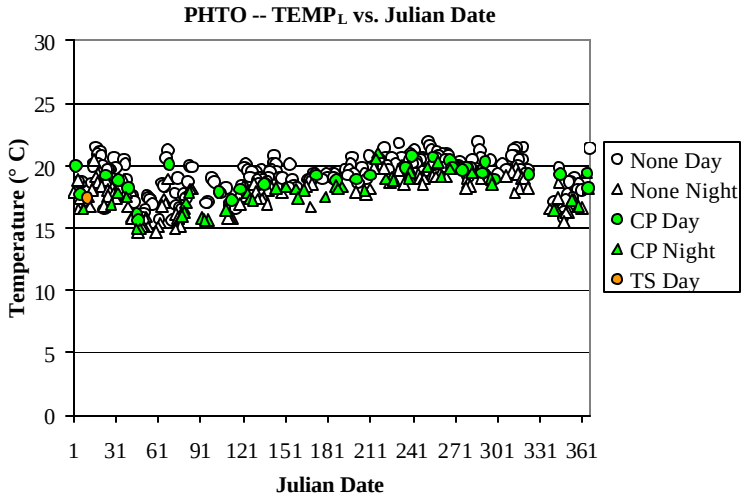
PHTO -- TEMP$_L$ vs. Julian Date
Temperature (° C)
30
25
20
15
10
5
0
1 31 61 91 121 151 181 211 241 271 301 331 361
Julian Date
None Day
None Night
CP Day
CP Night
TS Day

Total Totals Index (TT)

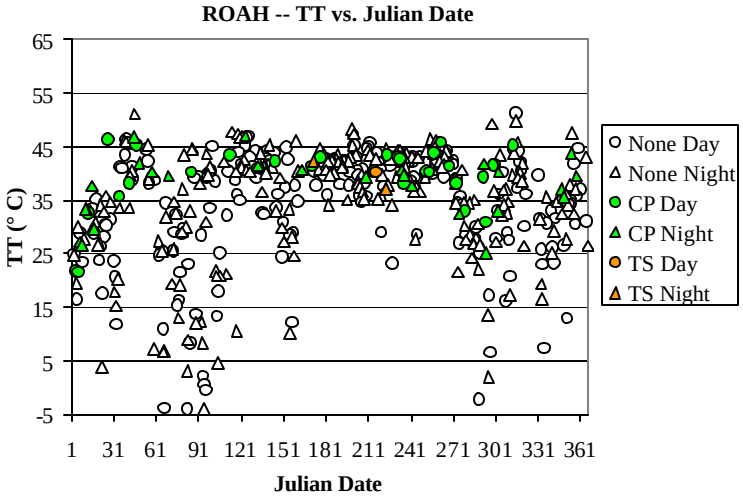

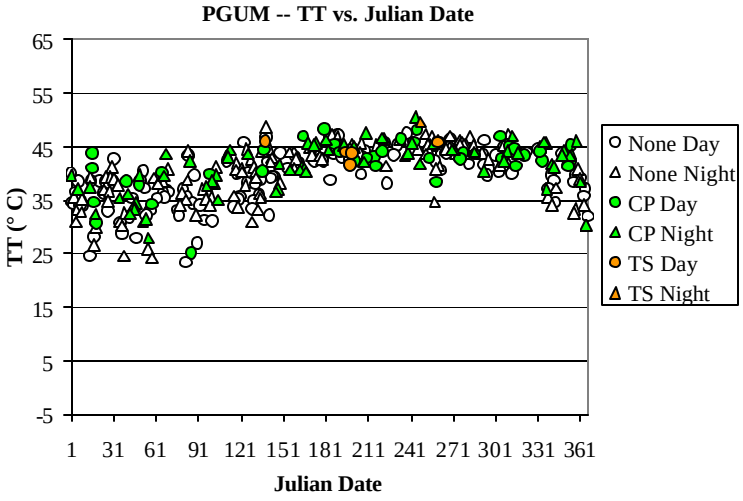

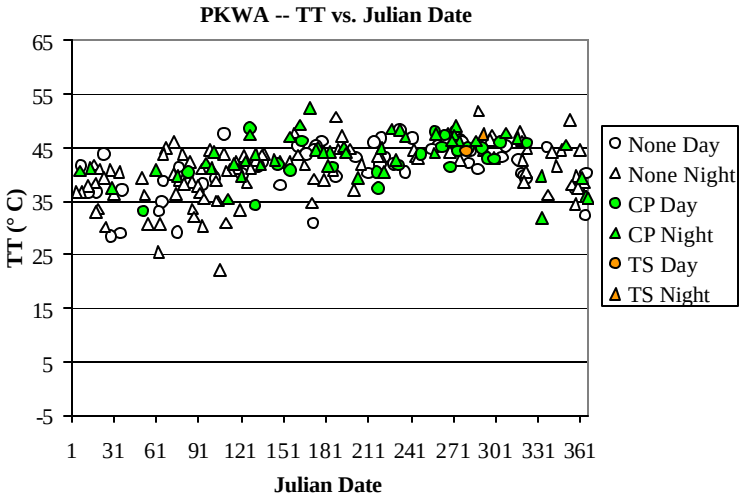

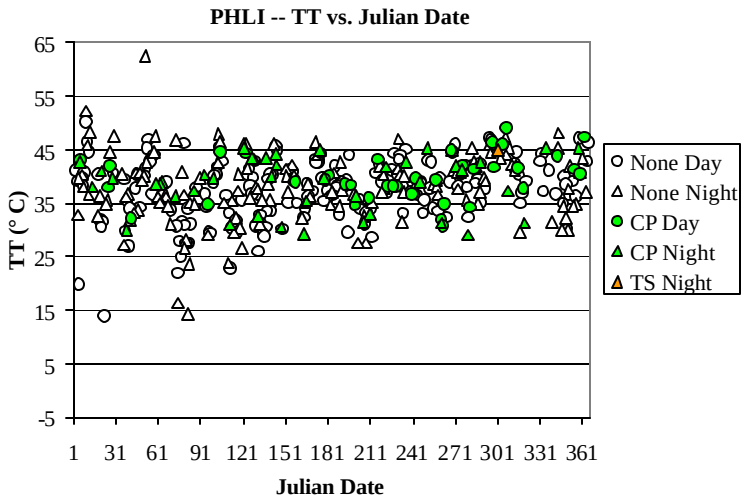
PHLI -- TT vs. Julian Date
TT (° C)
65
55
45
35
25
15
5
-5
1 31 61 91 121 151 181 211 241 271 301 331 361
Julian Date
None Day
None Night
CP Day
CP Night
TS Night

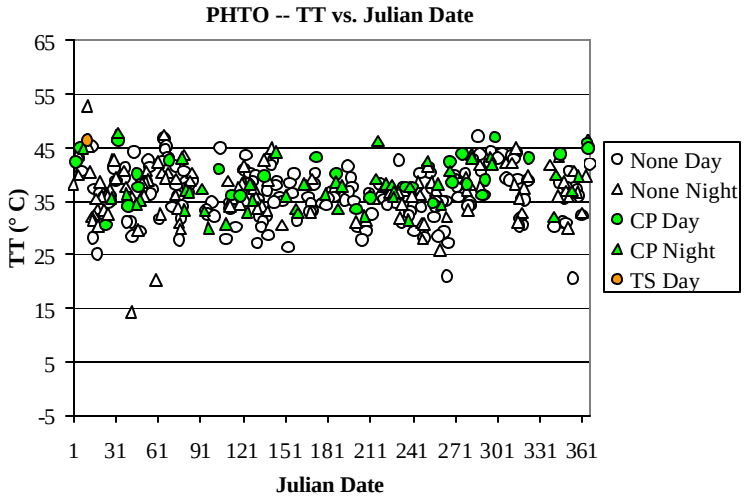
PHTO -- TT vs. Julian Date
TT (° C)
65
55
45
35
25
15
5
-5
1 31 61 91 121 151 181 211 241 271 301 331 361
Julian Date
None Day
None Night
CP Day
CP Night
TS Day

Vertical Totals Index (VT)

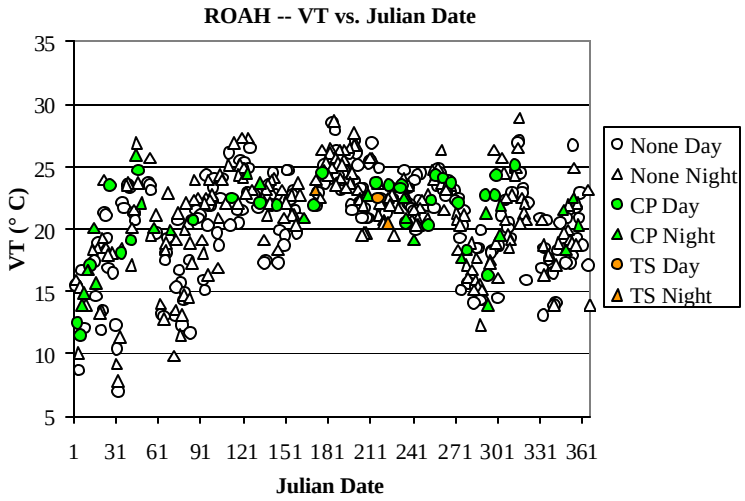

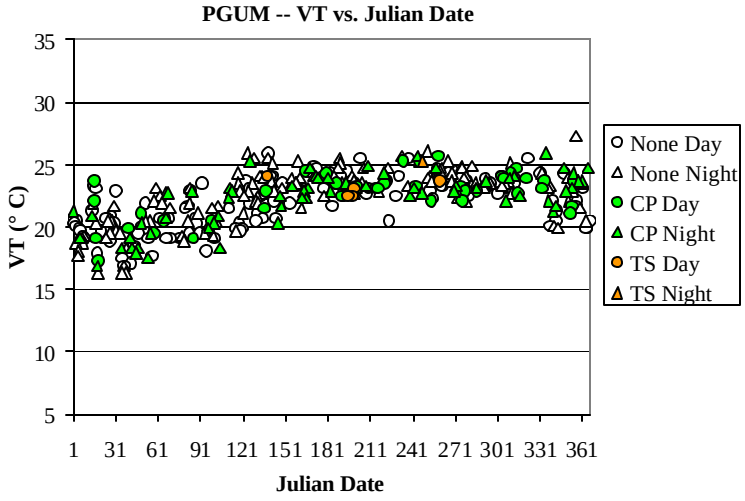

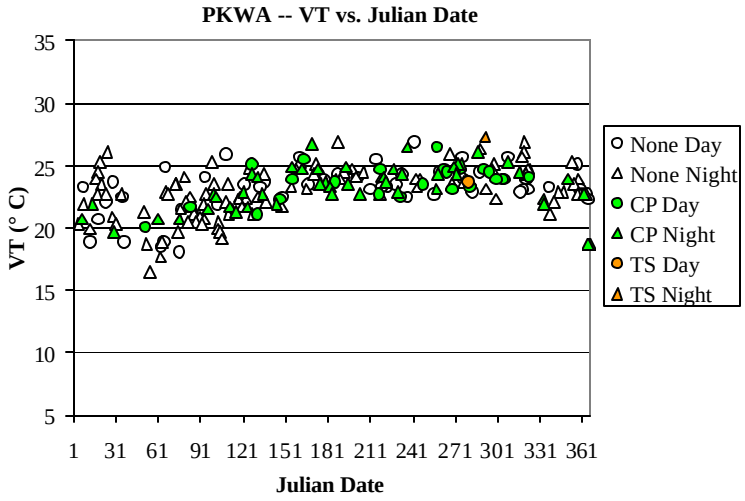

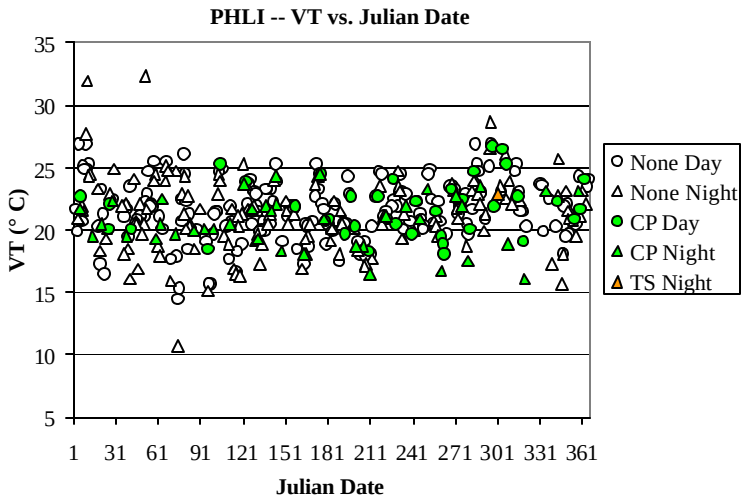
PHLI -- VT vs. Julian Date
VT (° C)
35
30
25
20
15
10
5
1 31 61 91 121 151 181 211 241 271 301 331 361
Julian Date
None Day
None Night
CP Day
CP Night
TS Night

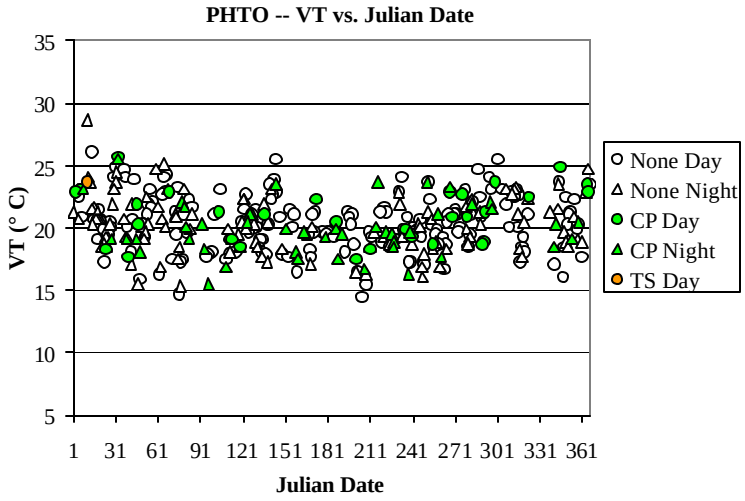
PHTO -- VT vs. Julian Date
VT (° C)
35
30
25
20
15
10
5
1 31 61 91 121 151 181 211 241 271 301 331 361
Julian Date
None Day
None Night
CP Day
CP Night
TS Day

APPENDIX C – MAXIMUM HEIDKE SKILL SCORES (MAX HSS)

Max HSS of Indices Predicting Convective Precipitation during Summer with Surface Observations as Truth

Index	ROAH	PGUM	PKWA	PHLI	PHTO
Best					
CAPEsfc	0.096	0.156	0.212	0.040	0.020
CINsfc	0.052	0.208	0.170	0.000	0.003
CT	0.105	0.109	0.191	0.163	0.253
DPTHneg	0.038	0.077	0.070	0.079	0.259
DPTHpos	0.145	0.196	0.221	0.049	0.043
KI	0.241	0.111	0.248	0.152	0.118
LIsfc	0.021	0.059	0.032	0.107	0.214
NCAPEsfc	0.066	0.102	0.195	0.040	0.000
RHL	0.247	0.211	0.177	0.225	0.379
RHM	0.234	0.141	0.245	0.161	0.099
SHRLM	0.074	0.120	0.108	0.109	0.049
SPDL	0.230	0.245	0.161	0.208	0.140
SSI	0.015	0.018	0.014	0.024	0.000
SWEAT	0.167	0.363	0.220	0.273	0.375
TEMPH	0.149	0.139	0.000	0.098	0.081
TEMPL	0.087	0.101	0.021	0.063	0.007
TT	0.063	0.090	0.201	0.136	0.194
VT	0.014	0.050	0.095	0.021	0.104

Threshold Values for above

Index	ROAH	PGUM	PKWA	PHLI	PHTO
Best					
CAPEsfc	1463.7	3057.4	2548.5	3210.3	1315.1
CINsfc	-23.17	-11.992	-28.528	0	-315.43
CT	17.6	18.565	20.127	19.7	17.22
DPTHneg	663.48	184.45	144.5	362	419.64
DPTHpos	12461	15403	14441	12752	11100
KI	34.02	26.74	34.376	16.01	21.148
LIsfc	-3.082	-4.052	-0.26	1.724	4.588
NCAPEsfc	0.1512	0.2008	0.2016	0.2324	0.13
RHL	0.904	0.8601	0.8532	0.822	0.803
RHM	0.7447	0.6665	0.7664	0.2506	0.2346
SHRLM	43.46	11.597	14.067	24.058	13.883
SPDL	31.094	14.148	14.324	14.48	9.68
SSI	0.3	-0.879	-4.35	8.747	15.8
SWEAT	328.44	237.04	192.64	182.05	174.69
TEMPH	-38.09	-40.065	-29.8	-42.98	-43.299
TEMPL	23.886	23.212	23.712	19.601	16.908
TT	40.016	47.479	44.76	41.75	37.632
VT	19.996	25.54	24.376	23.716	23.19

Max HSS of Indices Predicting Convective Precipitation during Winter with Surface Observations as Truth

Index	ROAH	PGUM	PKWA	PHLI	PHTO
Best					
CAPEsfc	0.149	0.161	0.161	0.196	0.112
CINsfc	0.005	0.105	0.131	0.038	0.013
CT	0.228	0.268	0.304	0.165	0.181
DPTHneg	0.070	0.109	0.035	0.177	0.298
DPTHpos	0.178	0.175	0.155	0.252	0.156
KI	0.219	0.207	0.220	0.145	0.140
LIsfc	0.006	0.023	0.044	0.000	0.004
NCAPEsfc	0.115	0.134	0.161	0.155	0.087
RHL	0.227	0.429	0.186	0.164	0.197
RHM	0.338	0.185	0.159	0.217	0.154
SHRLM	0.189	0.021	0.119	0.073	0.049
SPDL	0.146	0.226	0.210	0.179	0.029
SSI	0.006	0.000	0.000	0.005	0.004
SWEAT	0.282	0.441	0.345	0.210	0.139
TEMPH	0.215	0.085	0.073	0.023	0.004
TEMPL	0.217	0.146	0.146	0.164	0.004
TT	0.206	0.243	0.262	0.143	0.176
VT	0.069	0.092	0.087	0.033	0.062

Threshold values of Above

Index	ROAH	PGUM	PKWA	PHLI	PHTO
Best					
CAPEsfc	323.18	987.12	3486.8	680.68	592.48
CINsfc	-7.6761	-9.5524	-2.2827	-92.341	-437.82
CT	16.495	18.202	18.604	18.65	20.887
DPTHneg	1991.5	407.52	453.6	572.48	1020.6
DPTHpos	7739.1	11678	12831	9920.4	5605.1
KI	26.174	29.322	30.35	29.41	17.983
LIsfc	-4.58	6.792	-2.169	20.1	-5.103
NCAPEsfc	0.1005	0.08	0.232	0.093	0.0513
RHL	0.8614	0.8425	0.8534	0.8204	0.8408
RHM	0.7854	0.4432	0.502	0.5315	0.4336
SHRLM	53.315	18.694	11.332	32.01	28.132
SPDL	32.24	19.028	23.51	18.22	4.846
SSI	1.69	14.3	14.8	0.472	-1.115
SWEAT	230.33	228	231.85	165.04	185.56
TEMPH	-40.134	-38.948	-35.563	-39.499	-47.836
TEMPL	19.384	22.208	21.704	17.765	14.7
TT	37.475	39.528	39.624	37.28	42.305
VT	19.483	23.56	20.532	18.476	24.78

Max HSS of Indices Predicting Convective Precipitation during Summer with Rainrates as Truth

Index	ROAH	PGUM	PKWA	PHLI	PHTO
Best					
CAPEsfc	0.000	0.224	0.108	0.096	0.092
CINsfc	0.001	0.062	0.038	0.009	0.001
CT	0.077	0.107	0.189	0.125	0.028
DPTHneg	0.119	0.016	0.044	0.378	0.072
DPTHpos	0.085	0.135	0.078	0.061	0.092
KI	0.295	0.282	0.209	0.121	0.003
LIsfc	0.041	0.244	0.004	0.226	0.157
NCAPEsfc	0.000	0.240	0.076	0.108	0.092
RHL	0.119	0.295	0.137	0.121	0.073
RHM	0.341	0.278	0.171	0.192	0.000
SHRLM	0.166	0.133	0.047	0.044	0.079
SPDL	0.418	0.117	0.058	0.146	0.092
SSI	0.004	0.061	0.000	0.040	0.070
SWEAT	0.450	0.193	0.196	0.136	0.112
TEMPH	0.305	0.127	0.071	0.058	0.067
TEMPL	0.144	0.025	0.051	0.121	0.037
TT	0.056	0.089	0.131	0.125	0.028
VT	0.029	0.089	0.044	0.136	0.014

Threshold Values of Above

Index	ROAH	PGUM	PKWA	PHLI	PHTO
Best					
CAPEsfc	2870	3613	4361.3	3357.9	1808.8
CINsfc	-283.83	-2.9504	-9.5094	-10.525	-425.22
CT	20.372	21.4	22.084	22.074	15.24
DPTHneg	3317.4	1490.4	160.3	1303.2	1646.3
DPTHpos	13230	15617	14571	13133	12914
KI	33.691	35.696	34.815	36.494	-17.25
LIsfc	-2.86	-2.85	-3.935	4.092	4.588
NCAPEsfc	0.21	0.2404	0.2925	0.252	0.1411
RHL	0.8725	0.9018	0.8514	0.9722	0.851
RHM	0.703	0.8164	0.8121	0.3832	0.76
SHRLM	43.436	10.736	11.691	22.54	13.118
SPDL	34.241	17.616	10.206	20.988	15.8
SSI	-0.482	4.509	9.6	6.262	5.186
SWEAT	324.55	251.49	220.56	247.3	204.38
TEMPH	-35.934	-40.454	-40.525	-42.738	-42.772
TEMPL	23.886	23.602	23.674	21.539	21.211
TT	40.016	49.73	47.16	45.276	35.112
VT	20.948	26.126	23.902	25.79	16.767

Max HSS of Indices Predicting Convective Precipitation during Winter with Rainrates as Truth

Index	ROAH	PGUM	PKWA	PHLI	PHTO
Best					
CAPEsfc	0.085	0.090	0.124	0.153	0.000
CINsfc	0.004	0.032	0.062	0.027	0.010
CT	0.223	0.165	0.207	0.148	0.036
DPTHneg	0.274	0.015	0.040	0.097	0.190
DPTHpos	0.098	0.100	0.088	0.193	0.000
KI	0.188	0.316	0.415	0.228	0.042
LIsfc	0.129	0.003	0.080	0.002	0.183
NCAPEsfc	0.070	0.064	0.100	0.119	0.000
RHL	0.182	0.277	0.175	0.193	0.056
RHM	0.229	0.221	0.206	0.187	0.097
SHRLM	0.188	0.024	0.084	0.191	0.051
SPDL	0.176	0.153	0.031	0.096	0.181
SSI	0.050	0.038	0.009	0.001	0.084
SWEAT	0.198	0.168	0.146	0.127	0.065
TEMPH	0.083	0.060	0.066	0.094	0.068
TEMPL	0.061	0.045	0.125	0.133	0.055
TT	0.209	0.153	0.184	0.111	0.039
VT	0.126	0.083	0.041	0.063	0.012

Threshold Values of Above

Index	ROAH	PGUM	PKWA	PHLI	PHTO
Best					
CAPEsfc	86.16	3908	3985.2	1493.6	2576
CINsfc	-186.79	-28.657	-42.173	-65.958	-121.62
CT	20.516	23.228	20.644	21.376	16.58
DPTHneg	1770.2	543.36	1301.8	1860.6	1705.9
DPTHpos	2501.6	15692	12694	10947	13671
KI	26.609	35.832	33.505	20.884	14.02
LIsfc	15.43	-3.408	2.115	5.195	2.857
NCAPEsfc	0.06	0.2523	0.1421	0.16	0.19
RHL	0.8504	0.9204	0.9502	0.9105	0.903
RHM	0.5288	0.6115	0.5144	0.4746	0.6824
SHRLM	50.506	6.3596	23.221	30.133	37.897
SPDL	28.632	25.832	24.952	22.675	15.467
SSI	22.01	11.64	6.293	-4.09	4.334
SWEAT	304.68	245.88	231.7	197.6	153.49
TEMPH	-41.522	-39.974	-36.314	-37.424	-38.32
TEMPL	21.568	22.544	23.308	18.898	21.952
TT	46.336	47.136	42.264	42.89	32.674
VT	25.735	23.704	20.5	24.904	18.34

LIST OF REFERENCES

17 OWS Forecast Reference Notebook (FRN)-Area of Responsibility (AOR) [Available online at https://17ows.hickam.af.mil]. (Accessed 23 Jul 2005).

AFCCC narrative for Naha (ROAH) [Available online at https://www.afccc.af.mil]. (Accessed 20 Jan 2006).

Anthes, R. A., 1986: The general question of predictability. *Mesoscale Meteorology and Forecasting*, P. S. Ray, Ed., Amer. Meteor. Soc., Boston, MA, 636-656.

Barnes, G. M., 2001: Severe local storms in the tropics. Chap. 10, *Meteorological Monographs*, **28**, No. 50, 359-432.

Blanchard, D. O., 1998: Assessing the vertical distribution of convective available potential energy. *Wea. Forecasting*, **13**, 870-877.

Christian, H. J., R. J. Blakeslee, S. J. Goodman, D. A. Mach, M. F. Stewart, D. E. Buechler, W. J. Koshak, J. M. Hall, W. L. Boeck, K. T. Driscoll, D. J. Boccippio, 1999: The lightning imaging sensor. Proceedings, *11th Conf. on Atmos. Electricity,* Guntersville, AL, 746-749.

Doswell, C. A. III, 1996: On convective indices and sounding classification. Preprints, *5th Australian Severe Thunderstorm Conv*., Avoca Beach, NSW, Australia, Bureau of Meteor., 7-12.

_____, 2001: Severe Convective Storms—an overview. Chap. 1, *Meteorological Monographs*, **28**, No. 50, 1-26.

Fritsch, J. M., and G. S. Forbes, 2001: Mesoscale convective systems. Chap. 9, *Meteorological Monographs*, **28**, No. 50, 323-357.

Fujita, T. T., 1986: Mesoscale classifications: their history and their application to forecasting. *Mesoscale Meteorology and Forecasting*, P. S. Ray, Ed., Amer. Meteor. Soc., Boston, MA, 18-35.

Galway, J. G., 1956: The lifted index as a predictor of latent instability. *Bull. Amer. Meteor. Soc.*, **37**, 528-529.

George, J. J., 1960: *Weather Forecasting for Aeronautics*. Academic Press, 673 pp.

Houze, R. A., 1977: Structure and dynamics of a tropical squall-line system. *Mon. Wea. Rev*., **105**, 1540-1567.

_____, 1997: Stratiform precipitation in regions of convection. *Bull. Amer. Meteor. Soc.*, **78**, 2179-95.

Johnson, R. H., and B. E. Mapes, 2001: Mesoscale processes and severe convective weather. Chap. 3, *Meteorological Monographs*, **28**, No. 50, 71-122.

_____, T. M. Richenbach, S. A. Rutledge, P. E. Ciesielski, and W. H. Schubert, 1999: Trimodal characteristics of tropical convection. *J. Climate*, **12**, 2397-2418.

Kodama, K. R., and S. Businger, 1998: Weather and forecasting challenges in the Pacific region of the National Weather Service. *Wea. Forecasting*, **13**, 523-546.

Federal Meteorological Handbook No. 1, Surface Weather Observations and Reports, FCM-H1-2005. [Available online at http://www.ofcm.gov/fmh-1/fmh1.htm]. (Accessed 18 Oct 2005).

Federal Meteorological Handbook No. 3, Rawinsonde and Pibal Observations, FCM-H3-1997. [Available online at http://www.ofcm.gov/fmh3/text/default.htm]. (Accessed 18 Oct 2005).

Fox N. I., R. Webb, J. Bally, M. W. Sleigh, C. E. Pierce, D. M L. Sills, P. I. Joe, J. Wilson, and C. G. Collier, 2004: The impact of advanced nowcasting systems on severe weather warning during the Sydney 2000 Forecast Demonstration Project: 3 November 2000. *Wea. Forecasting*, **19**, 97-114.

Haklander A. J., and A. Van Delden, 2003: Thunderstorm predictors and their forecast skill for the Netherlands. *Atm. Research*, **67-68**, 273-299.

Lucas, C. E., E. J. Zipser, and M. A. LeMone, 1994: Vertical velocity in oceanic convection off tropical Australia. *J. Atmos. Sci.*, **51**, 3183-3193.

Miller, R. C., 1967: Notes on analysis and severe storm forecasting procedures of the Military Weather Warning Center. Tech. Rep. 200, AWS, U.S. Air Force. 94 pp. [Headquarters, AWS, Scott AFB, IL 62225].

_____, 1972: Notes on analysis and severe storm forecasting procedures of the Air Force Global Weather Center. Tech. Rep. 200 (Rev.), AWS, U.S. Air Force. 102 pp. [Headquarters, AWS, Scott AFB, IL 62225].

Ramage, C. S., 1995: Forecasters guide to tropical meteorology, AWS TR 240 Updated. AWS/TR-95/001, Air Weather Service, U.S. Air Force, 392 pp. [Available from AFWTL, 151 Patton Ave. Rm. 120, Asheville, NC 28801-5002.]

Raymond, D. J., 2001: Forecasting convection, precipitation, and vertical motion in the tropics. [Available online at New Mexico Tech website http://www.physics.nmt.edu/~raymond/papers/tropfcst/]. (Accessed 6 Sep 2005).

Rutledge S. A., E. R. Williams, and T. D. Keenan, 1992: The Down Under Doppler and Electricity Experiment (DUNDEE): Overview and preliminary results. *Bull. Amer. Meteor. Soc.*, **73**, 3-16.

RTS website for Kwajalein weather [Available online at http://www.rts-wx.com]. (Accessed 20 Jan 2006).

Sadler, J. C., M. A. Lander, A. M. Hori, and L. K. Oda, 1987: Tropical marine climatic atlas, Volume II, Pacific Ocean, UH-MET 87-02, Dept. of Meteorology, University of Hawaii, 27 pp., [Available from Dept. of Meteorology, University of Hawaii, 2525 Correa Rd., Honolulu, HI 96822.].

Sherwood, S. C., 1999: Convective precursors and predictability in the tropical wester Pacific. *Mon. Wea. Rev.*, **127**, 2977-2991.

Short, D. A., J. E. Sardonia, W. C. Lambert, M. M. Wheeler, 2004: Nowcasting thunderstorm anvil clouds over Kennedy Space Center and Canaveral Air Force Station. *Wea. Forecasting*, **19**, 706-713.

Showalter, A. K., 1953: A stability index for thunderstorm forecasting. *Bull. Amer. Meteor. Soc.*, **34**, 250-252.

Turk, F. J., E. E. Ebert, B.-J. Sohn, H.-J. Oh, V. Levizzani, E. A. Smith, and R. Ferraro, 2003: Validation of a global operational blended-satellite precipitation analysis at short time scales. Extended Abstract, *12th AMS Conf. on Sat. Meteor. and Ocean.*, Long Beach, CA, Amer. Meteor. Soc., J1.2.

Wilks, D. S., 2006: *Statistical Methods in the Atmospheric Sciences*. 2d ed. Academic Press, 627 pp.

Williams, E. R., S. A. Rutledge, S. G. Geotis, N. Renno, E. Rasmussen, and T. Rickenbach, 1992: A radar and electrical study of tropical 'hot towers'. *J. Atmos. Sci.*, **49**, 1386-1395.

Wilson J. W., R. E. Carbone, J. D. Tuttle, and T. D. Keenan, 2001: Tropical island convection in the absence of significant topography. Part II: Nowcasting storm evolution. *Mon. Wea. Rev.*, **129**, 1637-1655.

Zipser, E. J., 1977: Mesoscale and convective-scale downdrafts as distinct components of squall-line structure. *Mon. Wea. Rev.*, **105**, 1568-1589.

THIS PAGE INTENTIONALLY LEFT BLANK

INITIAL DISTRIBUTION LIST

1. Defense Technical Information Center
   Ft. Belvoir, Virginia

2. Dudley Knox Library
   Naval Postgraduate School
   Monterey, California

3. Air Force Weather Technical Library
   Air Force Combat Climatology Center
   Asheville, North Carolina

4. 17 OWS
   Hickam AFB, Hawaii

5. Dr. Pat Harr
   Naval Postgraduate School
   Monterey, California

6. Dr. Russell Elsberry
   Naval Postgraduate School
   Monterey, California

7. Dr. Joe Turk
   Naval Research Laboratory
   Monterey, California

8. Capt Matt Stratton
   General Delivery
   Hickam AFB, Hawaii